Harnessing Calcium Signaling in Dendritic Cells - A Potential Approach to Modulate the Immune Response In Vivo for Immunotherapy

Harnessing Calcium Signaling in Dendritic Cells – A Potential Approach to Modulate the Immune Response *In Vivo* for Immunotherapy

A dissertation presented

by

Gail Chan

to

The School of Engineering and Applied Sciences

in partial fulfillment of the requirements
for the degree of
Doctor of Philosophy
in the subject of
Engineering Sciences

Harvard University
Cambridge, Massachusetts

April 2013

Dr. David Mooney Gail Chan

Harnessing Calcium Signaling in Dendritic Cells – A Potential Approach to Modulate the Immune Response *In Vivo* for Immunotherapy

Abstract

Over the past several decades, our understanding of the immune system has advanced considerably. With it, an appreciation for its role in a number of diseases, such as cancer and infection has significantly grown. While our increased understanding of the immunological mechanisms underlying these diseases has improved treatment, considerable morbidity and mortality from these illnesses still exists signifying the need for more effective and innovative therapies. Dendritic cell (DC) therapy has been shown to be a promising approach to induce strong immune responses for immunotherapy, and biomaterial-based strategies have been developed to target DCs *in vivo* to facilitate this purpose. Given the importance of calcium in DC function and activation, we hypothesized that we could develop a biomaterial-based approach to locally and specifically control calcium signaling in DCs *in vivo* as a novel strategy for immunotherapy. Our first sub-hypothesis was that the calcium used to crosslink alginate gels, a commonly used biomaterial, could activate DCs *in vitro*; our second sub-hypothesis was that calcium ionophore A23187 could be delivered from biomaterials to activate DCs *in vitro*; and our third sub-hypothesis was that calcium used to crosslink alginate gels and/or controlled delivery of A23187 could increase local inflammation *in vivo*. We found that both the calcium released from calcium alginate gels and A23187 matured DCs and enhanced TLR-induced inflammatory cytokine secretion *in vitro*. Although we were unable to effectively deliver A23187 *in vivo*, calcium alginate gels injected subcutaneously were able to upregulate a number of inflammatory cytokines and chemokines relative to barium alginate gels. Likewise, when LPS was delivered from calcium alginate gels, the inflammatory effects of LPS on surrounding tissue were enhanced compared to when it was delivered from barium alginate gels. Thus, we confirmed that the calcium crosslinker in alginate gels could activate

DCs, and provided a proof-of-principle that calcium signaling could be harnessed *in vivo* to enhance the immune response. Not only does this work impact the future of biomaterial design, but it may also enhance our understanding of DC biology. This thesis lays the groundwork for a novel and potentially effective strategy for enhancing DC activation *in vivo*, and suggests that ion signaling pathways in other cell types (both immune and non-immune) could also be targeted using biomaterials.

Table of Contents

Chapters

Appendices

List of Figures and Tables

Figures

Tables

Acknowledgements

First and foremost, I would like to thank my mentor and thesis advisor, Dr. David Mooney, for his patience and guidance throughout my journey to getting a Ph.D. During my 6.5 years in his lab, Dave has actively supported my creativity and pursuit of my numerous ideas (even if most of them failed), and for that I am very grateful. I would also like to thank my committee members Dr. Shannon Turley, Dr. Neel Joshi, and former committee member, Dr. Debra Auguste, for their counsel and advice.

Of course, I have to give a huge thank you to all the Mooney Lab members, past and present. In particular I would like to thank Catia Verbeke, Dr. Omar Ali, Warren Sands, Aileen Li and Dr. Jaeyun Kim for insightful immunotherapy discussions and technical suggestions. My appreciation goes out to Beth Ann Lopez, a former summer REU student, for her help with preliminary alginate experiments. I would also like to recognize Erin Anderson, Dr. Sidi Bencherif, Dr. Thomas Braschler, Dr. Yevgeny Brudno, Dr. Lan Cao, Christine Cezar, Dr. Ovi Chaudhuri, Alex Cheung, Cristiana Cunha, Max Darnell, Rajiv Desai, Dr. Luo Guo, Dr. Cathal Kearney, Dr. Steve Kennedy, Darinka Klumpers, Anu Kod, Sandeep Koshy, Dr. Kangwon Lee, Dr. Evi Lippens, Angelo Mau, Dr. Manav Mehta, Dr. Dima Shvartsman, Dr. Eduardo Silva, Dr. Prakriti Tayalia, Dr. Will Yuen and Dr. Xuanhe Zhao for making my graduate school years both mentally stimulating and fun. Not only has the Mooney Lab helped me grow as a scientist, but many of them have become great friends. If it weren't for all the laughs, both in and out of lab, I'm not sure how I would have kept my sanity. Thanks for all of your support. To Kurt Schellenburg, I am so appreciative of your efforts in getting the lab into shape and keeping everything in working order. Your help has been invaluable and made my life that much easier – thank you is an understatement! Katie Parodi, Jill Larson, Arlene Stevens and Nora McDonald, thank you for all your hard work in keeping the lab running smoothly. Katie, working in the Mooney Lab is no easy feat, and you've really done a spectacular job at juggling all the ordering, expenses, scheduling, etc. these past few years. I don't know what I would have done without you.

I would like to express my gratitude to the Bauer Core staff, particularly Patricia Rogers, for her technical assistance with flow cytometry, and Chris Johnson at the Wyss Institute for his help with the LC-MS. I would like to acknowledge past and present lab assistants, and the facilities, delivery and BRI animal staff, who are always working diligently behind the scenes to support all the science.

I have to thank my teachers for their instruction and family and friends for their wisdom and support. To my mom, Anita Chan, and dad, Hung Fan Chan, thank you for all your love and encouragement and believing in me when sometimes I didn't believe in myself. To my sister, Faith Peak, and brother-in-law, Brendon Peak, thank you for always being there and giving me an excuse to hang out and escape from grad school every now and then. To my nephews, Charlie and Casey Peak, and my niece, Cora Peak, thanks for always putting a smile on my face – I love you guys! To Katie Yuan Dulaney and Juli Wong, thank you for being such amazing friends and having my back all these years. Hopefully now that I'm done with grad school you'll get to see more of me! To Chin Lin Wong, thanks for being such a great roommate these past few years; your support and kindness has been deeply appreciated.

Last but not least, I would like to thank the NIH for funding and the Wyss Institute for supporting the work in this thesis.

Gail Chan

April 2013

“Sometimes, Gail, God does you small favors.”

-Dr. David J. Mooney

Chapter 1
Calcium Signaling as a Potential Dendritic Cell Target for Immunotherapy

1.1 Background and Motivation

The Role of Dendritic Cells in Immunity

Dendritic cells (DCs) are white blood cells that are of significant interest in the field of medicine because they link the innate and adaptive immune systems and help dictate final immune responses towards specific antigens [1]. As professional antigen presenting cells (APCs), DCs reside in peripheral tissues where they continuously sample the environment and detect danger signals like those from invading pathogens (e.g. bacterial lipopolysaccharide (LPS), flagellin, unmethylated CpG DNA, double-stranded RNA, etc.) or those from damaged tissues (e.g. heat shock proteins, extracellular ATP, uric acid, cholesterol crystals, etc.) [2-4]. Non-microbial exogenous matter, such as asbestos and aluminum hydroxide (alum), can also act as threats [5, 6]. When naïve DCs become activated by these warning indicators, they home to the lymph nodes where they present three critical signals to T cells to trigger an adaptive immune response (Figure 1.1A) [2, 7]. Signal 1 is antigen presented on major histocompatibility complex (MHC) class II, a cell-surface molecule that binds to antigen-specific T cell receptors (TCRs); Signal 2 is a co-stimulatory signal, such as B7.1 (CD80) or B7.2 (CD86), which are cell surface molecules upregulated during DC activation; lastly, Signal 3 is a soluble signal, such as secreted cytokines, which play an important role in skewing the T cell response. For example, inflammatory cytokines, such as IL-12p70 and IFN-γ, drive naïve T cells towards a T-helper cell 1 (T_H1) phenotype (important for combating viruses and bacteria), whereas anti-inflammatory cytokines, such as TGF-β and IL-10, can drive naïve T cells to differentiate into a T regulatory (T_{reg}) phenotype (important for tolerogenic responses and suppressing inflammation) [2, 7, 8]. Figure 1.1B illustrates various cytokine-induced effector T cell responses.

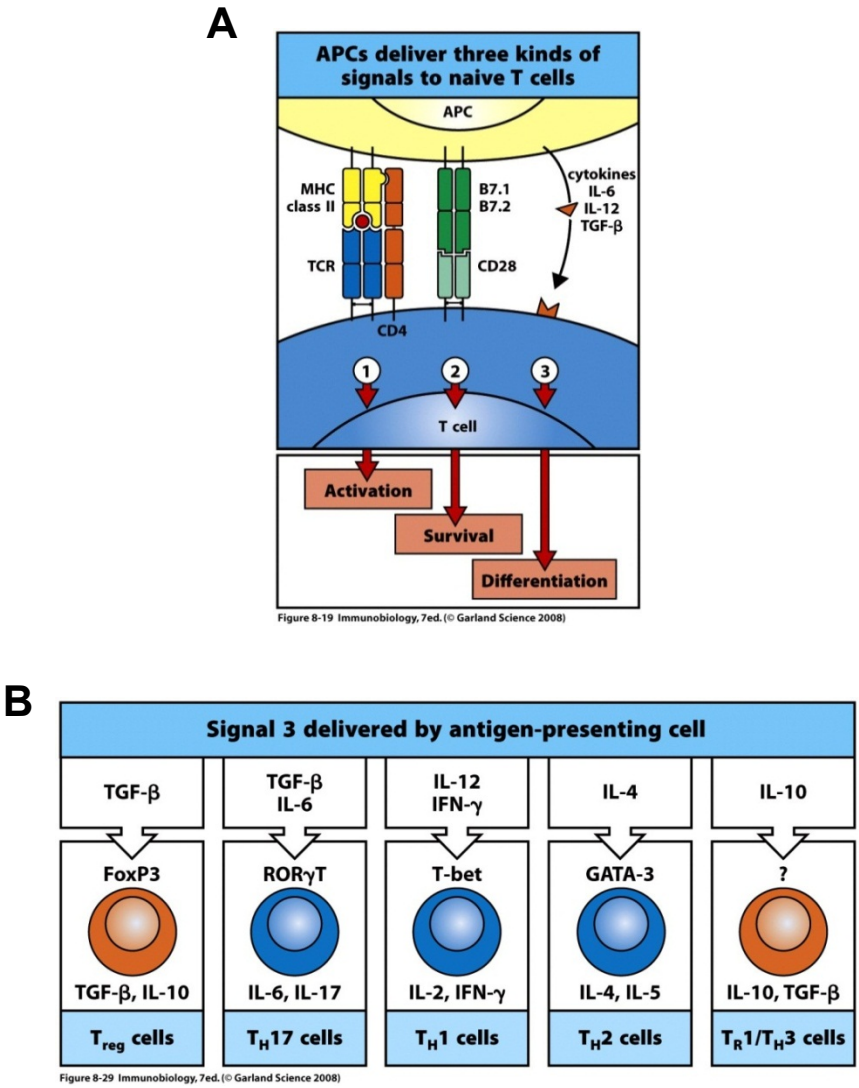

Figure 1.1: APCs deliver three important signals to naïve T cells. (A) Signal 1 is antigen bound to MHC class II; Signal 2 is a co-stimulatory signal, such as B7.1 (CD80) or B7.2 (CD86); lastly, Signal 3 is a soluble signal, such as secreted cytokines. (B) Signal 3 dictates inflammatory (T_H17/ T_H1/T_H2) or anti-inflammatory responses (T_{reg}/T_H3). Figures reproduced from [2].

Generally, the cytokine milieu expressed by DCs is dependent on the stimuli it encounters. Bacterial-derived signals, such as CpG DNA oligonucleotides, bind to toll-like receptors (TLRs) to promote T_H1 cytokines [9], whereas helminth antigens, such as soluble egg glycans bind to TLR4 to promote T_H2 cytokines [10]. Although our understanding of regulatory responses is not as well-understood, vitamin D and thymic stromal lymphopoietin (TSLP) have been found to induce tolerogenic DCs [11, 12].

In addition to external stimulatory signals controlling DC fate, certain DC subsets are intrinsically better at performing distinct functions [13, 14]. For instance, plasmacytoid DCs specialize in secreting type I interferons, which are critical for combating viral infections, while $CD8^{+}DEC205^{+}$ splenic DCs are better at cross-presenting antigens than other subsets [15]. Cross-presentation occurs when DCs uptake extracellular antigens, but rather than presenting them on MHC class II molecules, they present them on MHC class I molecules, which is important for activating cytotoxic T cells. Because DCs can be directed to initiate such diverse immune responses, they are popular therapeutic targets for immunotherapy.

Ca^{2+} Regulation of Dendritic Cells

Dendritic cells are highly dependent on Ca^{2+} to carry out their effector functions [16, 17]. While the Ca^{2+} concentration in the blood is approximately 2 mM, resting cells are able to maintain cytosolic Ca^{2+} concentrations of 10-100 nM by sequestering Ca^{2+} in organelles and employing ATP-driven Ca^{2+} pumps to pump Ca^{2+} against steep electrochemical gradients. When DCs encounter a stimulus, a rapid increase in cytosolic Ca^{2+} occurs [16, 17]. The exact mechanism of this Ca^{2+} spike is unclear, but it is thought that the stimulus activates tyrosine kinases and G-proteins, which trigger the formation of 1,4,5 inositol triphosphate (IP_3), a soluble molecule whose main function is to mobilize Ca^{2+} from organelles [16]. IP_3 binds to IP_3 receptors on the surface of organelles, such as the endoplasmic reticulum (ER), leading to the release of Ca^{2+} stores (Figure 1.2). In addition to IP_3, the phosphorylation of sphingosine to yield sphingosine-1-phosphate (S1P) has also been implicated in the release of Ca^{2+} from the ER [16].

When the ER becomes depleted of Ca^{2+}, Ca^{2+}- release activated current (CRAC) channels in the plasma membrane are activated causing an influx of extracellular calcium to replenish intracellular stores [17-19]. In turn, these large increases in cytosolic calcium activate several intracellular Ca^{2+}-sensing and -signaling molecules, which have been identified as having critical roles in DC activation and antigen presentation [16, 17]. For instance, when calmodulin (CaM), a Ca^{2+}-sensing protein, binds Ca^{2+}, it

can activate calcineurin and calcium-calmodulin dependent protein kinase II (CaMKII), which then activate transcription factors such as nuclear factor of activated T cells (NFAT) and nuclear factor kappa-light-chain-enhancer of activated B cells (NF-κB), respectively (Figure 1.2) [16, 17]. In DCs, these transcription factors lead to the synthesis of pro-inflammatory cytokines and co-stimulatory molecules such as CD80 and CD86. Additionally, studies demonstrate that the Ca^{2+}-CaM-CaMKII signaling pathway is essential for phagosome maturation [16].

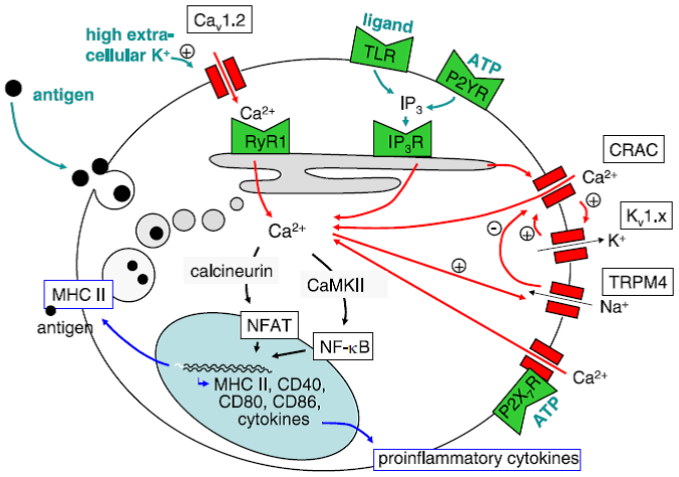

Figure 1.2: The role of calcium in dendritic cell activation. Stimuli bind to receptors that initiate signaling pathways leading to the release of Ca^{2+} from intracellular stores, such as the ER, and subsequently the influx of extracellular Ca^{2+} into the cell. Increases in cytosolic Ca^{2+} activate calcineurin and CaMKII leading to the activation of transcription factors, such as NF-κB and NFAT, and the synthesis of inflammatory molecules. P2YR, metabotropic purinoceptor; P2X, purinoceptor; RyR, ryanodine receptor; TRPM4, transient receptor potential melastatin channel. Figure reproduced from [17].

Typically, stimulation with danger signals such as LPS activates signaling pathways leading to increased cytosolic Ca^{2+} and DC maturation [17, 20], but strikingly, it has been shown that simply raising intracellular calcium levels using calcium ionophores in the absence of danger signals is enough to differentiate dendritic cells and other myeloid cells into a mature DC phenotype [21, 22]. In addition to intracellular Ca^{2+}-sensing proteins, the G-protein-coupled extracellular calcium-sensing receptor (CaR) has been implicated in the regulation of many cellular functions such as chemotaxis, apoptosis, proliferation, differentiation and ion-channel activity [23]. CaR can relay information about the local

extracellular Ca^{2+} concentration to the interior of the cell by activating the formation of IP_3 and has been associated with the activation of several mitogen-activated protein kinases (MAPKs), which play important roles in DC activation [23, 24]. Given the importance of Ca^{2+} signaling in DC function, it could be a strong therapeutic target.

Dendritic Cell-Based Immunotherapy

Dendritic cells were first discovered in 1973, and since then, research studying and exploiting DCs for immunotherapy has quickly grown [1, 25]. The first clinical study examining the efficacy of autologous dendritic cell therapy was conducted in the mid-1990s [26]. In this study, DCs were isolated from lymphoma patients, pulsed *ex vivo* with B cell lymphoma antigens, and injected back into the patients to induce anti-tumor T cell responses [27]. Although these initial trials were unsuccessful, a number of studies have been conducted since then that have had more promising outcomes due to improved *ex vivo* antigen loading and DC maturation protocols, such as using GM-CSF or monocyte-conditioned medium [28, 29]. DC therapy has also expanded to target many different types of cancers including melanoma, renal cell carcinoma, and leukemia [30, 31]. In 2010, the FDA approved the first *ex vivo* DC-based vaccine, Provenge®, to treat prostate cancer [32].

In addition to cancer vaccination, DCs are currently being tested for their ability to induce antigen-specific tolerogenic responses to treat autoimmunity and transplant rejection [33, 34]. Recently, a phase I study of autologous tolerogenic DC therapy was conducted to treat type I diabetes [35]. To generate an immunosuppressive phenotype, Signal 2 was knocked down by incubating DCs with phosphorothioate-modified antisense oligonucleotides targeting the 5' end of CD40, CD80 and CD86 gene primary transcripts. Although DCs were safely tolerated, only minimal effects were observed, indicating the need for more improved protocols in this area.

Despite advances in *ex vivo* therapy, it is expensive, labor-intensive, and difficult to isolate sufficient numbers of DCs to be cultured *in vitro* [26]. Furthermore, there is significant cell death, short signal duration, and poor distribution when these cells are re-injected into the patient [1, 26]. To address these limitations, scientists and engineers are developing novel methods to target antigens and adjuvants directly to DCs *in vivo*. Earlier strategies included fusing antigens to monoclonal antibodies specific for DC receptors, such as DEC-205 and DC-SIGN, or to TLR agonists, such as CpG, which could then be injected into the patient [36]. More recently, biomaterials have been integrated into immunotherapies because they can act as adjuvants themselves, they can sustain the delivery of multiple immune modulators and antigens leading to long-term, durable immune responses, and they can target specific organs, white blood cell types, and subcellular compartments [37-39].

One biomaterial-based approach is to implant porous polymer scaffolds to recruit and program DCs (Figure 1.3A) [40]. Poly(lactic-*co* glycolic acid) (PLG) scaffolds have been developed, which contain GM-CSF as a DC recruiting factor, CpG DNA as an adjuvant, and tumor lysates as an antigen source [41-43]. An injectable formulation made of covalently crosslinked alginate also has been recently developed. In animal studies, these scaffolds have been inserted subcutaneously to successfully create infection-mimicking niches that activate immune responses leading to the reduction of tumors.

Due to their versatility, nanoparticles are also widely studied in the field of immunoengineering. Nanoparticles can be modified to bind to a variety of DC receptors and can also target DC subsets based on size [44, 45]. Not only can they transport antigens and adjuvants to specific sites in the body, such as the lymph nodes and mucosal tissues, but they can be designed to target subcellular compartments, such as the cytoplasm or endosomes (Figure 1.3B) [39]. Nanoparticles have been fabricated using a number of materials, such as synthetic polymers, lipids, hydroxyapatite, silica, gold, and iron-oxide [46]. Most nanoparticle strategies are still in preclinical stages but seem very promising as they have been shown to induce strong and systemic immune responses [37-39].

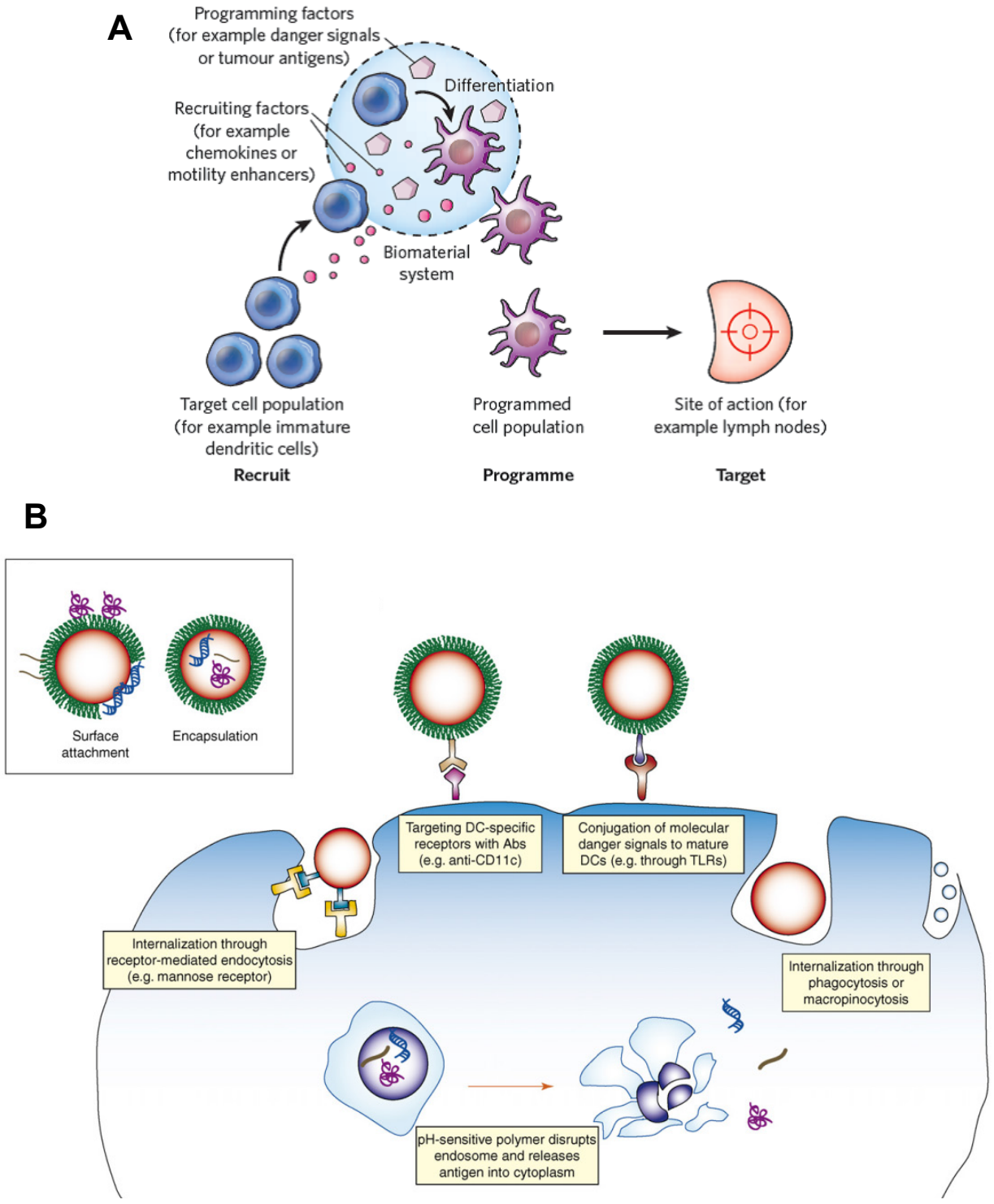

Figure 1.3: Biomaterial-based strategies for immunotherapy. (A) Scaffolds containing chemoattractants, danger signals, and antigens can recruit and program DCs for immunotherapy. Figure adapted from [40]. (B) Nanoparticles encapsulating antigen or displaying surface-bound antigen can be targeted to DCs by conjugating the nanoparticles with targeting antibodies or ligands that bind to DC-specific receptors. Figure adapted from [44].

Motivation

Although our increased understanding of the immunological mechanisms underlying many diseases, such as cancer and infectious diseases, has led to strides in vaccination and immunotherapy, suffering and mortality from these illnesses still exceeds tens of millions signifying the need for more effective and novel treatments [47]. Given the impact and versatility of DCs in medicine, the potent effect that calcium has on DC activation, and the development of new biomaterial-based strategies to target DCs, we propose that one could use biomaterials to specifically target and enhance calcium signaling in DCs *in vivo* as a means to activate them for immunotherapy. To date, we have not found a study examining this. We developed one main hypothesis and three sub-hypotheses based on this concept, and they are outlined below.

1.2 Hypotheses and Aims

Main Hypothesis

A biomaterial-based approach can be developed to locally enhance calcium signaling in DCs *in vivo* as a strategy to boost their activation for immunotherapy.

Sub-Hypothesis 1

Calcium used to crosslink alginate gels, a commonly used biomaterial, can promote DC activation *in vitro*.

Aim 1: Examine the effect of calcium-crosslinked alginate and other biomaterials on DC activation *in vitro*.

Aim 2: Determine if any differences between the materials are due to the polymer components of the materials and/or the calcium used to crosslink the alginate gels.

Sub-Hypothesis 2

Calcium ionophore A23187, a small molecule that increases intracellular calcium, can be delivered from biomaterials to activate DCs *in vitro.*

Aim 1: Test if A23187 can promote inflammatory cytokine secretion, co-stimulatory molecule expression and antigen presentation *in vitro*.

Aim 2: Test if A23187 can be delivered from biomaterials to activate DCs *in vitro*.

Sub-Hypothesis 3

Calcium used to crosslink alginate gels and/or controlled delivery of A23187 can increase local inflammation *in vivo*.

Aim 1: Determine if calcium-crosslinked alginate gels injected into mice can promote inflammatory cytokine secretion from surrounding tissue.

Aim 2: Test whether A23187 can be delivered from biomaterials to also promote local inflammatory cytokine secretion.

1.3 Thesis Outline

The next chapters describe the experiments performed to test the above hypotheses. Chapter 2 tests Sub-Hypothesis 1 (addressing Aims 1 and 2), Chapter 3 tests Sub-Hypothesis 2 (addressing Aims 1 and 2), and Chapter 4 tests Sub-Hypothesis 3 (addressing Aims 1 and 2). Chapter 5, the final chapter, discusses the conclusions, implications, and future directions of this work.

1.4 Significance

It is widely appreciated that Ca^{2+} is one of the most versatile second messengers in white blood cell signaling with important roles in transcription, apoptosis, cell adherence, activation, exocytosis,

metabolism and proliferation [18, 20, 48]. As discussed above, dendritic cells require Ca^{2+} signaling for cytokine secretion, maturation marker expression, and phagocytosis [16, 17]. This thesis proposes a unique way to enhance the immune response by exploiting calcium signaling in dendritic cells *in vivo*, and suggests that ion signaling pathways in other cell types (both immune and non-immune) could also be targeted using biomaterials.

1.5 References

[1] Steinman RM, Banchereau J. Taking dendritic cells into medicine. Nature 2007;449:419-26.

[2] Murphy K, Travers P, Walport M, Janeway C. Janeway's Immunobiology. 7th ed. New York: Garland Science; 2008.

[3] Kool M, Soullie T, van Nimwegen M, Willart MAM, Muskens F, Jung S, et al. Alum adjuvant boosts adaptive immunity by inducing uric acid and activating inflammatory dendritic cells. J Exp Med 2008;205:869-82.

[4] Duewell P, Kono H, Rayner KJ, Sirois CM, Vladimer G, Bauernfeind FG, et al. NLRP3 inflammasomes are required for atherogenesis and activated by cholesterol crystals. Nature 2010;464:1357-U7.

[5] Kool M, Pétrilli V, De Smedt T, Rolaz A, Hammad H, van Nimwegen M, et al. Cutting edge: alum adjuvant stimulates inflammatory dendritic cells through activation of the NALP3 inflammasome. J Immunol 2008;181:3755-9.

[6] Sharp FA, Ruane D, Claass B, Creagh E, Harris J, Malyala P, et al. Uptake of particulate vaccine adjuvants by dendritic cells activates the NALP3 inflammasome. Proc Natl Acad Sci U S A 2009;106:870-5.

[7] Kapsenberg ML. Dendritic-cell control of pathogen-driven T-cell polarization. Nat Rev Immunol 2003;3:984-93.

[8] Steinman RM, Hawiger D, Nussenzweig MC. Tolerogenic dendritic cells. Annu Rev Immunol 2003;21:685-711.

[9] Hartmann G, Weiner GJ, Krieg AM. CpG DNA: a potent signal for growth, activation, and maturation of human dendritic cells. Proc Natl Acad Sci U S A 1999;96:9305-10.

[10] Thomas PG, Carter MR, Atochina O, Da'Dara AA, Piskorska D, McGuire E, et al. Maturation of dendritic cell 2 phenotype by a helminth glycan uses a Toll-like receptor 4-dependent mechanism. J Immunol 2003;171:5837-41.

[11] Adorini L, Penna G, Giarratana N, Uskokovic M. Tolerogenic dendritic cells induced by vitamin D receptor ligands enhance regulatory T cells inhibiting allograft rejection and autoimmune diseases. J Cell Biochem 2003;88:227-33.

[12] Liu YJ, Soumelis V, Watanabe N, Ito T, Wang YH, Malefyt RD, et al. TSLP: an epithelial cell cytokine that regulates T cell differentiation by conditioning dendritic cell maturation. Annu Rev Immunol 2007;25:193-219.

[13] Steinman RM, Idoyaga J. Features of the dendritic cell lineage. Immunol Rev 2010;234:5-17.

[14] Satpathy AT, Wu XD, Albring JC, Murphy KM. Re(de)fining the dendritic cell lineage. Nat Immunol 2012;13:1145-54.

[15] Dudziak D, Kamphorst AO, Heidkamp GF, Buchholz VR, Trumpfheller C, Yamazaki S, et al. Differential antigen processing by dendritic cell subsets in vivo. Science 2007;315:107-11.

[16] Connolly SF, Kusner DJ. The regulation of dendritic cell function by calcium-signaling and its inhibition by microbial pathogens. Immunol Res 2007;39:115-27.

[17] Shumilina E, Huber SM, Lang F. Ca2+ signaling in the regulation of dendritic cell functions. Am J Physiol Cell Physiol 2011;300:C1205-14.

[18] Clapham DE. Calcium signaling. Cell 2007;131:1047-58.

[19] Hsu S, O'Connell PJ, Klyachko VA, Badminton MN, Thomson AW, Jackson MB, et al. Fundamental Ca2+ signaling mechanisms in mouse dendritic cells: CRAC is the major Ca2+ entry pathway. J Immunol 2001;166:6126-33.

[20] Berridge MJ, Lipp P, Bootman MD. The versatility and universality of calcium signalling. Nat Rev Mol Cell Biol 2000;1:11-21.

[21] Czerniecki BJ, Carter C, Rivoltini L, Koski GK, Kim HI, Weng DE, et al. Calcium ionophore-treated peripheral blood monocytes and dendritic cells rapidly display characteristics of activated dendritic cells. J Immunol 1997;159:3823-37.

[22] Koski GK, Schwartz GN, Weng DE, Czerniecki BJ, Carter C, Gress RE, et al. Calcium mobilization in human myeloid cells results in acquisition of individual dendritic cell-like characteristics through discrete signaling pathways. J Immunol 1999;163:82-92.

[23] Hofer AM, Brown EM. Extracellular calcium sensing and signalling. Nat Rev Mol Cell Biol 2003;4:530-8.

[24] Nakahara T, Moroi Y, Uchi H, Furue M. Differential role of MAPK signaling in human dendritic cell maturation and Th1/Th2 engagement. J Dermatol Sci 2006;42:1-11.

[25] Steinman RM, Cohn ZA. Identification of a novel cell type in peripheral lymphoid organs of mice: I. Morphology, quantitation, tissue distribution. J Exp Med 1973;137:1142-62.

[26] Tacken PJ, de Vries IJM, Torensma R, Figdor CG. Dendritic-cell immunotherapy: from ex vivo loading to in vivo targeting. Nat Rev Immunol 2007;7:790-802.

[27] Hsu FJ, Benike C, Fagnoni F, Liles TM, Czerwinski D, Taidi B, et al. Vaccination of patients with B-cell lymphoma using autologous antigen-pulsed dendritic cells. Nat Med 1996;2:52-8.

[28] Banchereau J, Palucka AK. Dendritic cells as therapeutic vaccines against cancer. Nat Rev Immunol 2005;5:296-306.

[29] Schuler G, Schuler-Thurner B, Steinman RM. The use of dendritic cells in cancer immunotherapy. Curr Opin Immunol 2003;15:138-47.

[30] Vulink A, Radford KJ, Melief C, Hart DNJ. Dendritic Cells in Cancer Immunotherapy. In: George FVW, George K, editors. Adv Cancer Res: Academic Press; 2008. p. 363-407.

[31] Fong L, Engleman EG. Dendritic cells in cancer immunotherapy. Annu Rev Immunol 2000;18:245-73.

[32] Lizée G, Overwijk WW, Radvanyi L, Gao J, Sharma P, Hwu P. Harnessing the power of the immune system to target cancer. Annu Rev Med 2013;64:71-90.

[33] Morelli AE, Thomson AW. Tolerogenic dendritic cells and the quest for transplant tolerance. Nat Rev Immunol 2007;7:610-21.

[34] Thomson AW, Robbins PD. Tolerogenic dendritic cells for autoimmune disease and transplantation. Ann Rheum Dis 2008;67:iii90-iii6.

[35] Giannoukakis N, Phillips B, Finegold D, Harnaha J, Trucco M. Phase 1 (safety) study of autologous tolerogenic dendritic cells in type 1 diabetic patients. Diabetes Care 2011;34:2026-32.

[36] Tacken PJ, Figdor CG. Targeted antigen delivery and activation of dendritic cells in vivo: steps towards cost effective vaccines. Semin Immunol 2011;23:12-20.

[37] Li WA, Mooney DJ. Materials based tumor immunotherapy vaccines. Curr Opin Immunol 2013:http://dx.doi.org/10.1016/j.coi.2012.12.008 (Article in Press).

[38] Kim J, Mooney DJ. In vivo modulation of dendritic cells by engineered materials: towards new cancer vaccines. Nano Today 2011;6:466-77.

[39] Swartz MA, Hirosue S, Hubbell JA. Engineering approaches to immunotherapy. Sci Transl Med 2012;4:148rv9.

[40] Huebsch N, Mooney DJ. Inspiration and application in the evolution of biomaterials. Nature 2009;462:426-32.

[41] Ali OA, Huebsch N, Cao L, Dranoff G, Mooney DJ. Infection-mimicking materials to program dendritic cells in situ. Nat Mater 2009;8:151-8.

[42] Ali OA, Emerich D, Dranoff G, Mooney DJ. In situ regulation of DC subsets and T cells mediates tumor regression in mice. Sci Transl Med 2009;1:1-10.

[43] Ali O, Doherty E, Bell W, Fradet T, Hudak J, Laliberte M-T, et al. Biomaterial-based vaccine induces regression of established intracranial glioma in rats. Pharm Res 2011;28:1074-80.

[44] Reddy ST, Swartz MA, Hubbell JA. Targeting dendritic cells with biomaterials: developing the next generation of vaccines. Trends Immunol 2006;27:573-9.

[45] Cruz LJ, Tacken PJ, Rueda F, Domingo JC, Albericio F, Figdor CG. Targeting nanoparticles to dendritic cells for immunotherapy. Methods Enzymol 2012;509:143-63.

[46] Faraji AH, Wipf P. Nanoparticles in cellular drug delivery. Bioorg Med Chem 2009;17:2950-62.

[47] World Health Organization. Disease and injury country estimates 2004. Online. 2013 February. Available from
URL: http://www.who.int/healthinfo/global_burden_disease/estimates_country/en/index.html.

[48] Dong Z, Saikumar P, Weinberg JM, Venkatachalam MA. Calcium in cell injury and death. Annu Rev Pathol-Mech 2006;1:405-34.

Chapter 2
Effect of Calcium Alginate Gels on Dendritic Cells *In Vitro*

2.1 Introduction

Alginate, also known as alginic acid, is an anionic, linear and unbranched polysaccharide isolated from algae or bacterial biofilms. Alginate is composed of (1, 4)-linked, β-D-mannuronate (M) and α-L-guluronate (G) sugar monomers that are arranged in M blocks (MMMMMM), G blocks (GGGGGG), or alternating M and G residues (MGMGMG), with the exact M and G composition being dependent on the algae or bacteria source. Alginate polymers have a high affinity for divalent cations (in the order Mg^{2+}<< Ca^{2+} < Sr^{2+} < Ba^{2+}) and can form a crosslinked network when these divalent cations associate with the G blocks in a proposed "egg-box" model to form crosslinks between the polymer chains (Figure 2.1) [1, 2]. Thus, alginate polymers rich in G blocks are able to create more crosslinks and stiffer gels [1, 3].

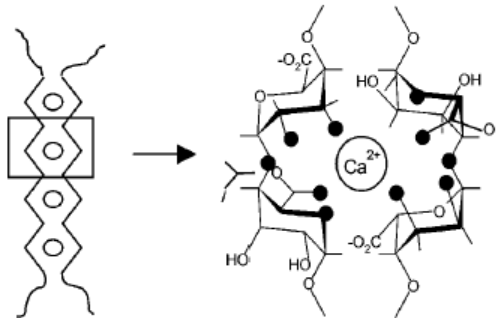

Figure 2.1: Ca^{2+} binds to the G blocks of alginate in a proposed "egg-box" leading to crosslinking of the polymer. Adapted from [1].

In physiological buffers, such as PBS, cell culture medium, or serum, monovalent cations (e.g. Na^{+}) compete with divalent cations crosslinking the alginate, which causes the release of crosslinker and weakening of the gel over time [4]. Because calcium-crosslinked alginate (calcium alginate) hydrogels are considered biocompatible, can encapsulate cells, drugs, and bioactive factors under physiological conditions, and can be tailored to have different mechanical properties and dissolution/degradation

rates depending on the M and G ratio, the molecular weight of the alginate, and the type and concentration of crosslinker used, they are widely used in tissue engineering and drug delivery [5-7].

Based on the importance of calcium signaling in white blood cell activation, we hypothesized that the calcium released from calcium alginate gels could mature and enhance the activation of DCs, which are highly sensitive to calcium. Despite calcium alginate's common use for biomedical purposes, we could not find a study examining the effects of calcium on leukocytes exposed to calcium alginate gels, even in studies where DCs were encapsulated in calcium-crosslinked alginate gels for immunotherapy [8, 9]. Contrary to this, the inflammatory properties of alginate polymers have been widely studied and disputed. For example, dissolved alginate polysaccharides (100-1000 μg/ml) have been shown to activate monocytes and macrophages depending on the molecular weight and the M and G ratio of the polymer [10, 11]. However, other studies have shown that alginate can actually suppress inflammatory disease [12] or have demonstrated no effect at all [13].

In the following study, calcium alginate was tested against three commonly used biomaterials (agarose, collagen and tissue culture polystyrene (TCPS)) for its ability to induce DC maturation and/or affect LPS-induced activation. The impact of both the alginate polymer itself and the calcium used to crosslink the alginate gels were assessed. To evaluate the immunostimulatory effects of alginate gels, DCs were cultured within alginate gels as well as externally in the presence of alginate gels. The cytokines IL-1β, IL-4, IL-6, IL-10, IL-12p70, IFN-γ and TNF-α and the activation markers CD86 and MHC class II were analyzed to gauge DC maturation.

2.2 Materials and Methods

Cell Culture

Dendritic cells were generated from bone marrow isolated from 4-16 week old C57BL/6J mice (Jackson Laboratory, Bar Harbor, ME) as described by Lutz *et al* [14]. On Day 0, mice were sacrificed and

their femurs and tibias removed. The bones were stripped of muscle and tendon with sterile scissors and washed three times in 10 ml of Hank's Balanced Salt Solution (HBSS) (Life Technologies, Carlsbad, CA) without calcium or magnesium and containing 1500 U/ml penicillin and 1500 μg/ml streptomycin (Life Technologies). The ends of the bones were cut and the marrow was flushed into a Petri dish using a 23 or 25 gauge needle and 10 ml syringe containing 10 ml of HBSS with 2% heat-inactivated FBS (Sigma-Aldrich, St. Louis, MO) and 1% 1 M HEPES buffer solution (Life Technologies). The bone marrow was then broken up with vigorous pipetting using a syringe and 18 gauge needle. The cells were passed through a 70 μm cell strainer and counted with a Z2 Coulter Counter® (Beckman Coulter, Brea, CA) using a range of 5 to 17 μm to exclude erythrocytes. Without lysing erythrocytes, $2x10^6$ cells were plated per 100x15 mm non-tissue culture treated Petri dish (BD Falcon, Franklin Lakes, NJ) in 10 ml of R10 medium (RPMI-1640 medium (Sigma-Aldrich) containing 2 mM L-glutamine, 10% heat-inactivated FBS, 100 U/ml penicillin, 100 μg/ml streptomycin, 50 μm of β-mercaptoethanol (Sigma-Aldrich) and 200 U/ml rmGM-CSF (PeproTech, Rocky Hill, NJ)). On Day 3, 10 ml of fresh R10 was added to each plate to bring the final volume to 20 ml. On Days 6, 8 and 10, 10 ml of medium were removed and centrifuged; the cell pellet was then resuspended in 10 ml of fresh medium and added back to culture. For experiments, only non-adherent cells between Days 8 and 12 were used, and the rmGM-CSF concentration was dropped to 100 U/ml. The non-adherent DCs generated with this protocol were determined to be greater than 90% CD11c positive by flow cytometry.

Endotoxin Testing

All polymer solutions, calcium crosslinkers and other ion-supplemented solutions used in this study were tested using the Limulus Amebocyte Lysate (LAL) Assay (Lonza, Walkersville, MD) according to the manufacturer's instructions.

Comparing DC Activation across TCPS, Collagen, Agarose and Alginate Gels

Cell-Seeding on TCPS

For TCPS conditions, DCs were plated at a concentration of 250,000 cells/100 μl PBS/well of a 48-well plate and incubated at 37°C for 30 minutes.

Collagen Gel Fabrication

Rat tail collagen, type I (BD Biosciences, Franklin Lakes, NJ) was certified to be negative for bacteria, fungi and mycoplasma and used without further purification. DCs were harvested, washed once in PBS, and resuspended at a concentration of $10x10^6$ cells/ml in a 3 mg/ml ice cold collagen solution prepared aseptically according to the manufacturer's instructions. 100 μl (10^6 cells) were pipetted into the wells of a 48-well plate and allowed to cure at 37°C for 30 minutes.

Agarose Gel Fabrication

A 1.2% SeaPlaque® agarose solution (Lonza, Allendale, NJ) in PBS was sterilized by autoclaving. For cell encapsulation, the solution was microwaved until fully dissolved. After cooling to 40°C in a water bath, DCs were resuspended in agarose at a concentration of $10x10^6$ cells/ml, and 100 μl (10^6 cells) were immediately pipetted into the wells of a 48-well plate. The agarose quickly cured at room temperature and was placed at 37°C for 30 minutes.

Alginate Gel Fabrication

PRONOVA™ Ultrapure medium viscosity alginate rich in α-L-guluronate residues (MVG) (FMC BioPolymer, Sandvika, Norway) was certified to be free of yeast, mold and bacteria and have an endotoxin content ≤100 EU/g. MVG alginate was further sterilized by dissolving it in deionized water and filtering it through a 0.22 μM pore diameter membrane (Millipore, Billerica, MA). The sterile alginate

solution was frozen, lyophilized and reconstituted aseptically in PBS to make a 2% solution. A $CaSO_4 \cdot 2H_2O$ slurry (183 mM) in deionized water was sterilized by autoclaving. DCs in PBS were mixed with the 2% alginate solution using two 1 ml syringes connected with a nylon female luer thread style coupler (Value Plastics, Fort Collins, CO) for a final concentration of $13x10^6$ cells/ml. 78 μl (10^6cells) of this suspension was added to wells of a 48-well plate using an 18 gauge needle, and 22 μl of thoroughly mixed $CaSO_4$ slurry was quickly pipetted and stirred into the alginate in each well. The alginate was allowed to cure at 37°C for 30 minutes. Final alginate gels contained 1.2% alginate, 40 mM $CaSO_4$, and 10^6 cells in a 100 μl gel volume.

DC Activation

After DC plating and encapsulation in hydrogels, 350 μl of R10 medium was added to each well and allowed to equilibrate at 37°C and 5% CO_2 for 1 hour before activation. For activation, 50 μl of 1000 ng/ml LPS (*E. coli* 0111:B4; Sigma-Aldrich) in R10 was added to each well so that the final concentration was 100 ng/ml; for LPS-free wells, 50 μl of R10 only was added. After 20-24 hours of activation on an orbital shaker, supernatant was collected and frozen at -20°C for cytokine analysis. For cytokine analysis, see below.

Soluble Polymer Studies with Collagen, Agarose and Alginate

Sterile 1 mg/ml solutions of dissolved collagen, agarose and alginate were made in PBS. In addition to the polymers used for gel fabrication, additional alginate polymers tested included pure G and β-D–mannuronate (M) blocks (provided by Dr. Kamal Bouhadir at the American University of Beirut, Lebanon) and PRONOVA™ Ultrapure medium viscosity (MV), low viscosity (LV) and very low viscosity (VLV) alginates rich in either G or M residues (FMC BioPolymer). Each polymer solution was then diluted 1:10 in R10 medium for a final concentration of 100 μg/ml (referred to as polymer R10). PBS was used

for the control. To prevent any potential differences in protein adsorption from affecting cell attachment across the different conditions, 200 μl of R10 medium was added to wells of a 96-well plate and incubated overnight to coat the wells with serum proteins prior to cell plating. DCs were harvested, washed in PBS, resuspended in the 100 μg/ml polymer solutions above, and plated at a density of 100,000 cells/180 μl/ serum-coated well. After 1 hour of incubation at 37°C and 5% CO_2, cells were stimulated with 20 μl of 1000 ng/ml LPS in basal R10 or polymer R10 to give a final concentration of 100 ng/ml; for LPS-free wells, 20 μl of basal R10 or polymer R10 only was added. After 20-24 hours, supernatant was collected and frozen at -20°C for cytokine analysis.

Calcium Studies on TCPS

Sterile, high calcium-containing medium was made by adding $CaCl_2 \cdot 2H_2O$ to deionized water, filtering it through a 0.22 μM membrane, and diluting it 1:100 in R10 so that the final calcium concentration equaled 3, 6 or 12 mM (basal R10=0.42 mM). Sterile deionized water was used for the control. To determine whether results were calcium-specific, magnesium, potassium and sodium ions were also screened for their ability to alter cytokine expression. Medium was supplemented with each ion so that its final concentration (Ca=3 mM; Mg=1 mM; K=5.6 mM, Na=162 mM) was 10% higher than the physiological upper limit; the calcium ionophore A23187 (400 ng/ml) (Sigma-Aldrich), which increases cytosolic calcium, was used as a positive control. DCs were harvested, washed once in PBS, and resuspended in basal medium or R10 containing high calcium, magnesium, potassium, sodium or A23187 (referred to as high ion R10). For cytokine analysis, 100,000 cells/180 μl of basal or high ion R10 were plated per well of a 96-well plate and allowed to equilibrate at 37°C and 5% CO_2. After 1 hour, 20 μl of 1000 ng/ml LPS in basal or high ion R10 was added to each well for a final concentration of 100 ng/ml; for LPS-free wells, 20 μl of basal or high ion R10 only was added. After 20-24 hours of activation supernatant was collected and frozen at -20°C. To measure surface marker expression, 10^6 cells/1.8 ml

basal or high calcium R10 were plated per well of a 6-well plate and stimulated with 200 μl of activation or LPS-free medium as above. Cytokines and cell-surface markers were detected and analyzed as described below.

Comparing DC Activation in Alginate Gels with Varying Calcium Concentration

Barium and Calcium Crosslinked Alginate Beads

DCs were harvested, washed once in PBS, and resuspended in R10 at a concentration of $125x10^6$ cells/ml. 800 μl of a sterile 2.5% Ultrapure MVG alginate solution in PBS was mixed with 200 μl of cell suspension using two 5 ml syringes connected with a coupler to give a final concentration of $25x10^6$ cells/ml of 2% alginate. A sterile beaker containing a sterile 10 mM $BaCl_2$ or 100 mM $CaCl_2$ solution with 0.1 M HEPES in ddH_2O (pH 7.4) was stirred using a stir plate while the alginate was ejected into the bath using a 30 gauge needle to create uniform alginate beads ~2 mm in diameter (~4 μl volume) with ~100,000 cells/bead. The beads were allowed to stir for 10 minutes for complete gelation, poured into a 0.22 μM filter, and washed twice with 50 ml of PBS. Ten beads ($\sim10^6$ cells) were placed in each well of a 48-well plate containing 500 μl medium and were allowed to equilibrate at 37°C and 5% CO_2. After 1 hour, 60 μl of 1000 ng/ml LPS in R10 was added so that the final concentration in each well was 100 ng/ml; for LPS-free wells, 60 μl of R10 only was added. Beads were incubated on an orbital shaker for 20-24 hours after which supernatant was collected and frozen at -20°C. For cytokine and cell-surface marker analysis, see below.

10 and 100 mM $CaCl_2$ Alginate Beads

DCs were harvested, washed once in PBS, and resuspended in PBS at a concentration of $100x10^6$ cells/ml. 750 μl of a sterile 2% Ultrapure MVG alginate solution in R10 was mixed with 250 μl of cell suspension using two 5 ml syringes connected with a coupler to give a final concentration of $25x10^6$

cells/ml of 1.5% alginate. A sterile beaker containing a sterile 10 or 100 mM $CaCl_2$ solution with 0.1 M HEPES in ddH_2O (pH 7.4) was stirred using a stir plate while the alginate was ejected into the $CaCl_2$ bath using a 30 gauge needle to create uniform alginate beads ~2 mm in diameter (~4 μl volume) with ~100,000 cells/bead. The beads were allowed to crosslink for 10 minutes and then were washed and cultured as above.

10 and 40 mM $CaSO_4$ Alginate Discs

DCs were harvested, washed once in PBS, and resuspended in R10 at a concentration of $128x10^6$ cells/ml. 1.2 ml of a sterile 2% Ultrapure MVG alginate solution in R10 was mixed with 300 μl of cell suspension using two 3 ml syringes connected with a coupler. The syringe containing the alginate-cell suspension was then connected to a third syringe containing 420 μl of 183 or 46 mM $CaSO_4$ crosslinker. The two syringes were pumped back and forth quickly 8-10 times to homogeneously mix the alginate with the crosslinker, and the mixture was cast between two Teflon-coated aluminum plates (McMaster-Carr, Elmhurst, IL) with 1 mm spacers. The alginate was allowed to cure for 10-20 minutes, after which 8 mm diameter discs were punched using a disposable biopsy punch (Premier, Plymouth Meeting, PA). Final discs were 8 x 1 mm (~50 μl) and contained 1.25% alginate, 10^6 cells, and either 10 or 40 mM $CaSO_4$. Discs were placed in 490 μl R10 in 48-well plates and allowed to equilibrate at 37°C and 5% CO_2. After 1 hour, 60 μl of 1000 ng/ml LPS in R10 was added so that the final concentration in each well was 100 ng/ml; for LPS-free wells, 60 μl of R10 only was added. Discs were incubated on an orbital shaker for 20-24 hours after which supernatant was collected and frozen at -20°C. For cytokine and cell-surface marker analysis, see below.

DCs Cultured in the Presence of Barium and Calcium Alginate Gels

For cytokine analysis, 10^6 DCs in 2 ml of medium were plated in 6-well plates. After 1 hour of culture, 200 μl of 4 mM barium- or 48.8 mM calcium-crosslinked alginate gels were added to wells. Gels were fabricated by mixing a 2.5% MVG alginate solution in R10 with 20 mM $BaCl_2$ or 244 mM $CaSO_4$ crosslinker solution in water in a 4:1 ratio using two syringes connected by a coupler. 200 μl was ejected through an 18 gauge needle onto a sterile plate and allowed to cure for 10 minutes. Final gels, containing 2% alginate, were then added to wells using a sterile spatula. After 20-24 hours of stagnant culture, supernatants were collected for IL-1β analysis. For surface marker analysis, the above procedure was repeated except gels were cast between two Teflon-coated aluminum plates and 8 mm discs were punched using a biopsy punch. Four gels were added per well and DCs were cultured on an orbital shaker. After 20-24 hours, cells were scraped from wells for surface marker staining as described below.

Cell-Surface Marker Analysis

For studies on TCPS, 1 ml of 50 mM EDTA in PBS (pH 7.4) was added to each well, and plates were placed in the incubator for 15 minutes to aid in cell detachment. Cells were then scraped from wells and washed with stain buffer (BD Pharmingen, Franklin Lakes, NJ). To retrieve DCs from the gels, 500 μl of 50 mM EDTA in PBS (pH 7.4) was added to each well. Gels were allowed to dissolve at 37°C and cells were collected and washed in stain buffer. Collected cells were stained with APC-conjugated anti-mouse CD11c, FITC-conjugated anti-mouse MHC class II and PE-conjugated anti-mouse CD86 (eBioscience, San Diego, CA). Cell-surface antigen staining was analyzed using an LSR II or LSR Fortessa™ flow cytometer (BD Biosciences). Cell viability was determined using SSC vs. FSC, and only viable cells were gated for surface marker analysis.

Cytokine Analysis

Cell culture supernatants were analyzed for mIL-1β, mIL-4, mIL-6, mIL-10, mIL-12p70, mIFN-γ and mTNF-α using the Bio-Plex Pro™ Magnetic Cytokine Assay System (Bio-Rad, Hercules, CA).

Calcium Release Assay

Alginate beads and discs were fabricated and incubated in R10 as above but without cells. Medium was collected at 1, 4 and 10 hours, frozen at -20°C, and later assayed using the QuantiChrom™ Calcium Assay Kit (BioAssay Systems, Hayward, CA) according to the manufacturer's instructions. R10 alone was assayed as t=0. Briefly, 5 μl of thawed sample or standard was added to a 96-well plate followed by 200 μl of Quantichrom™ working solution. Samples were mixed by gently tapping the plate and incubated for 3 minutes at room temperature before absorbance was read at 612 nm with a Synergy™ HT microplate reader (Bio-Tek, Winooski, VT).

Intracellular Calcium Assay

To measure intracellular calcium, cells were labeled with the fluorescent intracellular calcium probe Fluo-4 AM (Life Technologies). DCs were harvested, washed in PBS, and resuspended at a density of 10^6 cells/ml in 5 μM Fluo-4 AM in PBS for 30 minutes at room temperature. Labeled cells were then washed in PBS and allowed to sit for another 30 minutes to allow for complete de-esterification of the probe before plating or encapsulation. Immediately after plating on TCPS or being encapsulated within alginate gels, cells were imaged with an EVOS® fl microscope (AMG, Bothell, WA) using the FITC channel. For kinetic studies, DCs were plated on TCPS in increasing calcium concentrations as above and fluorescence was measured using a Synergy™ HT microplate reader (Ex. 488 nm, Em. 516) at multiple timepoints after plating. For all intracellular calcium studies, the anti-FITC antibody A889 (Life Technologies) was diluted in the medium 1:200 to quench background fluorescence.

Differential Interference Contrast (DIC) Microscopy and Photos of Whole Alginate Gels

DIC images of cells were taken using an Olympus IX81® inverted microscope (Olympus, Center Valley, PA). Photos of whole alginate gels were taken with a Nikon COOLPIX® p90 camera (Nikon, Melville, NY).

Graphs and Statistical Analysis

Flow cytometry data was analyzed and plotted using FlowJo® software (Tree Star, Ashland, OR), and all other graphs were made using Kaleidagraph® software (Synergy Software, Reading PA). Statistical analysis was performed using Microsoft® Excel (Microsoft, Redmond, WA) or Kaleidagraph® software. A two-tailed Student's t-test assuming equal variances was used when comparing two groups, and a one-way analysis of variance (ANOVA) followed by a post-hoc Tukey test was used when comparing multiple groups. For all experiments n=3-4. Data is reported as the mean ± standard deviation.

2.3 Results

Endotoxin Testing

All polymer solutions, calcium crosslinkers and other ion-supplemented solutions used in this study tested ≤0.1 EU/ml.

DC Comparison across Materials

To determine if calcium-crosslinked alginate gels had a distinct effect on DC behavior, DCs encapsulated in $CaSO_4$ alginate gels were compared to DCs encapsulated in agarose and collagen gels and DCs plated on TCPS. Agarose was chosen because like alginate, it is a polysaccharide that lacks integrin binding motifs and cannot be enzymatically degraded by mammalian cells; collagen and TCPS

were chosen as standard biomaterial controls. In order to cast DCs in alginate gels at the bottom of wells consistently with collagen and agarose gels, $CaSO_4$ was used as the crosslinker because it is less soluble in aqueous solution than $CaCl_2$ (a more commonly used calcium crosslinker) leading to a slower gelation rate and the ability to mold alginate gels in shapes other than rounded beads. $CaSO_4$ precipitates were visible immediately after casting (Figure 2.2), but by 24 hours were no longer present due to the alginate gel binding free Ca^{2+} ions and allowing the precipitates to solubilize. DCs in alginate or agarose gels had a rounded appearance throughout the duration of the experiment, while cells on TCPS and in collagen were able to migrate, spread and make direct cell-cell contacts (Figure 2.2).

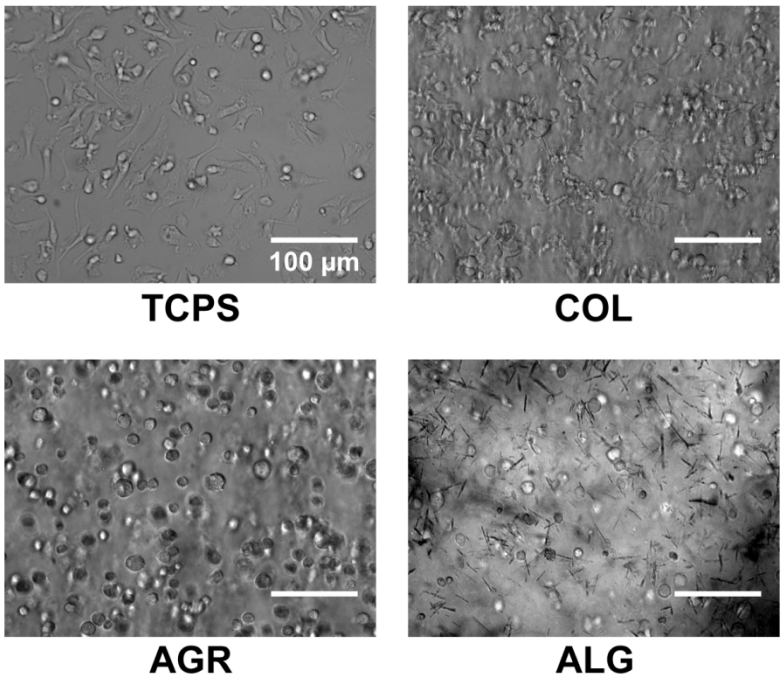

Figure 2.2: Photomicrographs of DCs cultured on TCPS and encapsulated in various hydrogels. Photomicrographs were taken of DCs adhered to TCPS or encapsulated in collagen (COL), agarose (AGR) or alginate (ALG) gels one hour after encapsulation.

To determine if there were differences in DC activation across the materials, cell culture supernatants were assayed for various inflammatory cytokines. DCs encapsulated in calcium-crosslinked alginate gels produced significantly higher levels of the inflammatory cytokine IL-1β when compared to

DCs encapsulated in agarose and collagen gels and DCs plated on TCPS (Figure 2.3). Overall cytokine expression increased for all conditions when cells were stimulated with LPS, but IL-1β was even further enhanced with alginate gels (Figure 2.3). Interestingly, with LPS stimulation, DCs in agarose gels produced significantly higher levels of TNF-α, while DCs plated on TCPS produced significantly higher levels of IL-6 (Figure 2.3). mIL-4 and mIFN-γ secretion were negligible for both LPS-free and LPS stimulated cells in all conditions and thus excluded from the rest of the study.

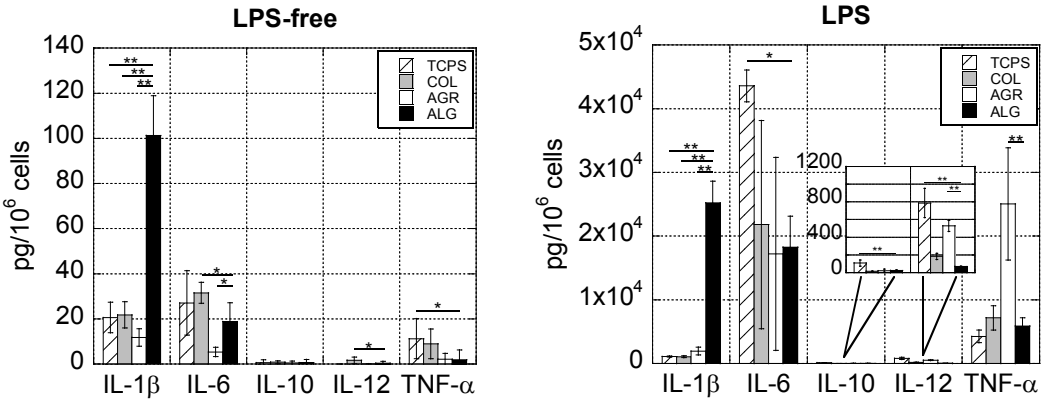

Figure 2.3: Alginate gels enhanced IL-1β secretion from encapsulated DCs. DCs were cultured without LPS or with LPS. After 24 hours, supernatant was collected and analyzed for multiple cytokines. Asterisks indicate that the condition is significantly different from the other material being compared. *P≤0.05; **P≤0.001.

The impact of each gel on soluble Ca^{2+} levels was next analyzed. As mentioned previously, in physiological buffers, such as PBS, cell culture medium, or serum, monovalent cations (e.g. Na^{+}) compete with divalent cations crosslinking the alginate, which causes the divalent cations to be released over time. Over a 10 hour period, calcium-crosslinked alginate gels increased Ca^{2+} in the surrounding medium to approximately 5 mM (indicating that ~43% of the calcium initially incorporated into the gel was released), while the other gels did not impact the Ca^{2+} concentration (Figure 2.4). These results indicated that calcium-crosslinked alginate gels elevated extracellular calcium levels and had a unique effect on DC behavior and activation when compared to other materials.

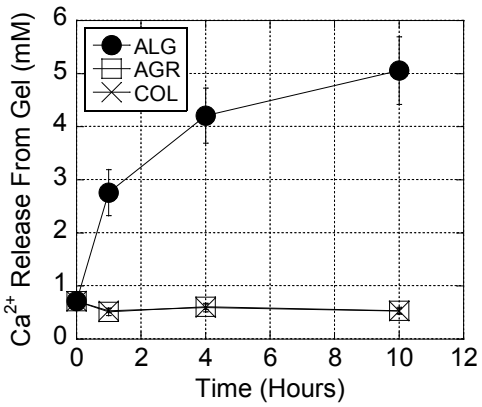

Figure 2.4: Alginate gels released high levels of calcium. The Ca^{2+} released into medium from each of the hydrogels was quantified over 10 hours.

Testing Polymer Components of Gels on TCPS-Cultured DCs

The impact of the polymer components of the three hydrogels tested were next examined by culturing DCs on TCPS overnight with each of the three dissolved polymers. In the absence of LPS, IL-6 secretion for alginate was slightly higher than the no polymer (NP) condition (Figure 2.5A), and in the presence of LPS, IL-1β and IL-12p70 secretion for collagen and agarose, respectively, were slightly different from NP (Figure 2.5A). However, these differences were minor and did not account for the trends seen with intact gels. Similarly, the various alginate polymers screened in Table 1 did not induce or enhance cytokine expression compared to NP (Figure 2.5B).

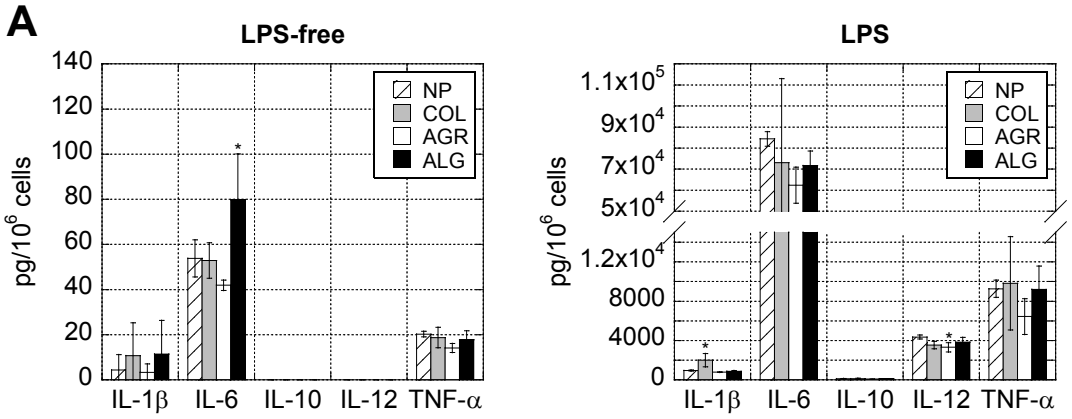

Figure 2.5

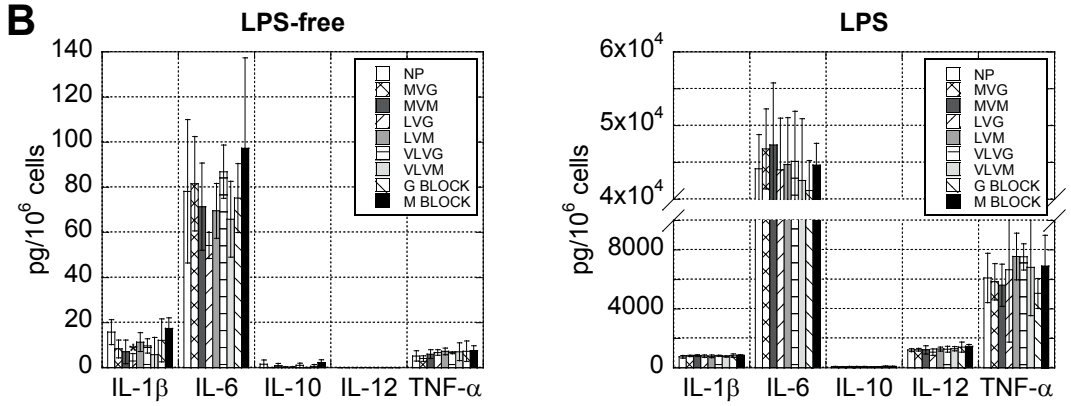

Figure 2.5 (Continued): Soluble polymer components of gels were not responsible for trends seen with intact gels. (A) DCs were cultured on TCPS with no polymer (NP), or dissolved collagen (COL), agarose (AGR) or alginate (ALG), in the absence of LPS or in the presence of LPS. After 24 hours, supernatant was collected and multiplexed for cytokines. (B) DCs were cultured on TCPS with dissolved alginate polymers of varying molecular weight and M and G ratio (see Table 1) in the absence of LPS or in the presence of LPS. After 24 hours, supernatant was collected and multiplexed for cytokines. Asterisks indicate that the polymer condition is significantly different from NP. *P≤0.05.

Table 1: Molecular weight and M and G percentage of alginate polymers tested in Figure 2.5.

Alginate	%M/G	MW (Da)
MVG	>60% G	>200,000
MVM	>50% M	>200,000
LVG	>60% G	75,000-200,000
LVM	>50% M	75,000-200,000
VLVG	>60% G	<75,000
VLVM	>50% M	<75,000
G Blocks	100% G	5,000-10,000
M Blocks	100% M	5,000-10,000

Testing Calcium-Supplemented Medium on DCs Cultured on TCPS

The impact of free Ca^{2+} on cytokine secretion was tested next. DCs were cultured on TCPS in medium supplemented with calcium up to 3, 6 or 12 mM. Interestingly, DCs extended longer processes as the calcium concentration in the medium increased, particularly for 12 mM calcium, and although LPS

stimulation caused cells to contract, the spindle-like morphology seen with 12 mM calcium was still apparent (Figure 2.6).

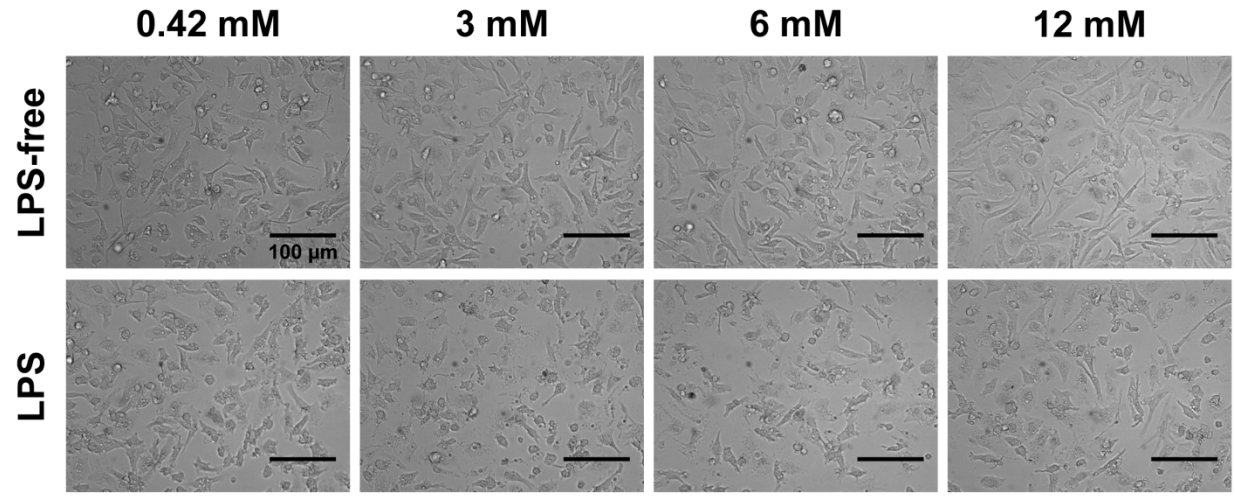

Figure 2.6: DCs altered their morphology when cultured in increasing concentrations of calcium. Photomicrographs were taken of DCs cultured on TCPS in medium containing 0.42 mM calcium (basal) or supplemented with 3, 6, or 12 mM calcium in the absence or presence of LPS.

Fluo-4, a fluorescent intracellular calcium probe, was used to quantify the levels of intracellular calcium for each of the calcium concentrations. Both photomicrographs and microplate readings revealed that the intracellular calcium levels rose with increasing extracellular calcium (Figure 2.7A and B). Although intracellular calcium concentrations were highest immediately after plating and fluctuated within the first hour, a sustained high intracellular Ca^{2+} concentration was observed and maintained for at least 10 hours (Figure 2.7B).

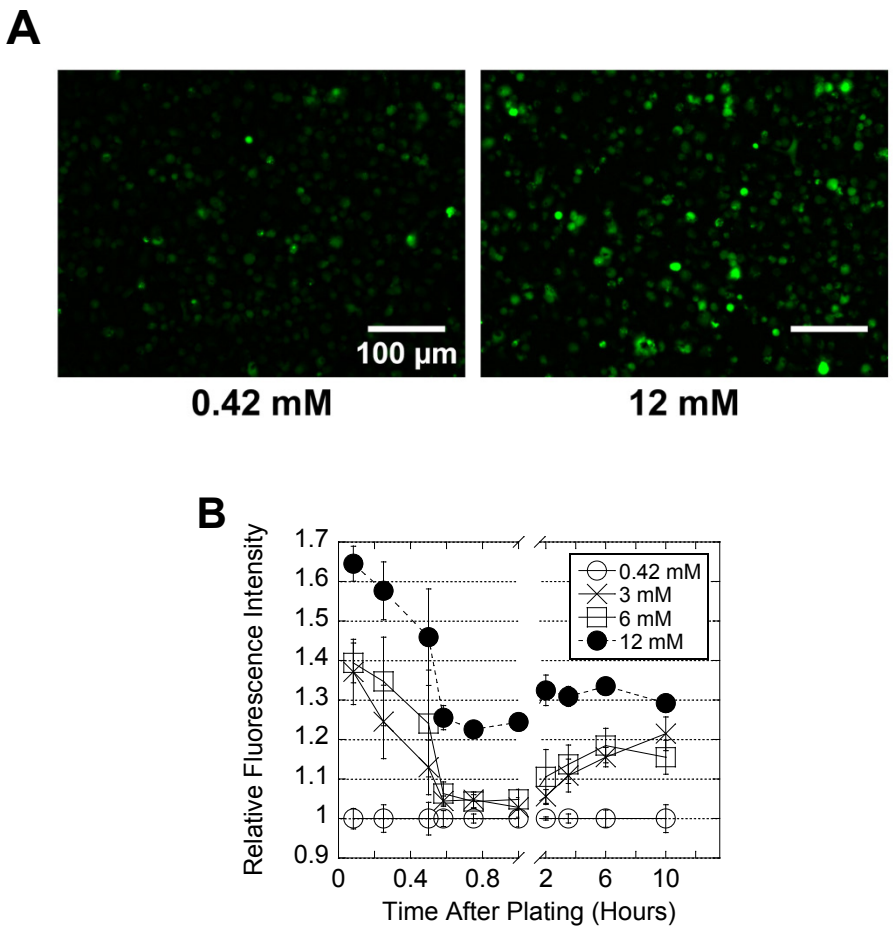

Figure 2.7: Intracellular calcium concentration positively correlated with extracellular calcium concentration. DCs were labeled with the intracellular calcium probe Fluo-4 and plated with increasing concentrations of calcium as above. (A) Cells were imaged immediately after plating (only 0.42 and 12 mM are shown) or (B) fluorescence was quantified over a 10 hour period using a plate reader.

Despite the fact that DCs in the 3, 6 and 12 mM calcium conditions looked equally as viable as the 0.42 mM conditions, forward-side scatter analysis using flow cytometry revealed that high levels of calcium reduced cell viability in a dose-dependent manner and that LPS stimulation further reduced cell viability (Figure 2.8).

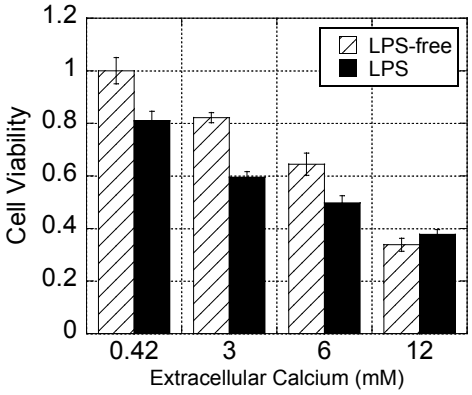

Figure 2.8: Increasing extracellular calcium and stimulating with LPS decreased cell viability. DCs were plated in increasing concentrations of calcium as above for 24 hours in the absence or presence of LPS. Cells were collected and viability was quantified based on forward-/side-scatter measurements obtained using flow cytometry.

Analysis of cell culture supernatants showed that high levels of extracellular calcium led to an increase in IL-1β both with and without LPS stimulation (with secretion peaking at 3 mM calcium) (Figure 2.9). This data was consistent with DCs cultured in alginate gels. Interestingly, in the LPS-free condition, high levels of extracellular calcium also upregulated IL-6 and TNF-α secretion, but in the presence of LPS, had no effect on IL-6 and actually downregulated IL-12p70 and TNF-α (Figure 2.9).

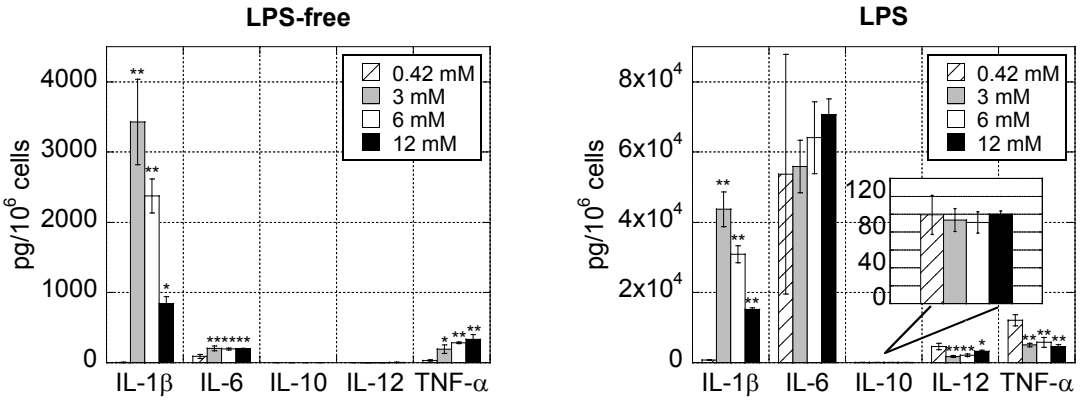

Figure 2.9: Supplementing medium with excess calcium induced IL-1β secretion. DCs were cultured in R10 supplemented with increasing concentrations of calcium in the absence or presence of LPS. After 24 hours, supernatants were multiplexed for cytokines. Asterisks indicate that the calcium-supplemented condition is significantly different from the 0.42 mM (basal) condition. *P≤0.05; **P≤0.001.

To determine whether these trends were calcium-specific, and not due to an increase in osmolality, several physiologically relevant ions were screened for their ability to alter cytokine expression. R10 was supplemented with calcium, magnesium, sodium, or potassium so that the concentration of the ion was 10% higher than the physiological upper limit; the calcium ionophore A23187, which increases cytosolic calcium, was used as a positive control. The increase in IL-1β, IL-6 and TNF-α observed with calcium was repeated only with A23187, which demonstrated that the effect was specific to calcium (Figure 2.10).

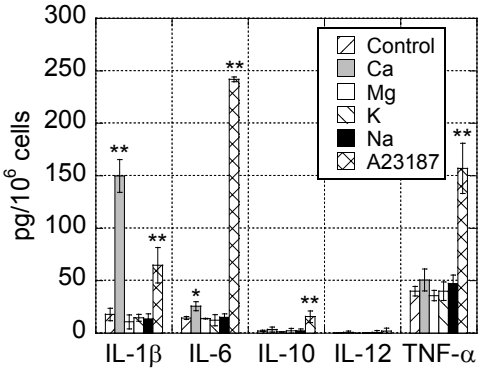

Figure 2.10: Cytokine secretion induced by excess calcium was calcium-specific. DCs were cultured on TCPS in medium supplemented with calcium, magnesium, potassium, or sodium at a concentration ~10% higher than the physiological upper limit. The calcium ionophore A23187 was tested as a positive control. After 24 hours, supernatants were collected and analyzed for cytokines. Asterisks indicate that the ion-supplemented condition is significantly different from the control condition. *P≤0.05; **P≤0.001.

DCs cultured in increasing concentrations of calcium were stained with anti-CD86 and anti-MHC class II antibodies, and live cells were gated into populations of negative, low or high expression of each marker based on flow cytometry histograms (Figure 2.11A). In LPS-free medium, increasing extracellular calcium correlated with increasing MHC class $II^{hi}CD86^{hi}$ double-positive expression in a dose-dependent manner, while LPS stimulation caused MHC class $II^{hi}CD86^{hi}$ double-positive cells to plateau at approximately 80% across all calcium concentrations (Figure 2.11B).

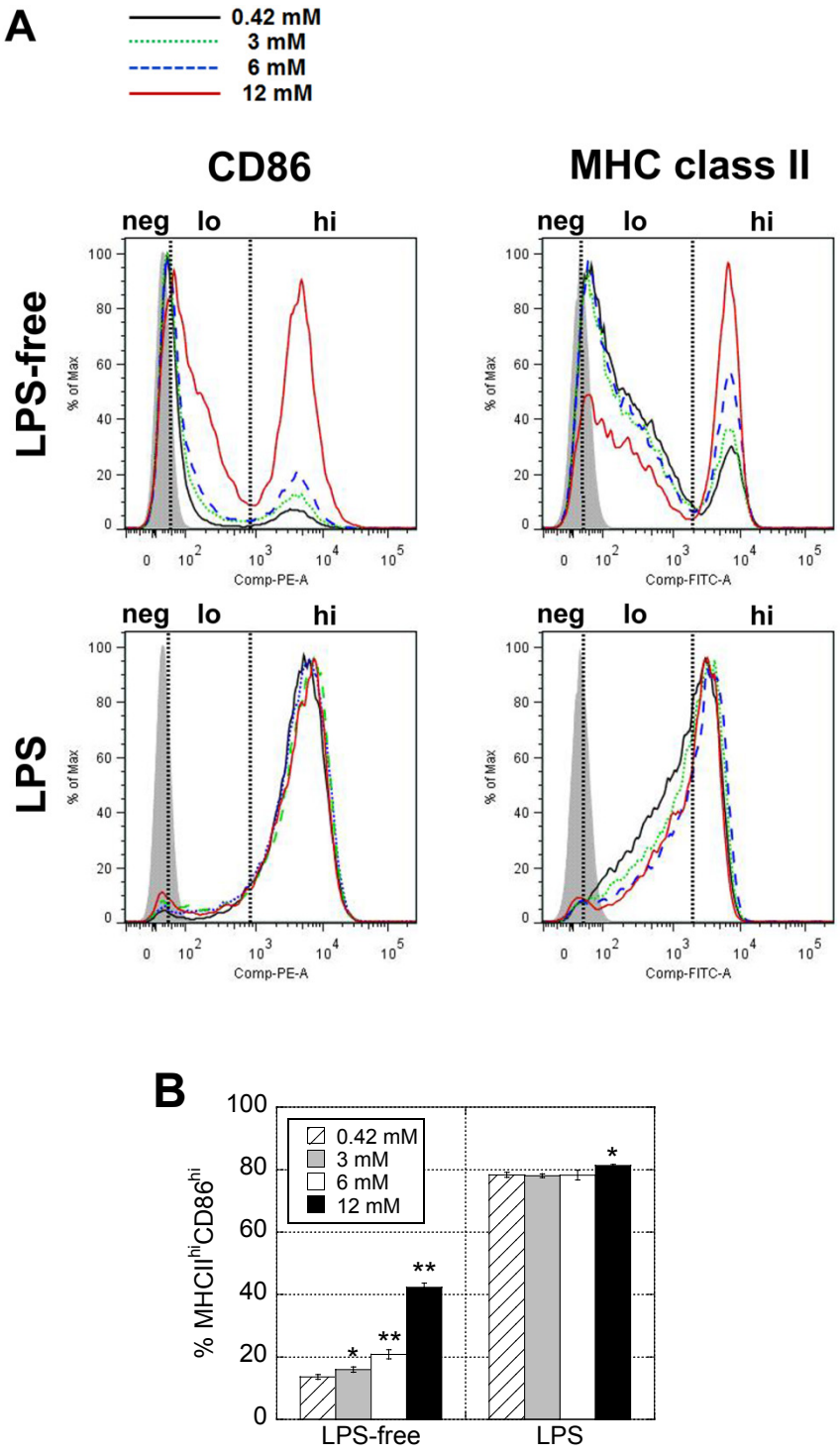

Figure 2.11: Supplementing medium with excess calcium upregulated DC activation markers. DCs cultured in increasing concentrations of calcium, in the absence or presence of LPS, were detached from the TCPS, stained with PE-labeled anti-CD86 and FITC-labeled anti-MHC class II, and analyzed using flow cytometry. (A) Live cells were gated into negative (neg), low (lo), or high (hi) populations. Filled gray histograms are isotype controls. (B) The percentage of MHC class II^{hi}CD86^{hi} double-positive cells were calculated based on neg/lo/hi gating. Asterisks indicate that the calcium-supplemented condition is significantly different from the basal (0.42 mM) condition. *P≤0.05; **P≤0.001.

Testing Calcium Crosslinker in Alginate Gels

Given evidence that it was the calcium crosslinker and not the alginate polymer accounting for enhanced DC maturation, we hypothesized that DCs encapsulated in calcium-crosslinked alginate would have a greater degree of maturation than DCs encapsulated in barium-crosslinked alginate. To test this, DCs were encapsulated in alginate droplets crosslinked in a 10 mM $BaCl_2$ or 100 mM $CaCl_2$ bath (the most standard method for crosslinking alginate) and analyzed for their ability to induce DC maturation. 100 mM $CaCl_2$ was chosen because it is a concentration typically used for biomedical applications, and 10 mM $BaCl_2$ was selected because it yielded beads approximately the same size as 100 mM $CaCl_2$. Because barium has such a high affinity for alginate, less was needed for gel fabrication [2].

As hypothesized, DCs encapsulated in calcium-crosslinked alginate secreted significantly more IL-1β compared to DCs in barium-crosslinked gels (Figure 2.12A). LPS stimulation caused an overall increase in IL-1β, but the presence of calcium even further enhanced its secretion. Likewise, for both LPS-free and LPS conditions, DCs extracted from calcium-crosslinked alginate gels had increased expression of CD86 and MHC class II compared to DCs extracted from barium-crosslinked alginate gels (Figure 2.12B).

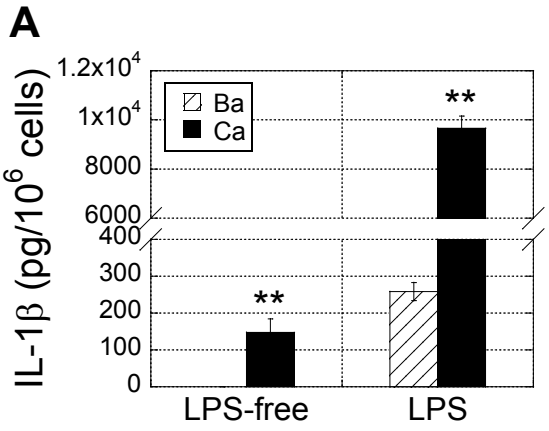

Figure 2.12

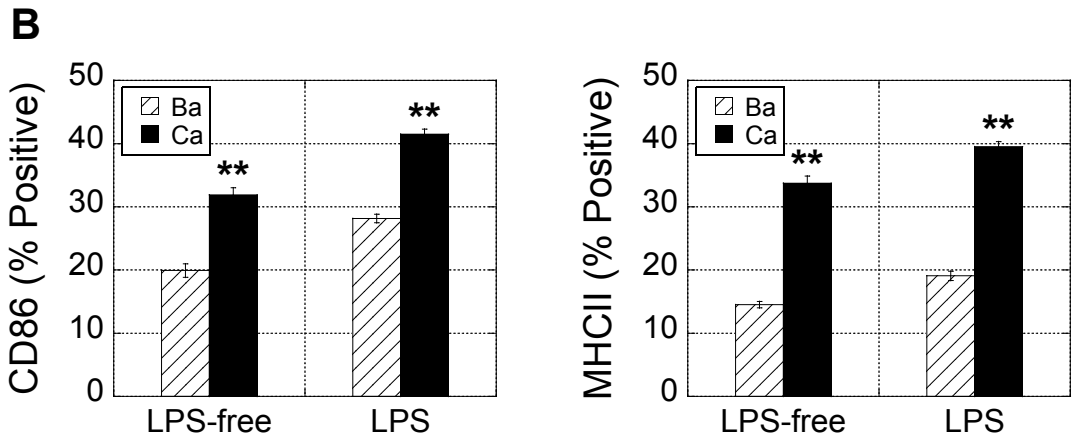

Figure 2.12 (Continued): Calcium crosslinker enhanced DC activation markers compared to barium crosslinker. (A) After 24 hours in culture, supernatants from DCs encapsulated in barium or calcium alginate beads, in the absence or presence of LPS, were collected and assayed for IL-1β. (B) DCs were extracted from beads and analyzed for CD86 and MHC class II using flow cytometry. Asterisks indicate that the calcium condition is significantly different from the barium condition. **P≤0.001.

Since the calcium crosslinker was responsible for the enhanced IL-1β secretion and maturation marker expression observed with alginate gels, we hypothesized that DCs encapsulated in alginate gels with increasing concentrations of calcium crosslinker would have a dose-dependent response. Alginate droplets were crosslinked in a 10 or 100 mM $CaCl_2$ bath as described above. Alginate beads crosslinked with 100 mM $CaCl_2$ had slightly more precipitates than 10 mM $CaCl_2$ gels (Figure 2.13A), which were formed during washing with PBS. Beads crosslinked with 100 mM $CaCl_2$ raised the Ca^{2+} concentration of the medium up to 1.5 times higher than 10 mM gels (Figure 2.13B). Over time, the calcium released from both gel formulations began to precipitate in the medium, potentially accounting for the decrease in free Ca^{2+} seen at 4 and 10 hours. As expected, DCs in 100 mM gels stained more brightly with Fluo-4 indicating that intracellular calcium concentration positively correlated with extracellular calcium concentration (Figure 2.13C).

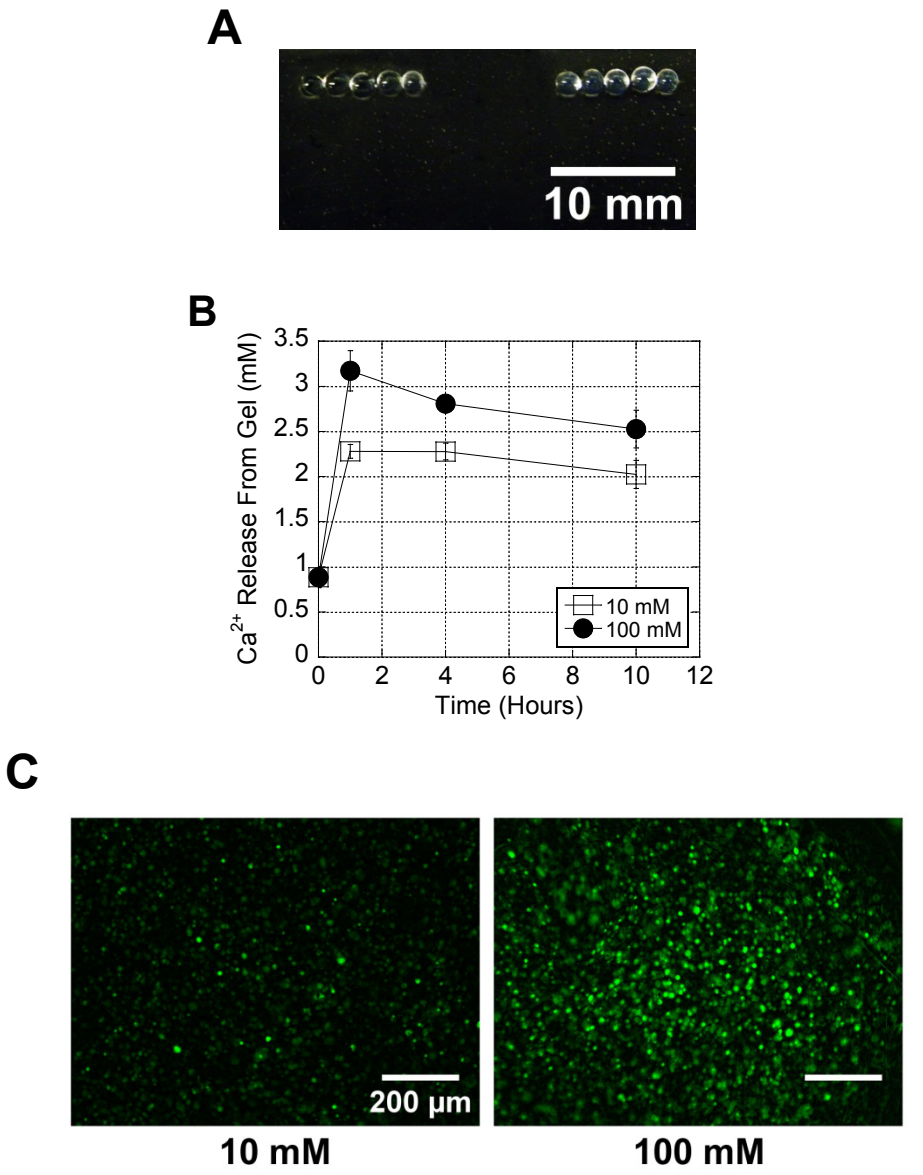

Figure 2.13: Increasing $CaCl_2$ crosslinker in alginate discs increased extracellular and intracellular Ca^{2+}. (A) Alginate beads (diameter≈2 mm) were crosslinked with 10 (left) or 100 mM (right) $CaCl_2$. (B) Ca^{2+} released into medium from 10 and 100 mM $CaCl_2$ alginate gels was quantified over 10 hours. (C) DCs were labeled with Fluo-4, encapsulated in 10 or 100 mM $CaCl_2$ alginate beads, and imaged with a fluorescent microscope to determine relative intracellular Ca^{2+} levels.

DCs in $CaCl_2$ gels appeared viable immediately after encapsulation but by 24 hours appeared necrotic (Figure 2.14A). Forward-side scatter analysis of DCs retrieved 24 hours after encapsulation confirmed that increasing $CaCl_2$ crosslinker concentration by 10 fold decreased cell viability from 80% to 50% and that LPS stimulation further decreased cell viability by 8 to 10 fold (Figure 2.14B).

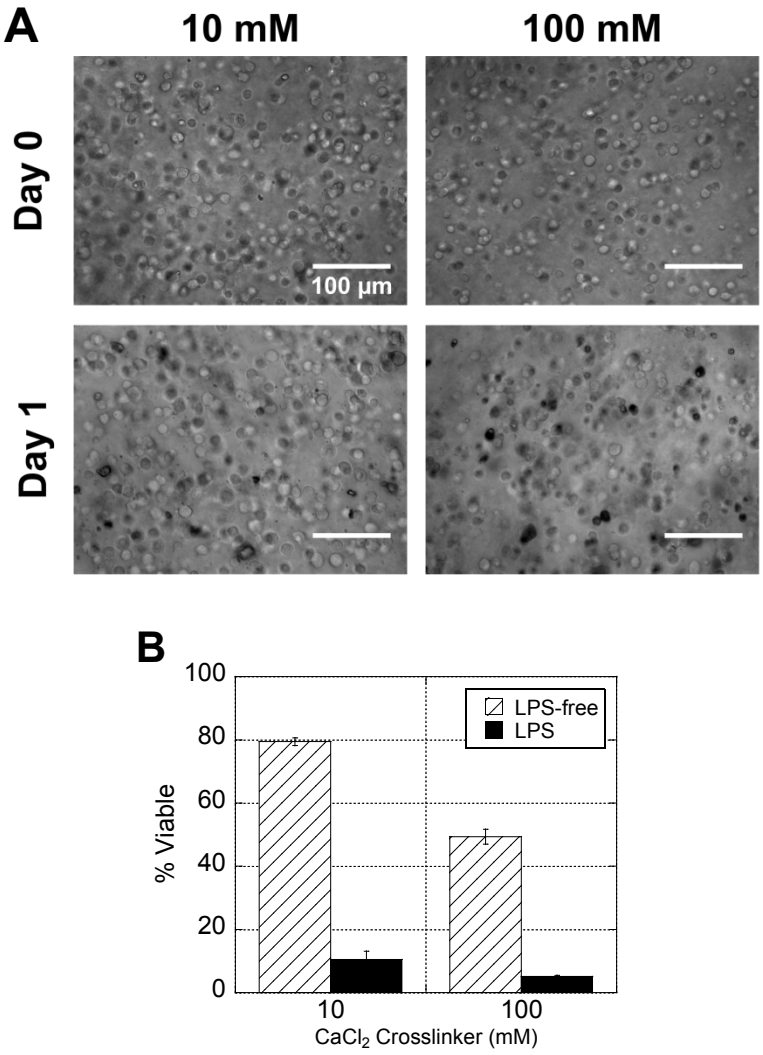

Figure 2.14: Increasing $CaCl_2$ crosslinker decreased cell viability. (A) Photomicrographs were taken of DCs immediately after encapsulation (top) and 24 hours later (bottom). Images shown are the most representative. (B) DCs were extracted from beads and cell viability was quantified based on forward-/side-scatter measurements obtained using flow cytometry.

Consistent with trends seen with calcium-supplemented R10, increasing the $CaCl_2$ crosslinker from 10 mM to 100 mM induced secretion of all cytokines tested, particularly IL-1β, and enhanced LPS-stimulated IL-1β secretion (Figure 2.15). Increasing $CaCl_2$ also strongly enhanced the mean fluorescence intensity (MFI) of $CD86^{lo}$ for both LPS-free and LPS-stimulated cells (Figure 2.16A), enhanced the MFI of

MHC class II^{lo} for LPS-stimulated cells (Figure 2.16A), and significantly increased MHC class II^{hi}CD86^{hi} double-positive expression (Figure 2.16B).

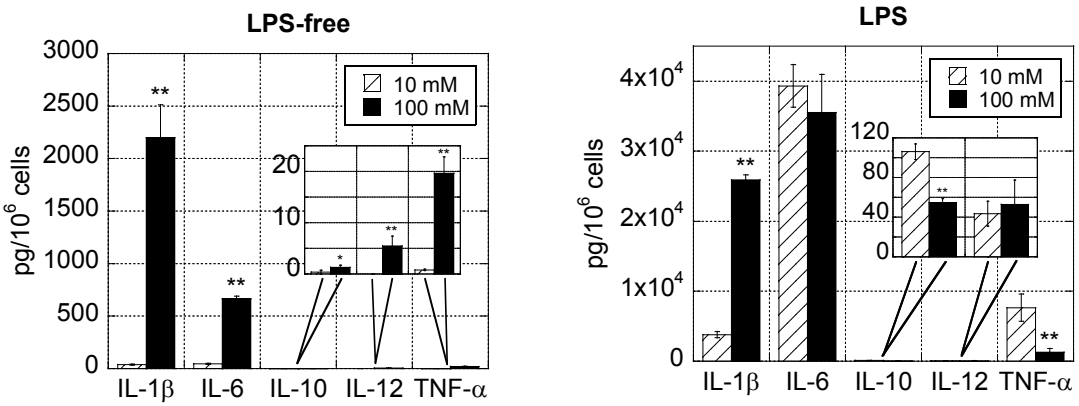

Figure 2.15: Increasing $CaCl_2$ crosslinker increased IL-1β secretion. After 24 hours in culture, supernatants from DCs encapsulated in alginate beads, in the absence or presence of LPS, were collected and multiplexed for cytokines. Asterisks indicate that the 100 mM condition is significantly different from the 10 mM condition. *P≤0.05; **P≤0.001.

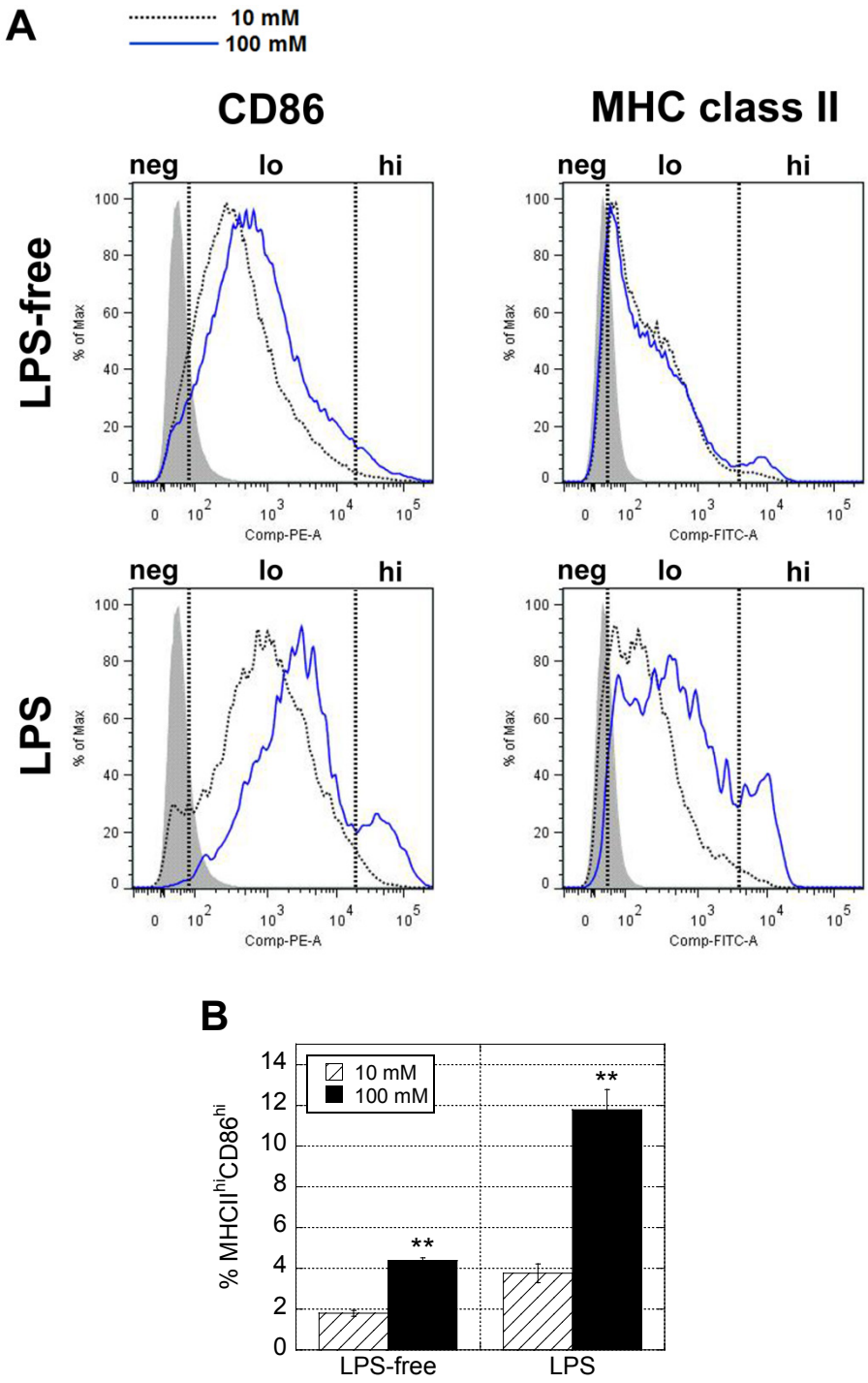

Figure 2.16: Increasing $CaCl_2$ crosslinker upregulated DC activation markers. DCs were extracted from beads, stained with PE-labeled anti-CD86 and FITC-labeled anti-MHC class II, and analyzed using flow cytometry. (A) Live cells were gated into negative (neg), low (lo), or high (hi) populations. Filled gray histograms are isotype controls. (B) The percentage of MHC class $II^{hi}CD86^{hi}$ double-positive cells were calculated based on neg/lo/hi gating. Asterisks indicate that the 100 mM condition is significantly different from the 10 mM condition. **P≤0.001.

To confirm that these results were not unique to $CaCl_2$ crosslinked alginate gels and could extend to alginate gels crosslinked with other calcium crosslinkers, we tested alginate discs cured with 10 or 40 mM $CaSO_4$. Alginate gels cured with 40 mM $CaSO_4$ crosslinker contained more calcium precipitates than 10 mM gels (Figure 2.17A) and increased the Ca^{2+} concentration of the surrounding medium to approximately 3 mM - about 2.5 times more than 10 mM gels (Figure 2.17B). For 40 mM gels the amount of calcium released over a 10 hour period equaled ~61% of the calcium initially incorporated into the gel, and for 10 mM gels the amount was ~34%. DCs in 40 mM gels stained more brightly with Fluo-4, indicating that intracellular calcium concentration positively correlated with extracellular calcium concentration (Figure 2.17C).

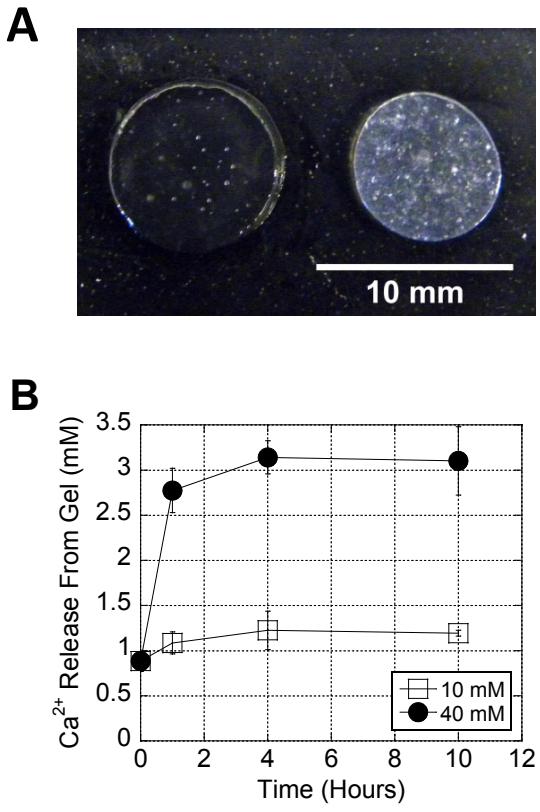

Figure 2.17

C

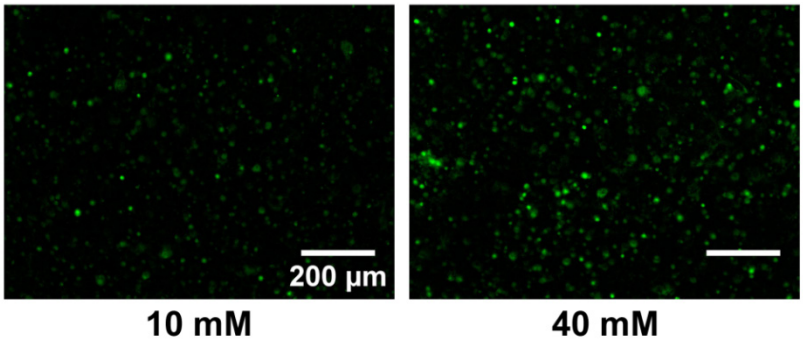

Figure 2.17 (Continued): Increasing $CaSO_4$ crosslinker in alginate discs increased extracellular and intracellular Ca^{2+}. (A) Alginate discs (diameter=8 mm) were crosslinked with 10 (left) or 40 mM (right) $CaSO_4$. (B) Ca^{2+} released into medium from 10 and 40 mM $CaSO_4$ alginate gels was quantified over 10 hours. (C) DCs were labeled with Fluo-4, encapsulated in 10 or 40 mM $CaSO_4$ alginate discs, and imaged with a fluorescent microscope to determine intracellular Ca^{2+} levels.

Like DCs in CaCl2 crosslinked gels, cells immediately after encapsulation appeared viable, but by 24 hours they were noticeably unhealthy, with DCs in 40 mM gels appearing dark and granular (Figure 2.18A). Forward-side scatter analysis of DCs retrieved 24 hours after encapsulation revealed that increasing $CaSO_4$ crosslinker from 10 mM to 40 mM reduced the viability of encapsulated cells from 60% to 55% and that LPS stimulation further reduced cell viability by 2-3 fold (Figure 2.18B).

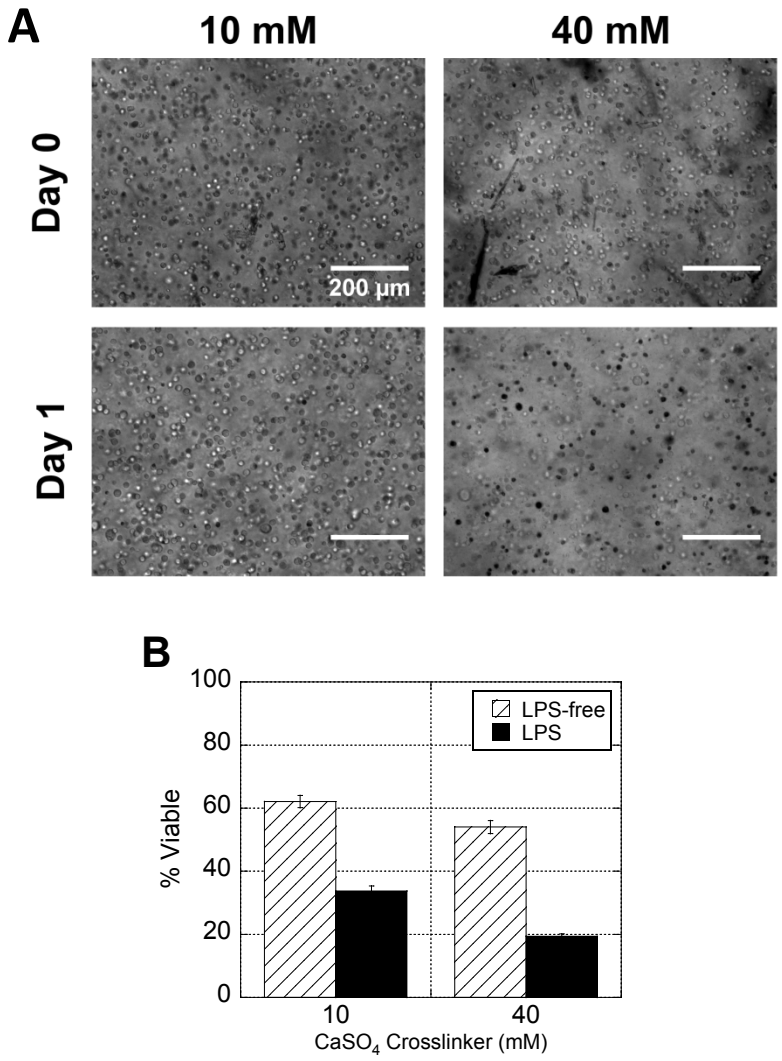

Figure 2.18: Increasing $CaSO_4$ crosslinker decreased cell viability. (A) Photomicrographs were taken of DCs immediately after encapsulation (top) and 24 hours later (bottom). Images shown are the most representative. (B) DCs were extracted from discs and cell viability was quantified based on forward-/side-scatter measurements obtained using flow cytometry.

Consistent with results from $CaCl_2$ crosslinked gels, supernatants collected and analyzed after 24 hours showed that IL-1β secretion increased with increasing $CaSO_4$ crosslinker (Figure 2.19). Additionally, increasing $CaSO_4$ crosslinker from 10 mM to 40 mM noticeably enhanced the percentage of $CD86^{hi}$ cells for both LPS-free and LPS conditions (Figure 2.20A) as well as MHC class $II^{hi}CD86^{hi}$ double-positive cells for the LPS condition (Figure 2.20B).

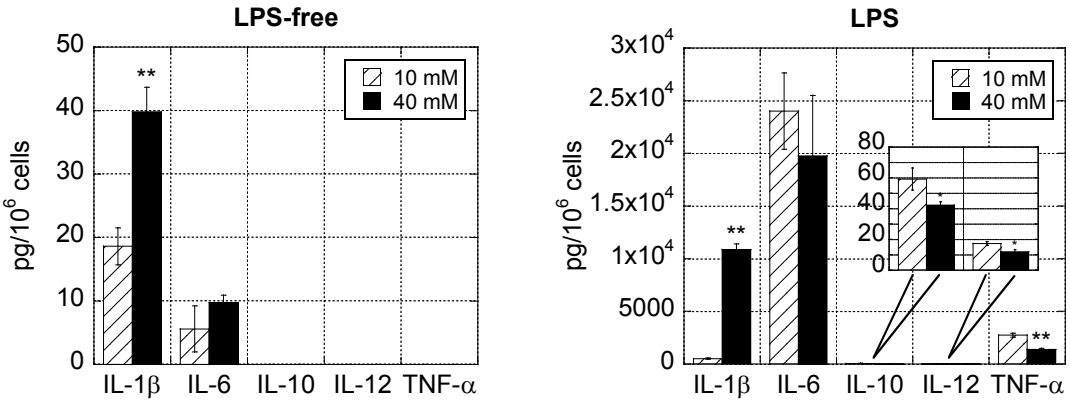

Figure 2.19: Increasing $CaSO_4$ crosslinker increased IL-1β secretion. After 24 hours in culture, supernatants from DCs encapsulated in alginate discs, in the absence of LPS or with LPS stimulation, were collected and multiplexed for cytokines. Asterisks indicate that the 40 mM condition is significantly different from the 10 mM condition. *P≤0.05; **P≤0.001.

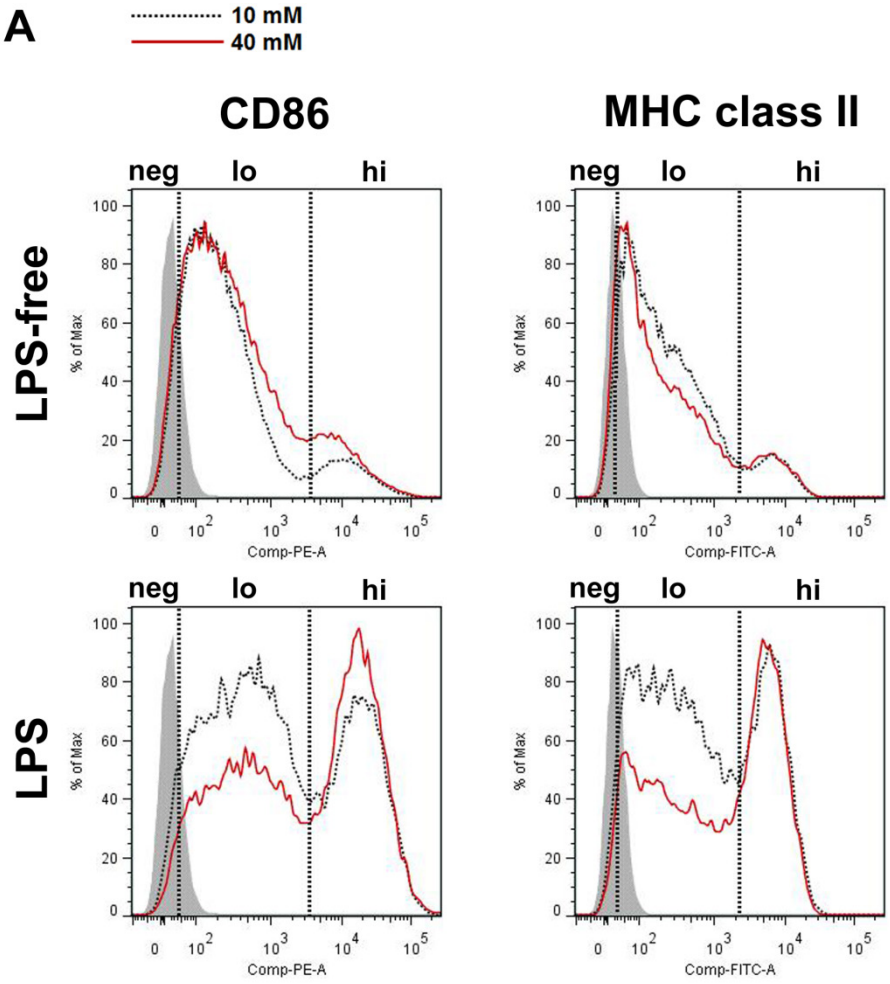

Figure 2.20

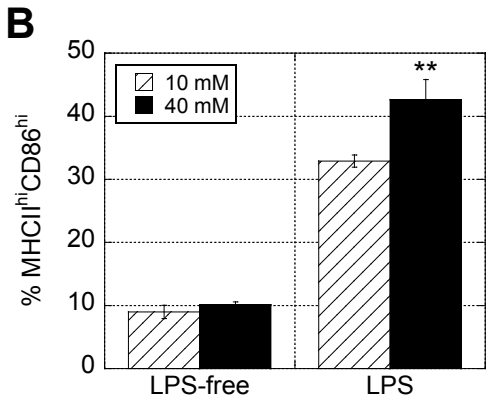

Figure 2.20 (Continued): Increasing $CaSO_4$ crosslinker upregulated DC activation markers. DCs were extracted from discs, stained with PE-labeled anti-CD86 and FITC-labeled anti-MHC class II, and analyzed using flow cytometry. (A) Live cells were gated into negative (neg), low (lo), or high (hi) populations. Filled gray histograms are isotype controls. (B) The percentage of MHC class $II^{hi}CD86^{hi}$ double-positive cells were calculated based on neg/lo/hi gating. Asterisks indicate that the 40 mM condition is significantly different from the 10 mM condition. **P≤0.001.

To establish that DCs cultured externally from gels could also be matured by calcium alginate gels, DCs were plated on TCPS in the absence or presence of alginate gels crosslinked with barium or calcium. DCs cultured in the presence of calcium alginate gels secreted significantly higher concentrations of IL-1β (Figure 2.21A) and expressed higher levels of CD86 and MHC class II (Figure 2.21B) compared to control and barium alginate conditions.

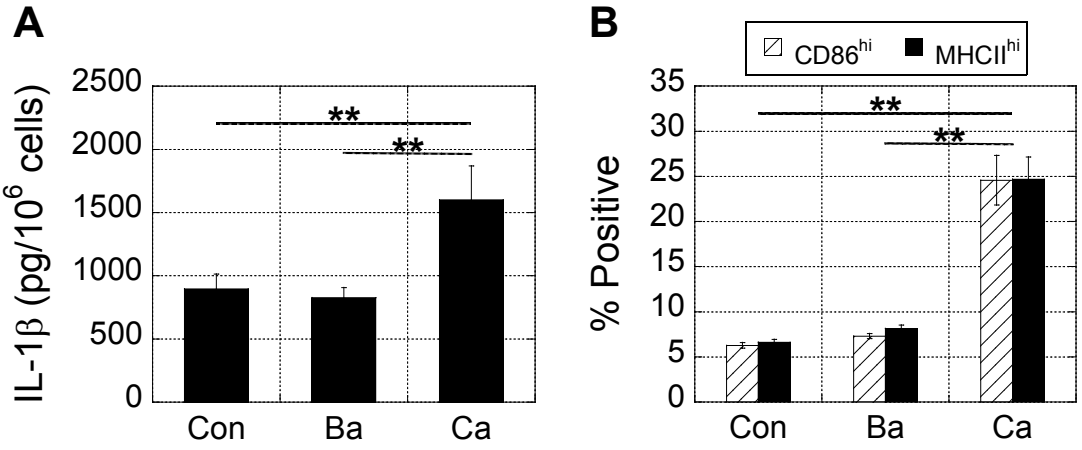

Figure 2.21: Calcium crosslinker enhanced DC activation markers compared to barium crosslinker. (A) After 24 hours in culture, supernatants from DCs plated on TCPS and cultured in the presence of barium or calcium alginate gels were collected and assayed for IL-1β. (B) DCs were scraped from wells and analyzed for CD86 and MHC class II using flow cytometry. **P≤0.001.

2.4 Discussion

The results of this study indicate that the Ca^{2+} used to crosslink alginate gels was released over time and promoted IL-1β, CD86 and MHC class II expression by DCs, whether they were encapsulated within gels or cultured externally from gels *in vitro*. In addition to increasing DC maturation, increasing calcium crosslinker was also associated with increasing intracellular Ca^{2+} and reduced cell viability.

Contrary to published data showing that alginate polysaccharides could stimulate inflammatory cytokine production from monocyte populations, the various soluble alginate polysaccharides used in these experiments did not stimulate DCs. Alginate has been suggested to activate monocytes and macrophages, potentially via the NF-κB pathway [10, 11, 15-17], and several studies have reported the detection of antibodies against alginate *in vivo* [18-20]. Conflicting with this, alginate has been used as an anti-inflammatory to suppress experimental glomerulonephritis and ulcerative colitis [12, 21]. The literature on alginate immunogenicity is abundant yet controversial, and many of these results must be interpreted with caution as alginates used in past studies may have contained impurities such as endotoxins, residual proteins, or polyphenols, all of which affect the immunogenicity of alginate [13, 22-24]. The alginate used in this study was of ultrapure grade, which may explain why no immunostimulatory effects were seen.

Although agarose polymers did not induce or affect DC activation, it was observed that whole agarose gels had a unique effect on DC activation. The gels themselves did not induce cytokine secretion from DCs but greatly enhanced TNF-α production when DCs were pulsed with LPS. It has been shown that heat shock proteins (HSPs) play an important role as molecular chaperones of the LPS-signaling pathway [25, 26], and it is possible that the heated agarose, although cooled near body temperature before use, elicited the production of HSPs by DCs, subsequently enhancing TNF-α secretion when the cells were exposed to LPS. Although further testing would have to be done to confirm this, it is an interesting idea that could be used advantageously to activate white blood cells.

Calcium alginate gels increased the concentration of calcium in the medium up to 5 mM (2.5 times what is physiologically relevant) over a 10 hour period, and Fluo-4 labeling revealed that the elevated level of extracellular calcium, whether it be on TCPS or with alginate gels, resulted in a sustained increase in intracellular Ca^{2+}. The exact mechanism(s) of increased cytosolic Ca^{2+} in this study was not determined, but it was likely due to a series of events leading to contributions from both extracellular Ca^{2+} and intracellular Ca^{2+} stores [27, 28]. Given the intricately intertwined activities of ion channels, pumps, transporters, intracellular buffers, Ca^{2+}-binding proteins and organelles, all of which affect cytosolic Ca^{2+} [28], one would have to use more sophisticated techniques, such as patch clamp techniques, to precisely determine the mechanisms of increased intracellular Ca^{2+} in these experiments.

A critical finding of this study was that increasing calcium matured DCs and enhanced LPS-induced DC activation. As discussed in Chapter 1, dendritic cells are highly dependent on Ca^{2+} to carry out their effector functions, and several intracellular Ca^{2+}-sensing and -signaling molecules have been identified as having necessary roles in DC activation and antigen presentation [29, 30]. It is likely that the increases in intracellular calcium induced by raising extracellular calcium activated these Ca^{2+} signaling molecules leading to the upregulation of activation marker expression and inflammatory cytokine secretion. These results illustrate how one can amplify gene expression by increasing a second messenger (in this case calcium) that is downstream of a signaling event (such as TLR signaling). It is also plausible that the calcium being released from the alginate gels was sensed externally by CaR, initiating various signaling pathways leading to expression of inflammatory markers.

One of the most striking findings was the increase in IL-1β observed with calcium alginate gels. IL-1β is a critical mediator of inflammation, with important roles in neutrophil mobilization, cellular adhesion to the endothelium, and white blood cell infiltration [31, 32]. Cleavage of pro-IL-1β into its functional, secreted form is predominantly mediated by the NRLP3 inflammasome, an important molecular platform expressed by myeloid cells in innate immune defense that can be activated by a

number of danger signals and stress factors [33]. A connection has been made between Ca^{2+}-induced mitochondrial damage and activation of the NLRP3 inflammasome, which likely explains the increase in IL-1β [33-35]. Inflammasome activation has been implicated in the success of adjuvants, such as alum [36, 37], which suggests that calcium alginate induction of IL-1β (and potentially inflammasome activation) may have interesting implications in the field of vaccination.

The calcium levels in this study correlated with reduced cell viability in a dose-dependent manner. This is consistent with past reports showing that elevations in intracellular calcium can directly and indirectly induce cell injury and death [38]. The largest contributor to Ca^{2+} toxicity is believed to be Ca^{2+}-induced mitochondrial permeability transition (MPT), which is the formation of a large pore in the mitochondrial membrane during mitochondrial stress [38]. When cytosolic Ca^{2+} is elevated (>500 nM), mitochondria can be destabilized, initiating MPT, and resulting in the release of pro-apoptotic proteins. Cell death due to Ca^{2+} toxicity may have accounted for decreases in IL-1β seen with TCPS for calcium concentrations above 3 mM. Additionally, LPS-induced TNF-α secretion could have triggered apoptosis via the TNF pathway and accounted for the decreased viability seen with LPS-treated conditions [39].

Increasing calcium crosslinker increases alginate gel stiffness [3], which could potentially affect the behavior of encapsulated DCs as reported for other adherent cells [40]. However, since the alginate used in this study was not modified with integrin ligands, such as Arg-Gly-Asp (RGD) peptide, the DCs were not able to attach to the surrounding matrix, and it is questionable whether the DCs encapsulated within the gels could sense or be strongly affected by gel stiffness. Further studies are needed to confirm this. In contrast, the high stiffness of TCPS could account for the high levels of IL-6 secreted by DCs cultured on TCPS compared to the other materials. DCs on TCPS also appeared more elongated as calcium increased. It is unclear whether this was an indirect consequence of the calcium activating DCs (and subsequently the formation of dendrites), a direct consequence of the calcium affecting integrin binding, or other mechanisms.

In conclusion, the data collected in this study suggests that the calcium used to crosslink alginate gels matures DCs and opens the idea that other biomaterials, aside from alginate, may be useful in controlling calcium signaling to affect DC behavior.

2.5 References

[1] Braccini I, Pérez S. Molecular basis of Ca2+-induced gelation in alginates and pectins: the egg-box model revisited. Biomacromolecules 2001;2:1089-96.

[2] Mørch ÝA, Donati I, Strand BL. Effect of Ca2+, Ba2+, and Sr2+ on alginate microbeads. Biomacromolecules 2006;7:1471-80.

[3] Kuo CK, Ma PX. Ionically crosslinked alginate hydrogels as scaffolds for tissue engineering: Part 1. Structure, gelation rate and mechanical properties. Biomaterials 2001;22:511-21.

[4] LeRoux MA, Guilak F, Setton LA. Compressive and shear properties of alginate gel: effects of sodium ions and alginate concentration. J Biomed Mater Res 1999;47:46-53.

[5] Augst AD, Kong HJ, Mooney DJ. Alginate hydrogels as biomaterials. Macromol Biosci 2006;6:623-33.

[6] Tønnesen HH, Karlsen J. Alginate in drug delivery systems. Drug Dev Ind Pharm 2002;28:621-30.

[7] Lee KY, Mooney DJ. Alginate: properties and biomedical applications. Prog Polym Sci 2012;37:106-26.

[8] Hori Y, Winans AM, Huang CC, Horrigan EM, Irvine DJ. Injectable dendritic cell-carrying alginate gels for immunization and immunotherapy. Biomaterials 2008;29:3671-82.

[9] Hori Y, Stern PJ, Hynes RO, Irvine DJ. Engulfing tumors with synthetic extracellular matrices for cancer immunotherapy. Biomaterials 2009;30:6757-67.

[10] Otterlei M, Sundan A, Skjak-Braek G, Ryan L, Smidsrod O, Espevik T. Similar mechanisms of action of defined polysaccharides and lipopolysaccharides: characterization of binding and tumor necrosis factor alpha induction. Infect Immun 1993;61:1917-25.

[11] Iwamoto M, Kurachi M, Nakashima T, Kim D, Yamaguchi K, Oda T, et al. Structure-activity relationship of alginate oligosaccharides in the induction of cytokine production from RAW264.7 cells. FEBS Lett 2005;579:4423-9.

[12] Razavi A, Khodadadi A, Eslami MB, Eshraghi S, Mirshafiey A. Therapeutic effect of sodium alginate in experimental chronic ulcerative colitis. Iran J Allergy Asthm 2008;7:13-8.

[13] Zimmermann U, Klöck G, Federlin K, Hannig K, Kowalski M, Bretzel RG, et al. Production of mitogen-contamination free alginates with variable ratios of mannuronic acid to guluronic acid by free flow electrophoresis. Electrophoresis 1992;13:269-74.

[14] Lutz MB, Kukutsch N, Ogilvie ALJ, Rößner S, Koch F, Romani N, et al. An advanced culture method for generating large quantities of highly pure dendritic cells from mouse bone marrow. J Immunol Methods 1999;223:77-92.

[15] Yamamoto Y, Kurachi M, Yamaguchi K, Oda T. Induction of multiple cytokine secretion from RAW264.7 cells by alginate oligosaccharides. Biosci Biotech Bioch 2007;71:238-41.

[16] Flo TH, Ryan L, Latz E, Takeuchi O, Monks BG, Lien E, et al. Involvement of toll-like receptor (TLR) 2 and TLR4 in cell activation by mannuronic acid polymers. J Biol Chem 2002;277:35489-95.

[17] Yang D, Jones KS. Effect of alginate on innate immune activation of macrophages. J Biomed Mater Res A 2009;90:411-8.

[18] Johansen HK, Hoiby N, Pedersen SS. Experimental immunization with Pseudomonas aeruginosa alginate induces IgA and IgG antibody responses. APMIS 1991;99:1061-8.

[19] Pressler T, Pedersen SS, Espersen F, Hoiby N, Koch C. IgG subclass antibody responses to alginate from Pseudomonas aeruginosa in patients with cystic fibrosis and chronic P. aeruginosa infection. Pediatr Pulmonol 1992;14:44-51.

[20] Kulseng B, Skjak-Braek G, Ryan L, Andersson A, King A, Faxvaag A, et al. Transplantation of alginate microcapsules: generation of antibodies against alginates and encapsulated porcine islet-like cell clusters. Transplantation 1999;67:978-84.

[21] Mirshafiey A, Borzooy Z, Abhari RS, Razavi A, Tavangar M, Rehm BHA. Treatment of experimental immune complex glomerulonephritis by sodium alginate. Vasc Pharmacol 2005;43:30-5.

[22] Orive G, Tam SK, Pedraz JL, Halle JP. Biocompatibility of alginate-poly-L-lysine microcapsules for cell therapy. Biomaterials 2006;27:3691-700.

[23] Orive G, Carcaboso AM, Hernández RM, Gascón AR, Pedraz JL. Biocompatibility evaluation of different alginates and alginate-based microcapsules. Biomacromolecules 2005;6:927-31.

[24] Dusseault J, Tam SK, Ménard M, Polizu S, Jourdan G, Yahia LH, et al. Evaluation of alginate purification methods: effect on polyphenol, endotoxin, and protein contamination. J Biomed Mater Res A 2006;76A:243-51.

[25] Triantafilou K, Triantafilou M, Ladha S, Mackie A, Fernandez N, Dedrick RL, et al. Fluorescence recovery after photobleaching reveals that LPS rapidly transfers from CD14 to hsp70 and hsp90 on the cell membrane. J Cell Sci 2001;114:2535-45.

[26] Triantafilou M, Triantafilou K. Heat-shock protein 70 and heat-shock protein 90 associate with Toll-like receptor 4 in response to bacterial lipopolysaccharide. Biochem Soc Trans 2004;32:636-9.

[27] Hsu S, O'Connell PJ, Klyachko VA, Badminton MN, Thomson AW, Jackson MB, et al. Fundamental Ca2+ signaling mechanisms in mouse dendritic cells: CRAC is the major Ca2+ entry pathway. J Immunol 2001;166:6126-33.

[28] Lewis RS. The molecular choreography of a store-operated calcium channel. Nature 2007;446:284-7.

[29] Connolly SF, Kusner DJ. The regulation of dendritic cell function by calcium-signaling and its inhibition by microbial pathogens. Immunol Res 2007;39:115-27.

[30] Shumilina E, Huber SM, Lang F. Ca2+ signaling in the regulation of dendritic cell functions. Am J Physiol Cell Physiol 2011;300:C1205-14.

[31] Allantaz F, Chaussabel D, Banchereau J, Pascual V. Microarray-based identification of novel biomarkers in IL-1-mediated diseases. Curr Opin Immunol 2007;19:623-32.

[32] Dinarello CA. Biologic basis for interleukin-1 in disease. Blood 1996;87:2095-147.

[33] Davis BK, Wen HT, Ting JPY. The Inflammasome NLRs in immunity, inflammation, and associated diseases. Annu Rev Immunol 2011;29:707-35.

[34] Murakami T, Ockinger J, Yu J, Byles V, McColl A, Hofer AM, et al. Critical role for calcium mobilization in activation of the NLRP3 inflammasome. Proc Natl Acad Sci U S A 2012;109:11282-7.

[35] Zhou RB, Yazdi AS, Menu P, Tschopp J. A role for mitochondria in NLRP3 inflammasome activation. Nature 2011;469:221-5.

[36] Li HF, Willingham SB, Ting JPY, Re F. Cutting edge: Inflammasome activation by alum and alum's adjuvant effect are mediated by NLRP3. J Immunol 2008;181:17-21.

[37] Eisenbarth SC, Colegio OR, O'Connor W, Sutterwala FS, Flavell RA. Crucial role for the Nalp3 inflammasome in the immunostimulatory properties of aluminium adjuvants. Nature 2008;453:1122-U13.

[38] Dong Z, Saikumar P, Weinberg JM, Venkatachalam MA. Calcium in cell injury and death. Annu Rev Pathol-Mech 2006;1:405-34.

[39] Elmore S. Apoptosis: a review of programmed cell death. Toxicol Pathol 2007;35:495-516.

[40] Discher DE, Janmey P, Wang YL. Tissue cells feel and respond to the stiffness of their substrate. Science 2005;310:1139-43.

Chapter 3
Effect of Calcium Ionophore A23187 on Dendritic Cells *In Vitro*

3.1 Introduction

The ionophore A23187 is a lipid-soluble mobile ion carrier (523.62 g/mol) that is commonly used to raise cytosolic calcium levels (Figure 3.1A) [1]. It binds to divalent cations in a 1:2 ratio with high affinity, in the order Mn^{2+}>>Ca^{2+}>Mg^{2+}>>Sr^{2+}>Ba^{2+} [2], and very weakly to monovalent ions making it capable of inducing Ca^{2+}-dependent signaling pathways without perturbing the balance of Na^{+} and K^{+} [3]. A23187 and other calcium ionophores are thought to increase cytosolic calcium by depleting intracellular stores of Ca^{2+} leading to the influx of extracellular calcium to replenish intracellular stores [4-8]. Studies show that in myeloid cells, A23187-induced elevations in cytosolic calcium are associated with the activation of calcineurin phosphatase and protein kinase C leading to the acquisition of morphologic, phenotypic, and functional traits of mature DCs [9, 10]. Because of its ability to induce mature DC characteristics, A23187 has been tested on monocytes and dendritic cells isolated from peripheral blood as a means to mature them *ex vivo* for dendritic cell-based immunotherapy [11, 12]. Additionally, it has been studied for its ability to differentiate myeloid leukemia cells into antigen presenting cells *ex vivo* for anti-leukemia therapy (for more information, see Appendix 2) [13-16].

A23187 is a potent dendritic cell stimulator, but given the universality of calcium signaling, it is impractical to administer it systemically. We hypothesized that we could demonstrate A23187's release from biomaterials *in vitro*, which could then be used to target A23187 to dendritic cells for potential use in immunotherapy *in vivo*. Our starting approach was modeled after PLG scaffolds described in Chapter 1 that contained GM-CSF to recruit DCs and danger signals and tumor lysates to program an anti-cancer response [17]. First, we verified the immunostimulatory effects of A23187 on bone marrow-derived dendritic cells *in vitro* and compared its effects to monensin, a lipid-soluble sodium ionophore. To gauge DC maturation we analyzed cytokine secretion, activation marker expression, and antigen cross-

presentation. Second, we encapsulated A23187 (a hydrophobic molecule) in both PLG matrices (a hydrophobic material) and calcium alginate gels (a hydrophilic material) to determine if it could be released *in vitro*. Delivery from calcium alginate gels could be appealing given the high concentration of immunostimulatory calcium in the gels and the ability to inject it making it easier to introduce in the body. If successful, an implantable or injectable scaffold containing a chemoattractant and A23187 could be used to recruit local DCs and enhance their activation *in situ*.

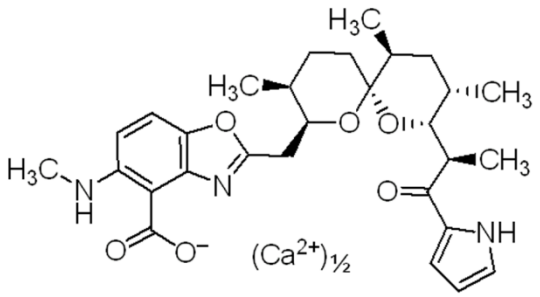

Figure 3.1: Structure of A23187. A23187 (523.62 g/mol) binds to divalent cations, such as Ca^{2+}, with high affinity. Two A23187 molecules bind to every one Ca^{2+} ion.

3.2 Materials and Methods

Cell Culture

Bone marrow-derived DCs were cultured according to methods described in Chapter 2 and used for all experiments.

Cell Viability

DCs were harvested, washed, and resuspended in R10 at a concentration of 555,556 cells/ml, and 1.8 ml (10^6 cells) were plated in 6-well plates. After 1 hour of incubation, 200 μl of control R10 or R10 containing A23187 (Sigma-Aldrich) was added so that the final concentration equaled 400, 800, 1600, or 2000 ng/ml A23187. After 20-24 hours of activation, cells were scraped from wells and cell viability was quantified based on forward-/side-scatter measurements obtained using flow cytometry.

Intracellular Calcium Assay

To measure intracellular calcium, cells were labeled with the fluorescent intracellular calcium probe Fluo-4 AM. DCs were harvested, washed in PBS, and resuspended at a density of 10^6 cells/ml in 5 μM Fluo-4 AM in PBS for 30 minutes at room temperature. Labeled cells were then washed in PBS and allowed to sit for another 30 minutes to allow for complete de-esterification of the probe. Cells were spun and resuspended at a density of 888,889 cells/ml in control R10 or R10 containing 400 ng/ml A23187, and 180 μl (160,000 cells) were plated into 96-well plates. Immediately, fluorescence was measured using a Synergy™ HT microplate reader (Ex. 488 nm, Em. 516) at multiple timepoints after plating. For all intracellular calcium studies, the anti-FITC antibody A889 was diluted in the medium 1:200 to quench background fluorescence.

Cell-Surface Marker Analysis

Cells were harvested, washed, and resuspended in R10 at a density of 666,667 cells/ml, and 1.5 ml (10^6 cells) were plated in 6-well plates. After an hour of adherence, 500 μl of control R10 or R10 containing A23187, CpG (InvivoGen, San Diego, CA), or both, were added to the wells for a final concentration of 400 ng/ml A23187 and/or 1 μM CpG. After 20-24 hours of activation, cells were scraped from wells and stained with APC-conjugated anti-mouse CD11c, FITC-conjugated anti-mouse MHC class II, PE-conjugated anti-mouse CD86, and PE-Cy7-conjuated anti-mouse CCR7 (eBioscience). Cell-surface antigen staining was analyzed using an LSR II or LSR Fortessa™ flow cytometer. Cell viability was determined using SSC vs. FSC, and only viable cells were gated for surface marker analysis. Supernatants were frozen at -20°C for cytokine analysis.

For monensin studies, DCs were resuspended in R10 at a density of 555,556 cells/ml, and 1.8 ml (10^6 cells) were plated in 6-well plates. After one hour of adherence, 200 μl of control R10 or R10 containing A23187 or monensin sodium salt (Sigma-Aldrich) was added so that the final concentration

equaled 400 ng/ml A23187 (0.76 μM) or 526.6 ng/ml monensin (0.76 μM). After 20-24 hours, cells were collected, stained, and analyzed as above. Supernatants were frozen at -20°C for cytokine analysis.

Cytokine Analysis

Cell culture supernatants were analyzed with the Bio-Plex Pro™ Mouse Cytokine 23-plex Assay System or IL-1β and TNF-α Quantikine® Colorimetric Sandwich ELISA kits (R&D Systems, Minneapolis, MN).

Microscopy

Cells were imaged with an EVOS® fl microscope 20-24 hours after plating.

Cross Presentation Studies

To determine if A23187 could enhance cross presentation, DCs were harvested, washed, and resuspended in R10 at a concentration of 555,556 cells/ml. 1.8 ml (10^6 cells) were plated in 6-well plates. After 1 hour of incubation, 200 μl of control R10 or R10 containing A23187, ovalbumin (Sigma-Aldrich), OVA257-264 (SIINFEKL) (21st Century Biochemicals, Marlboro, MA), ovalbumin+A23187, or SIINFEKL+A23187 were added to wells for a final concentration of 400 ng/ml A23187, 10 μM ovalbumin, and/or 10 μM SIINFEKL. After 20 hours, DCs were scraped from wells, stained with PE-conjugated anti-mouse OVA257-264 peptide bound to H2Kb (eBioscience) and analyzed using flow cytometry.

To determine if maturation by A23187 prior to addition of antigen would downregulate cross presentation, DCs were harvested, washed, and resuspended in R10 at a concentration of 555,556 cells/ml. 1.8 ml (10^6 cells) were plated in 6-well plates. After 1 hour of incubation, 200 μl of control R10 or R10 containing A23187, SIINFEKL, or both were added to wells for a final concentration of 400 ng/ml A23187 and/or 10 μM SIINFEKL. After another 2 hours of incubation, 20 μl of 1 mg/ml SIINFEKL in water

was added to control wells or wells treated with A23187 so that the final concentration equaled 10 μM. 20 μl of water was added to the remaining wells. After 22 hours, cells were scraped from wells, stained, and analyzed as above. This procedure was repeated for 7 and 20 hours.

To determine if A23187 treatment could affect cross presentation after the addition of SIINFEKL, similar experiments as above were repeated, except at 2, 7 and 20 hours, 0.8 μl of 1 mg/ml A23187 in DMSO was added to wells treated with SIINFEKL so that the final concentration equaled 400 ng/ml. 0.8 μl of DMSO was added to the remaining wells.

Delivery of A23187 from PLG Scaffolds

85:15 PLG (DLG 7E; Lakeshore Biomaterials, Birmingham, AL) microspheres encapsulating A23187 were fabricated by dissolving A23187 in a PLG/ethyl acetate solution and using an oil-in-water emulsion method as previously described [17, 18]. Lyophilized microspheres were then mixed and compressed with sucrose porogen and leached into macroporous scaffolds; ethanol sterilization was skipped [17, 18]. The amount of A23187 added to the PLG/oil phase during microsphere fabrication was such that the final amount in each 18 mg scaffold (8.5 mm diameter) equaled 180 μg A23187 assuming 100% encapsulation efficiency. To measure release, leached scaffolds were placed in 15 ml polypropylene tubes containing 1 ml PBS and placed on an orbital shaker at 37°C. On days 1, 2, 3, 5, 9, 13, and 25, the PBS was collected and frozen, and 1 ml of fresh PBS was added back to the tube. At the end of the study, scaffolds and PLG microspheres used to make the scaffolds were dissolved in ethyl acetate, and an A23187 standard curve (1, 0.5, 0.1, 0.05, 0.01, 0.005, and 0.001 mg/ml) was made in ethanol. The amount of A23187 in the dissolved microspheres, dissolved scaffolds, sucrose leach, and PBS release solutions were quantified using liquid chromatography-mass spectrometry (LC-MS) (Agilent 1290 Infinity LC/6140 Quadrupole MSD) (Agilent Technologies, Santa Clara, CA). A Zorbax Eclipse Plus C18 Rapid Resolution HD column (1.8 μm, 2.1 mm x 50 mm i.d.) (Agilent Technologies) was used with a

gradient of 5% solvent B (0.1% formic acid in acetonitrile) to 100% solvent B over 10 minutes at a flow rate of 1 ml/min. Solvent A was 0.1% formic acid in water.

Delivery of A23187 from Alginate Gels

DCs were harvested, washed, and resuspended in R10 at a concentration of 10^6 cells/ml, and 1 ml (10^6 cells) was plated in 12-well plates. ThinCert™ cell culture transwells (translucent, 8 μm pore) (Grenier Bio-One) were placed on top of wells. After 1 hour of incubation, barium alginate gels (with or without A23187) or calcium alginate gels (with or without A23187) were added to the inserts so that the total concentration of A23187 in the wells equaled 400 ng/ml. To fabricate gels, a 2.5% Ultrapure MVG alginate solution in PBS containing 5 μg/ml A23187 was made by adding 5 μl of a 1 mg/ml A23187 solution in DMSO to every 1 ml PBS and reconstituting a known mass of lyophilized alginate with the appropriate volume. The alginate solution was mixed with a 20 mM $BaCl_2$ or 244 mM $CaSO_4$ crosslinker solution in water using two syringes connected by a coupler in a 4:1 volume ratio so that the final gel contained 2% alginate and 4 mM barium or 48.8 mM calcium. 200 μl of gel was ejected into the ThinCerts and allowed to cure for 10 minutes, after which 600 μl of R10 was pipetted on top. For control wells, 600 μl of R10 was added directly to wells followed by 200 μl of control R10 or R10 containing A23187 for a final concentration of 400 ng/ml A23187. After 20-24 hours of culture on an orbital shaker, ThinCerts were removed, supernatants were collected and frozen at -20°C, and 1 ml of 50 mM EDTA was added to each well to aid in cell detachment. Cells were incubated at 37°C for 10 minutes and then scraped, washed, and stained with APC-conjugated anti-mouse CD11c, FITC-conjugated anti-mouse MHC class II, and PE-conjugated anti-mouse CD86 for flow cytometry analysis.

Graphs and Statistical Analysis

Flow cytometry data was analyzed and plotted using FlowJo® software, and all other graphs were made using Kaleidagraph® software. Statistical analysis was performed using Microsoft® Excel or Kaleidagraph® software. A two-tailed Student's t-test assuming equal variances was used when comparing two groups, and an ANOVA followed by a post-hoc Tukey test was used when comparing multiple groups. For all experiments n=3-4. Data is reported as the mean ± standard deviation.

3.3 Results

Effect of A23187 on DC Maturation In Vitro

To analyze the effects of A23187, DCs were cultured in control medium or medium containing 400 ng/ml A23187 (0.76 μM; a concentration typically used *in vitro*). Cells exposed to A23187 extended long dendritic cell processes, which is a characteristic of activated DCs (Figure 3.2). Their appearance was similar to cells cultured in medium containing 12 mM calcium, which was shown in Chapter 2. As the concentration of the ionophore increased above 400 ng/ml, a significant decrease in viability was observed (Figure 3.3). Thus, 400 ng/ml A23187 was used for all experiments.

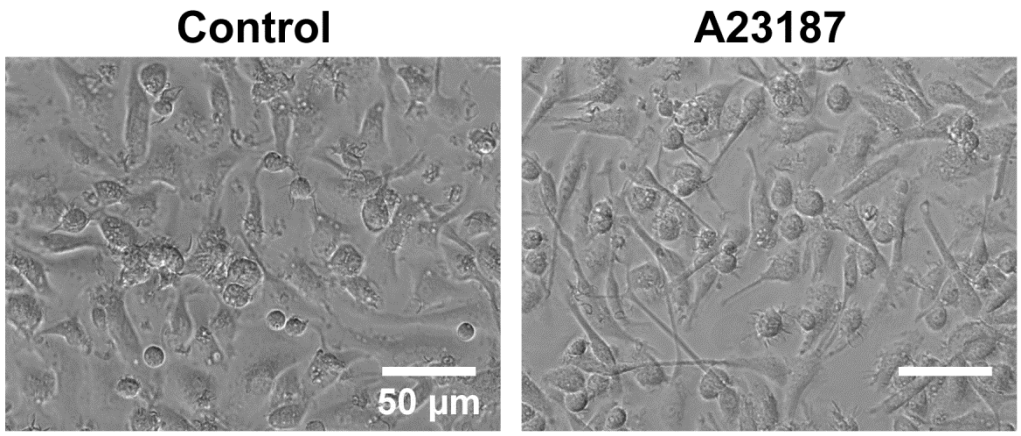

Figure 3.2: A23187 induced an activated DC morphology. Immature DCs were cultured in control medium or medium containing 400 ng/ml A23187. Photomicrographs were taken after 24 hours.

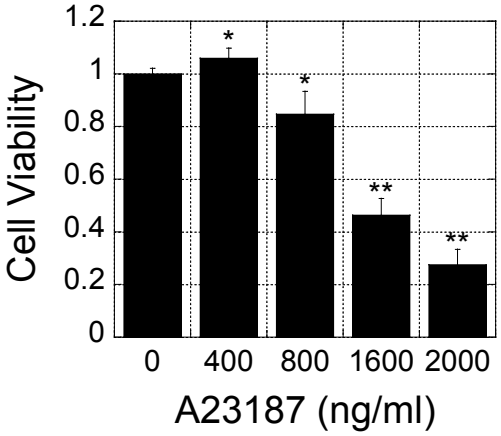

Figure 3.3: 400 ng/ml A23187 did not reduce cell viability. DCs were cultured in increasing concentrations of A23187. After 24 hours, cell viability was determined using FSC/SSC measurements obtained with flow cytometry. Asterisks indicate that the condition is significantly different from the control condition. *P≤0.05; **P≤0.001.

Fluo-4 staining revealed that treatment with A23187 elevated intracellular calcium for the first hour before it returned to baseline (Figure 3.4). This is in contrast to high calcium-containing medium, which caused DCs to maintain high intracellular calcium levels over several hours.

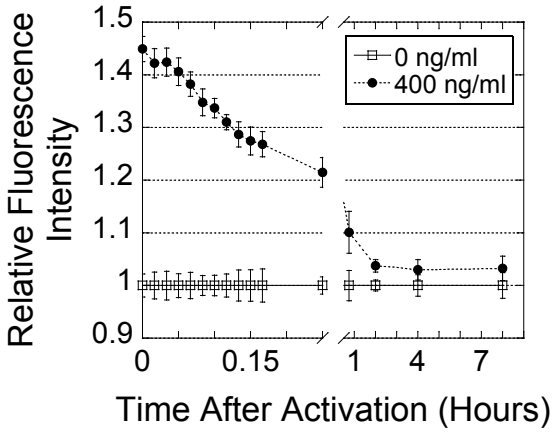

Figure 3.4: A23187 increased intracellular calcium for the first hour. DCs were labeled with Fluo-4 and cultured in control medium or medium containing 400 ng/ml of A23187. Fluorescence was measured at various timepoints using a plate reader.

Supernatants were next multiplexed for 22 pro-inflammatory cytokines and chemokines as well as IL-10, which is often considered a regulatory cytokine. We found that A23187 alone upregulated a

number of inflammatory mediators (Figure 3.5A and B), but even more striking was that A23187 was able to significantly enhance CpG-induced cytokine secretion (Figure 3.5A and C). One interesting observation was that chemokines such as MIP-1β (CCL4), RANTES (CCL5), MIP-1α (CCL3), KC (CXCL1) and MCP-1 (CCL2), which are all chemokines secreted by a number of immune cells, such as monocytes, macrophages, dendritic cells and neutrophils, to enhance granulocyte infiltration, tended to be secreted in higher concentrations with stimulation (Figure 3.5A). In terms of fold upregulation, A23187 alone upregulated IL-4 (a T_H2 cytokine) the most, by ~40 fold (Figure 3.5B). A23187 alone also induced large fold increases in TNF-α, MIP-1α, IL-1α, and IL-6 (Figure 3.5B). Interestingly, when DCs were treated with CpG, not only was overall cytokine secretion significantly higher, but a different profile of inflammatory cytokines was upregulated (Figure 3.5C). With CpG alone, the greatest fold increase was observed with IL-6 (~1500 fold increase) followed by IL-12p40 (~500 fold increase) (Figure 3.5C); when A23187 was present, the effect of CpG activation was more than tripled (Figure 3.5C).

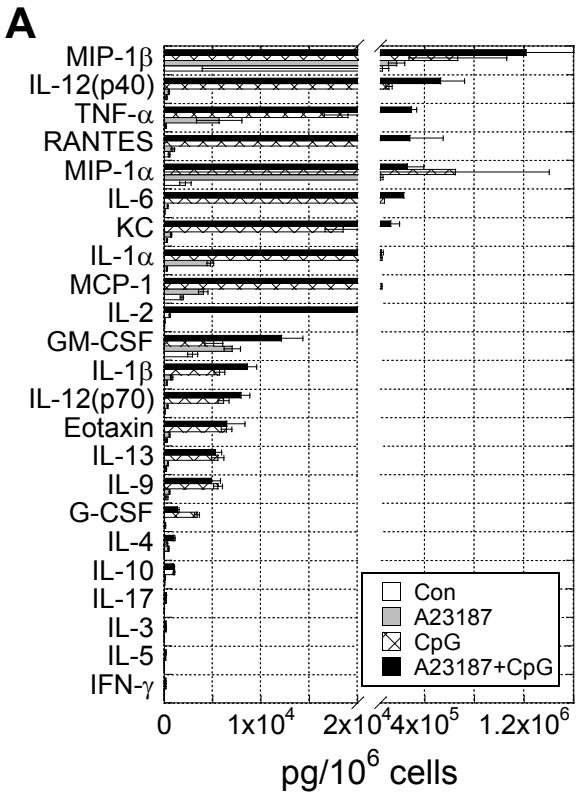

Figure 3.5

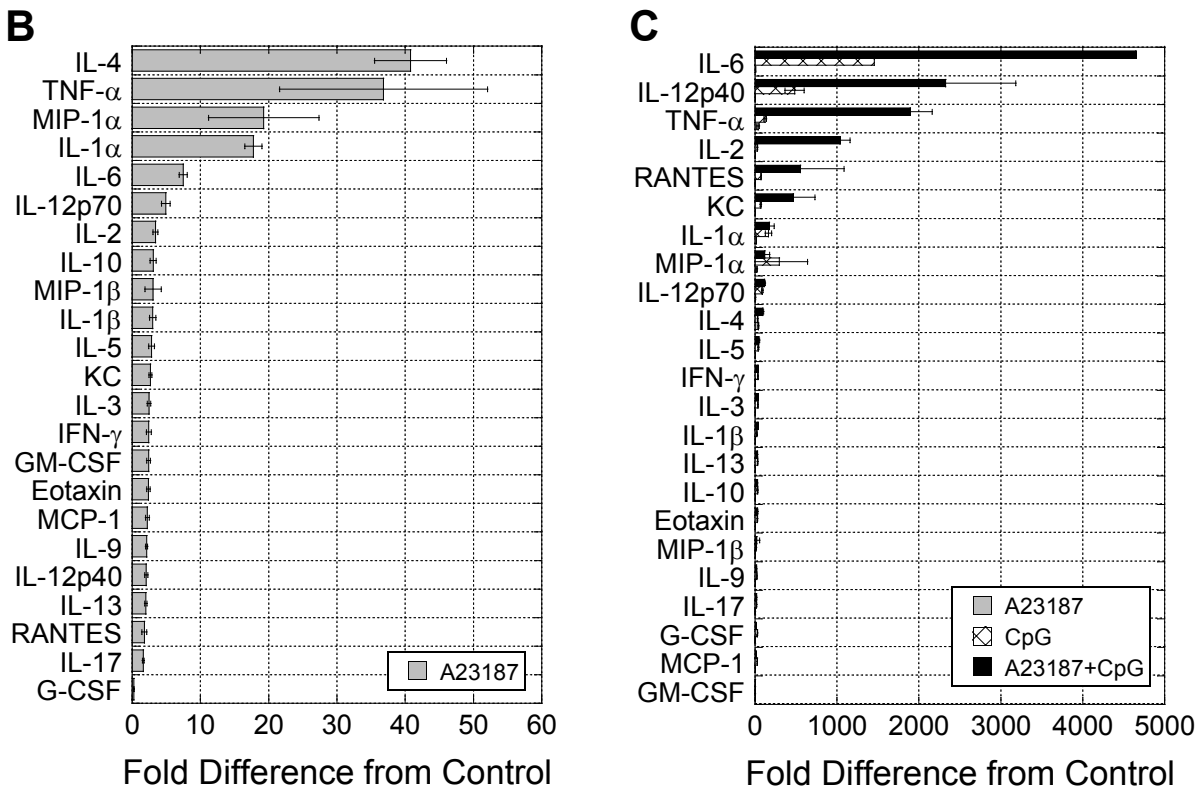

Figure 3.5 (Continued): A23187 promoted inflammatory cytokine secretion. DCs were cultured in control R10 or R10 containing A23187, CpG, or both. After 24 hours, supernatants were collected and multiplexed for cytokines. (A) The absolute amounts of cytokines and chemokines secreted by DCs were determined. (B) The fold increase in cytokine secretion that A23187 induced over control cells was calculated. (C) The fold increases in cytokine secretion induced by CpG and A23187+CpG over control cells were calculated.

The expression of cell surface activation markers followed a similar trend as cytokine secretion. CpG induced greater MHC class II, CD86, and CCR7 expression than A23187 alone, but the combination of CpG and A23187 had the strongest effect (with the exception of MHC class II, which decreased) (Figure 3.6). The presence of A23187 during CpG activation was able to increase CD86 expression from ~57% to ~87% and increase CCR7 expression from ~46% to ~82%.

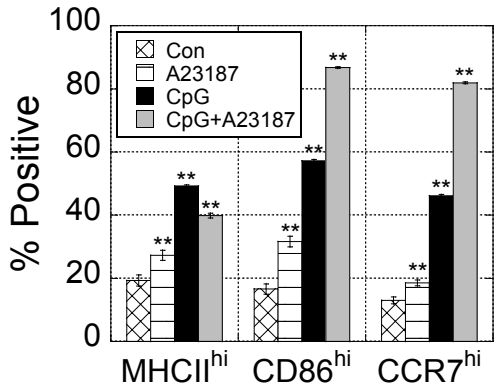

Figure 3.6: A23187 promoted expression of cell surface activation markers. DCs were cultured in control R10 or R10 containing A23187, CpG, or both. After 24 hours, cells were collected and stained with fluorescently-tagged antibodies specific for MHC class II, CD86, and CCR7. Cells were analyzed by flow cytometry and gated into negative, low, and high (hi) populations for quantification. Asterisks indicate that the condition is significantly different from the control condition. **P≤0.001.

To verify that A23187 was upregulating inflammatory markers by specifically enhancing calcium signaling, monensin sodium salt, a lipid-soluble ionophore that binds strongly to Na^+ and is commonly used to block intracellular transport (and thus, having the opposite effect of A23187) [19], was tested as a negative control (Figure 3.7A). As expected, A23187 enhanced IL-1β, TNF-α, MHC class II, and CD86 compared to control cells, whereas monensin downregulated these markers (Figure 3.7B and C). This data indicated that maturation of DCs by A23187 was specifically due to calcium modulation and not because of a non-specific effect of lipid-soluble ionophores.

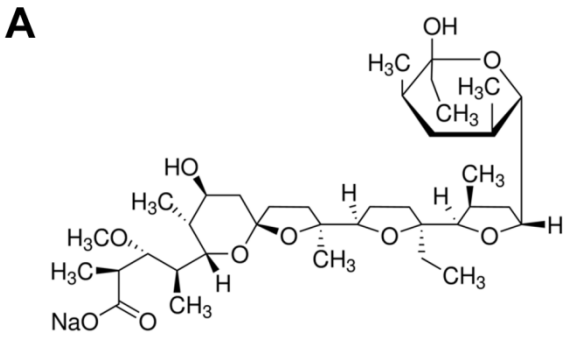

Figure 3.7

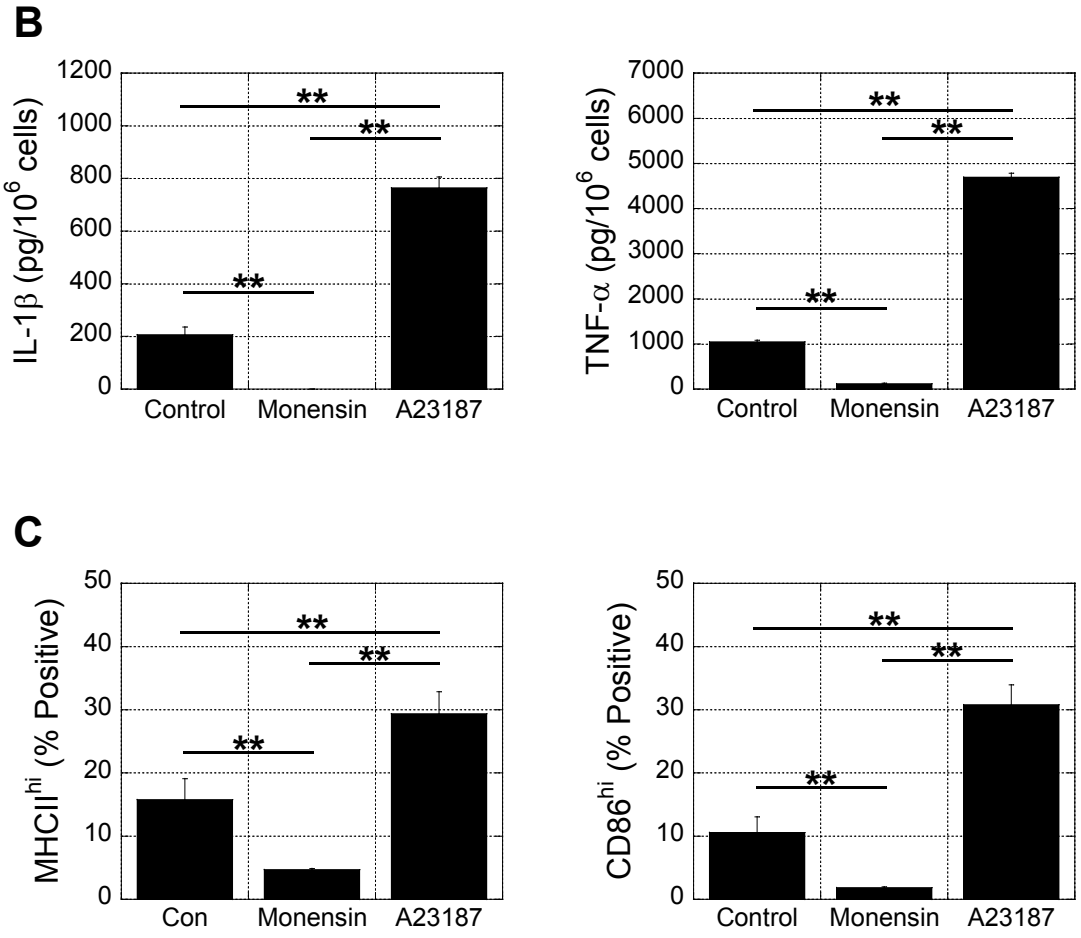

Figure 3.7 (Continued): A23187 had the opposite effect of monensin, a lipid-soluble sodium ionophore. (A) Monensin sodium salt (692.85 g/mol) binds to monovalent cations, such as Na^+, with high affinity. (B) Cells were cultured in control R10 or R10 containing 0.76 μM monensin or 0.76 μM A23187. After 24 hours, supernatants were collected and analyzed for IL-1β and TNF-α by ELISA. (C) Cells were also collected and stained for MHC class II and CD86. Cells were analyzed by flow cytometry and gated into negative, low, and high (hi) populations for quantification. **P≤0.001.

The effect of A23187 on cross-presentation was next examined by culturing DCs with ovalbumin (OVA) or SIINFEKL, a peptide derived from ovalbumin, with or without A23187. The presence of A23187 was able to increase the brightness of MHCI-SIINFEKL staining by more than 2-fold for cells exposed to SIINFEKL and almost 3-fold for cells exposed to ovalbumin (Figure 3.8). Because DCs exposed to SIINFEKL had overall brighter staining than cells exposed to OVA, it was used for subsequent experiments.

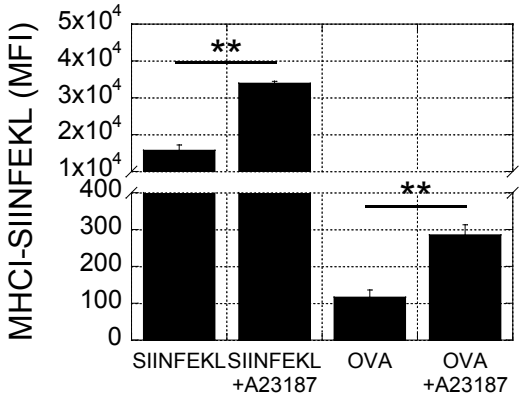

Figure 3.8: A23187 enhanced cross-presentation. DCs were cultured with SIINFEKL or OVA with or without A23187. After 20 hours, cells were collected, stained with anti-SIINFEKL bound to MHC class I, and analyzed by flow cytometry. **P≤0.001.

When co-delivering multiple factors from biomaterials, it is important to determine the optimal sequence of drug delivery. It has been demonstrated that when DCs mature, their ability to uptake, process, and present antigen is downregulated [20]. Thus, it was important to determine if pretreatment of DCs with A23187 inhibited cross presentation, as this would impact the design of a material that could co-deliver A23187 with antigens and other signals. To test this *in vitro*, DCs were pre-treated with A23187 for 2, 7, or 20 hours and then exposed to SIINFEKL for an additional 22 hours. Staining for SIINFEKL bound to MHC class I revealed that pretreatment of DCs with ionophore did not downregulate cross presentation. In fact, for all pretreatment times, A23187 continued to strongly upregulate cross presentation (Figure 3.9A). When DCs were exposed to SIINFEKL for 2, 7, or 20 hours prior to 22 hours of A23187 treatment, A23187 continued to enhance cross presentation (Figure 3.9B). However, for the 20 hour condition, DCs had an overall reduced expression of MHCI-SIINFEKL, which was potentially due to degradation of the peptide.

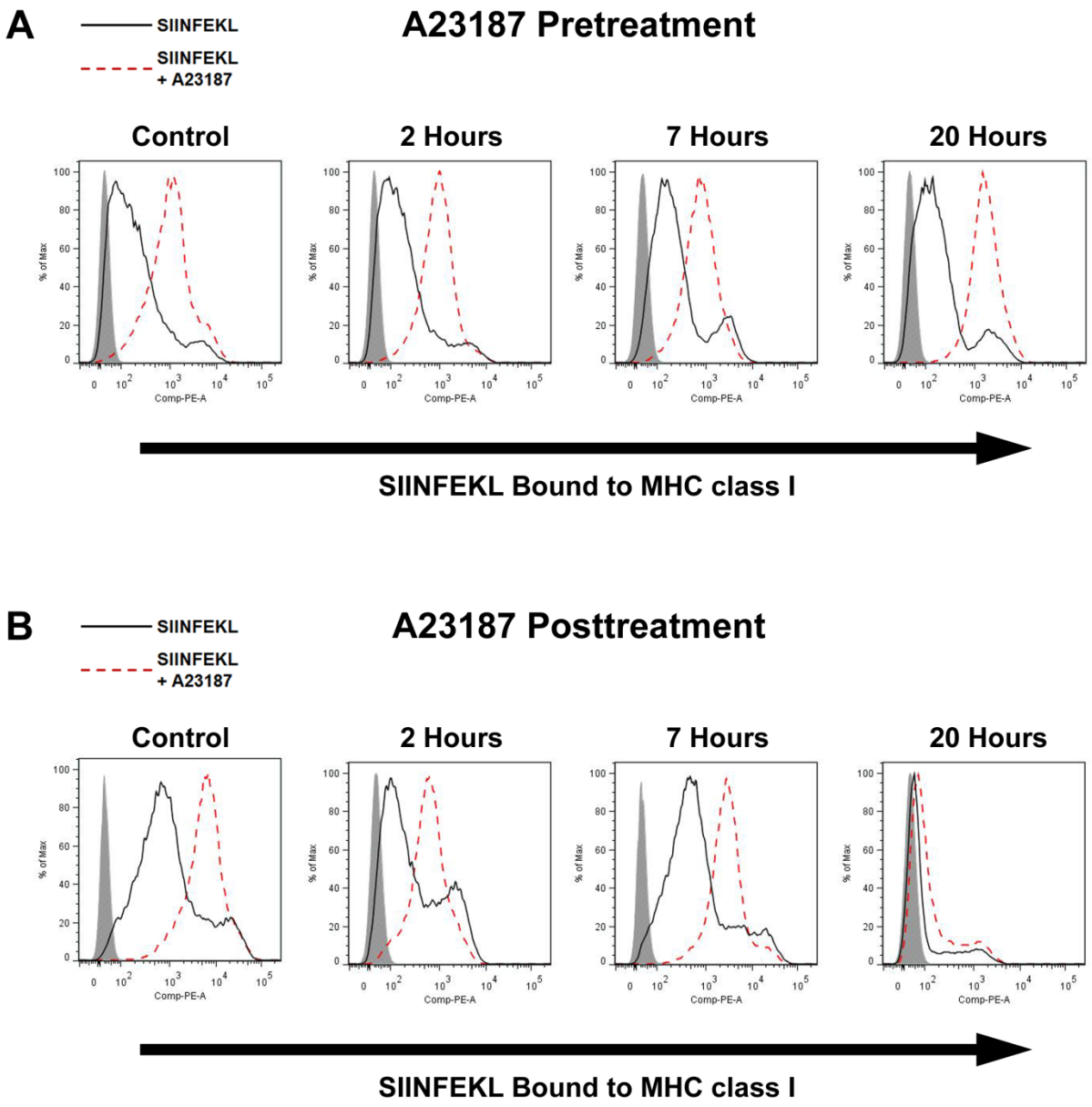

Figure 3.9: A23187 enhanced cross presentation whether it was administered to DCs before or after SIINFEKL addition. (A) DCs were pretreated with A23187 for 2, 7, or 20 hours before SIINFEKL addition. 22 hours after SIINFEKL addition, cells were stained with anti-SIINFEKL bound to MHC class I and analyzed by flow cytometry. (B) DCs were exposed to SIINFEKL 2, 7, or 20 hours prior to A23187 treatment. 22 hours after A23187 treatment, cells were stained and analyzed as above. For control conditions, DCs were treated simultaneously with A23187 and SIINFEKL. Filled gray histograms are isotype controls.

Delivery of A23187 from PLG and Alginate Scaffolds

As a starting point, we tested whether A23187 could be released from PLG scaffolds that were previously developed for immunotherapy [17, 18]. LC-MS was used to quantify the release of A23187 from these scaffolds. Using the protocol described in 2.2 Materials and Methods, A23187 was found to elute at approximately 7.38 minutes and have a mass of 522.2 g/mol (Figure 3.10A and B). The lower limit of detection was ~0.001 mg/ml.

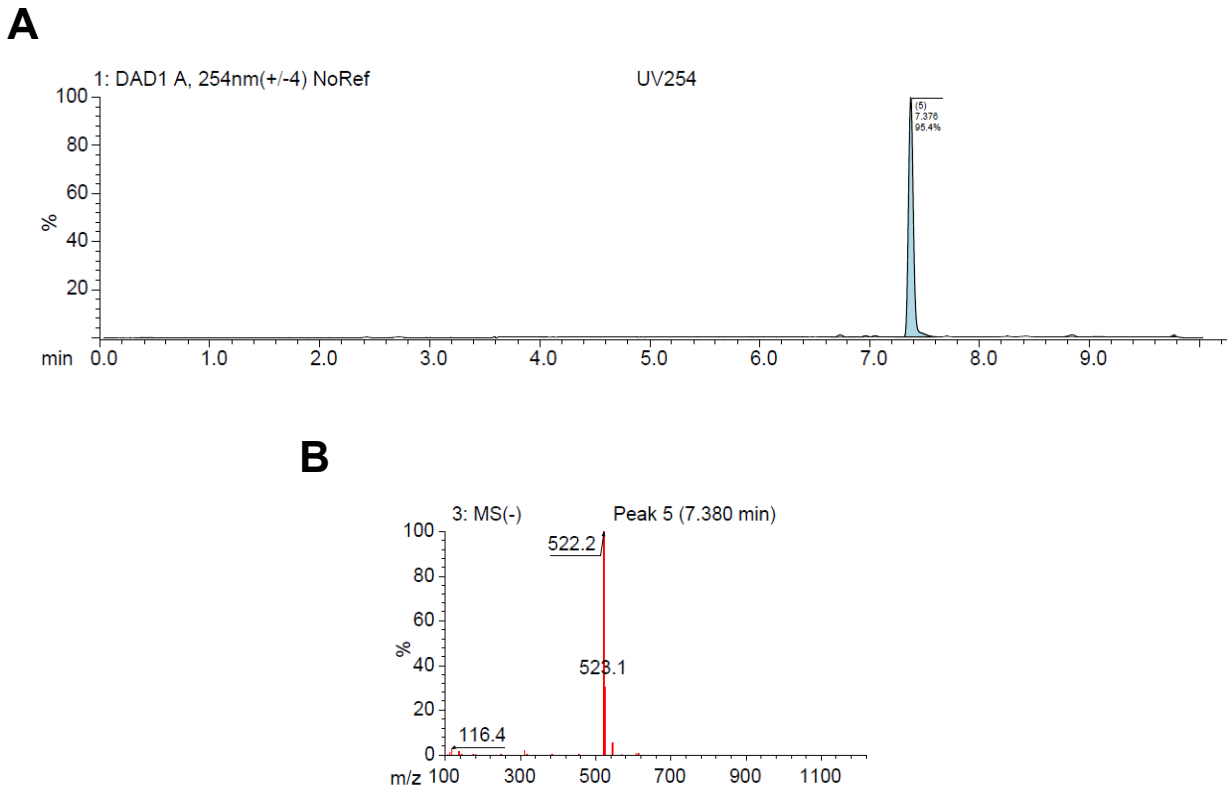

Figure 3.10: A23187 was detected by LC-MS. (A) Chromatogram of 1 mg/ml A23187. A23187 eluted at ~7.38 minutes. (B) Mass spectrum of A23187.

Encapsulation efficiency was determined to be ~65-89%; of the original 180 μg of A23187 used for scaffold fabrication, only 118-160 μg was actually encapsulated within scaffolds. A23187 was not detected in the porogen leach or throughout the release study (Figure 3.11). At the end of the study, the

total amount of A23187 initially incorporated still remained in the scaffolds, demonstrating that although A23187 had a high encapsulation efficiency in PLG scaffolds, it was released poorly into PBS.

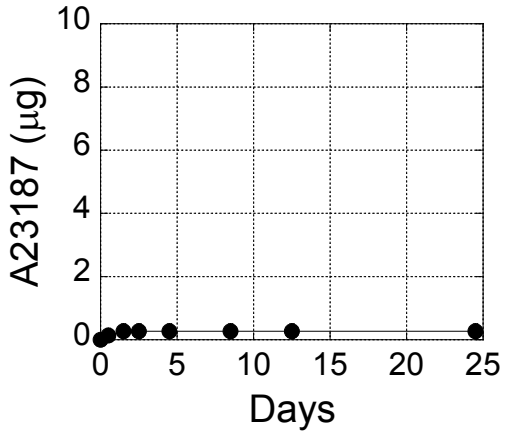

Figure 3.11: A23187 released poorly into PBS from PLG scaffolds. A23187 was encapsulated in PLG scaffolds, which were placed at 37°C on a rocker in 1 ml PBS. PBS was collected and replaced at various timepoints over 24 days. At the end of the study, collected samples were tested for A23187 using LC-MS.

We next tested whether A23187 could be delivered from calcium alginate hydrogels to activate DCs *in vitro*. Because the amount of ionophore encapsulated in gels fell below the LC-MS level of detection, functional assays were used to determine its release. In these studies, the total amount of A23187 added to each well for the ionophore conditions was identical, whether it was added directly to the medium or via alginate hydrogels. Interestingly, in contrast to previous studies, calcium alginate gels alone (Ca) did not stimulate detectable IL-1β, but A23187 delivered from calcium alginate gels (Ca+A23187) in the first 24 hours more than tripled IL-1β secretion compared to A23187 delivered from barium alginate gels (Ba+A23187) and A23187 pipetted directly into the medium (A23187) (Figure 3.12A). Calcium alginate gels alone elevated CD86 expression (~53%) compared to barium alginate gels alone (Ba) (~49%) and the control condition (Con) (~48%), whereas all conditions containing A23187 increased CD86 expression to ~90% or higher (Figure 3.12B). Given that the A23187 released from alginate gels induced a similar or more enhanced degree of DC maturation compared to A23187 added

directly to wells, it is likely that all of the A23187 encapsulated in gels was released over the first 24 hours.

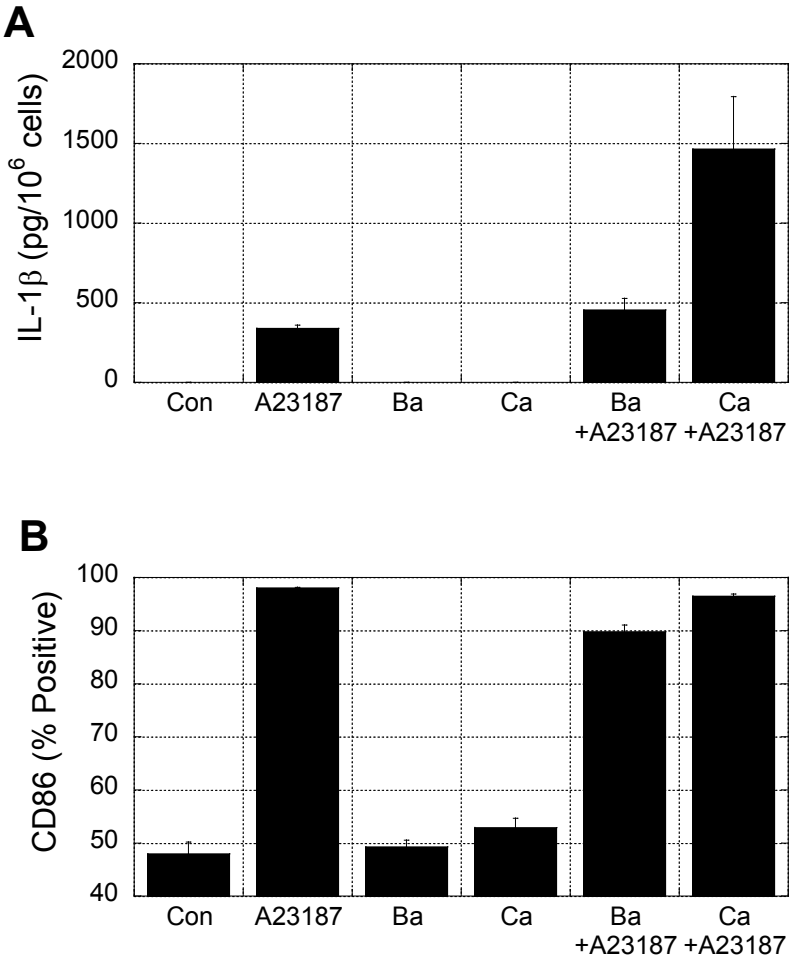

Figure 3.12: A23187 was released from barium and calcium alginate matrices. DCs were cultured in 12-well plates, and barium or calcium alginate gels with or without A23187 were cured in transwells placed above the cells. As a positive control, A23187 was added directly to wells. (A) Cells were cultured for 24 hours on an orbital shaker and supernatants were collected and analyzed for IL-1β. (B) Cells were also collected and stained with anti-CD86 and analyzed by flow cytometry.

3.4 Discussion

The results of this study confirm that A23187, a lipid-soluble calcium ionophore, is a potent activator of DCs, upregulating pro-inflammatory cytokines, cell surface activation markers, and antigen cross-presentation. The ionophore had a high encapsulation efficiency in PLG microspheres, but due to

its high affinity for the polymer, released very poorly into PBS. In contrast, A23187 released readily from barium and calcium alginate matrices.

Maturation of DCs by calcium ionophores is associated with the activation of NF-κB and the CaMKII pathway, which promote Signal 1 (antigen presentation on MHC molecules), Signal 2 (co-stimulatory molecules such as CD86), and Signal 3 (cytokine secretion) [20-22]. In our studies, A23187 promoted DC maturation, which was indicated by DC morphology, cytokine secretion, co-stimulatory molecule expression, and cross-presentation. Additionally, we observed that CCR7, a chemokine receptor that allows DCs to home to lymph nodes and prime T-cell responses, was also upregulated upon A23187 treatment – another sign of DC maturation [23]. These changes were accompanied by increases in cytosolic calcium. Although A23187 alone did not induce DC maturation as strongly as CpG, A23187 dramatically increased CpG-induced cytokine secretion by several orders of magnitude and enhanced CpG-induced CD86 and CCR7 expression. This suggests that calcium ionophores could be extremely useful in boosting the effects of adjuvants for vaccination.

Interestingly, when DCs were treated with ionophore only, a different profile of inflammatory cytokines was upregulated when compared to CpG only. IL-4, a T_H2 cytokine, dominated the response to A23187 alone, possibly suggesting that DC maturation in the absence of TLR signaling can skew DCs towards a T_H2 phenotype. Additionally, A23187 induced a different cytokine profile compared to calcium alginate gels. For instance, IL-6 and TNF-α were more strongly upregulated by A23187, whereas IL-1β was more strongly upregulated by calcium alginate gels. This could potentially be due to differences in inflammasome activation, which demonstrates that although A23187 and calcium crosslinker activate many overlapping signaling pathways, their effects are not completely identical. These results could have an important impact on our understanding of DC biology.

Dendritic cells are highly sensitive to external stimuli and we wanted to verify that the immunostimulatory effects induced by A23187 were not a non-specific effect of lipid-soluble

ionophores. Thus, monensin, a lipid-soluble ionophore that binds to monovalent cations, was also tested for its ability to stimulate dendritic cells. Monensin binds strongly to Na^+ ions and is capable of disrupting the Na^+/H^+ exchange across the Golgi apparatus. This occurs when increases in intracellular Na^+ induced by monensin cause an efflux of H^+ from the Golgi, leading to neutralization of acidic Golgi compartments and a reduction in protein transport to the cell surface [19]. Because of this effect, monensin is a common experimental tool used to block intracellular transport for intracellular cytokine staining. We hypothesized that if the ionophores were acting specifically on DCs and altering ion signaling, A23187 and monensin would have opposite effects. As hypothesized, monensin reduced the expression of inflammatory markers, while A23187 enhanced them compared to control cells. Not only do these results validate that monensin and A23187 are specifically altering intracellular Na^+ and Ca^{2+}, respectively, but they also make it evident that other ions, such as sodium, can be targeted *in vivo* to control other aspects of cell behavior.

Past studies have shown that maturation causes DCs to reduce their antigen uptake and processing capabilities, so it was important to determine if A23187 would have this effect, as this would affect drug delivery design. Surprisingly, we did not observe a reduction in antigen presentation in studies where DCs were pre-treated with A23187 prior to antigen exposure. This could potentially be due to the fact that the DCs in these particular studies were not exposed to traditional danger signals, which may have an important role in dictating phagocytosis and antigen presentation signaling pathways. To test this, the experiments could be repeated but include a positive control such as LPS or CpG.

A23187 had a high encapsulation efficiency (65-89%) in PLG scaffolds and released poorly into PBS. This is not surprising given the hydrophobicity of ionophores. It is possible that if release studies were performed in complete medium containing carrier proteins, A23187 would release more readily from scaffolds. However, these studies were not performed because it would have been difficult to use

LC-MS to detect A23187 in the presence of serum proteins. Future studies could involve *in vitro* functional assays where DCs were seeded directly onto scaffolds or at the bottom of wells with scaffolds placed in transwells above. Experiments in complete medium such as these would better recapitulate the *in vivo* environment than PBS. Another option would be to implant scaffolds directly *in vivo*, remove them periodically, and analyze them for remaining A23187 using more sophisticated analyses. If A23187 release kinetics were still poor, the properties of the PLG could be tuned to accelerate the release of ionophore from the scaffolds.

Given the high concentration of calcium in calcium alginate gels, the strong interactions between calcium and A23187, and the hydrophilic nature of the material, we were interested in seeing if A23187 could be encapsulated and released from calcium alginate matrices. Delivery from calcium alginate matrices is attractive, not only because it provides an immunostimulatory calcium source, but because it can be injected minimally-invasively making it easier to administer. Here, we did not have to worry about the ionophore significantly chelating the calcium crosslinker, since the concentration of A23187 incorporated in gels (7.6 μM) was approximately 4 orders of magnitude lower than the calcium crosslinker concentration (48.8 mM). However, we considered that the high concentration of calcium in the gel could sequester the ionophore and prevent it from leaving the gel; our results indicated that this was not the case. The A23187 released from barium gels induced a similar magnitude of IL-1β secretion as cells exposed to A23187 added directly to the medium, suggesting that all of the A23187 was released from gels within the first day. Moreover, A23187 released from calcium-crosslinked gels induced significantly more IL-1β secretion compared to all other conditions, demonstrating that A23187 and calcium released from the gels had an additive impact. These results demonstrated that in contrast to PLG scaffolds, A23187 was released quickly from calcium alginate gels and had a strong effect on DC activation *in vitro*.

Unlike earlier studies (see Chapter 2), IL-1β could not be detected from DCs exposed to calcium alginate gels only. This is possibly due to gels being in a separate compartment during culture leading to altered calcium diffusion and a weaker impact on DC maturation. In earlier studies, cells were also cultured on a larger surface area and alginate gels were in direct contact with cells, which could account for the differences in IL-1β and CD86 seen between the different experiments. Lastly, control cells in past experiments secreted detectable levels of IL-1β, whereas control DCs in this experiment did not, suggesting that cells used in these experiments inherently produced less IL-1β.

This chapter illustrates both the potent effect of ionophores on dendritic cell behavior and A23187's ability to be incorporated into both hydrophobic (PLG) and hydrophilic (alginate) materials. More work will have to be done to better characterize ionophore release from these materials and to optimize them, or other potential materials, for ionophore delivery *in vivo*. For example, delivering too much ionophore could lead to destabilization of cell membranes of target cells and toxicity. In contrast, if cleared too quickly after released, the ionophore may have minimal, transient, or off-target effects. If calcium ionophores can be successfully delivered from biomaterials to have a strong, but safe impact on cells and tissues, this could be a powerful tool to manipulate cell behavior *in vivo*.

3.5 References

[1] Reed PW, Lardy HA. A23187 - divalent cation ionophore. J Biol Chem 1972;247:6970-&.

[2] Pfeiffer DR, Reed PW, Lardy HA. Ultraviolet and fluorescent spectral properties of divalent-cation ionophore A23187 and its metal-ion complexes. Biochemistry (Mosc) 1974;13:4007-14.

[3] Pressman BC. Biological applications of ionophores. Annu Rev Biochem 1976;45:501-30.

[4] Luckasen JR, White JG, Kersey JH. Mitogenic properties of a calcium ionophore, A23187. Proc Natl Acad Sci U S A 1974;71:5088-90.

[5] Drummond IA, Lee AS, Resendez E, Jr., Steinhardt RA. Depletion of intracellular calcium stores by calcium ionophore A23187 induces the genes for glucose-regulated proteins in hamster fibroblasts. J Biol Chem 1987;262:12801-5.

[6] Dolmetsch RE, Lewis RS. Signaling between intracellular Ca2+ stores and depletion-activated Ca2+ channels generates [Ca2+](I) oscillations in T-lymphocytes. J Gen Physiol 1994;103:365-88.

[7] Bird GS, DeHaven WI, Smyth JT, Putney JW, Jr. Methods for studying store-operated calcium entry. Methods 2008;46:204-12.

[8] Morgan AJ, Jacob R. Ionomycin enhances Ca2+ influx by stimulating store-regulated cation entry and not by a direct action at the plasma-membrane. Biochem J 1994;300:665-72.

[9] Engels FH, Kreisel D, Faries MB, Bedrosian I, Koski GK, Cohen PA, et al. Calcium ionophore activation of chronic myelogenous leukemia progenitor cells into dendritic cells is mediated by calcineurin phosphatase. Leuk Res 2000;24:795-804.

[10] Li Q, Ozer H, Lindner I, Lee KP, Kharfan-Dabaja MA. Protein kinase C blockade inhibits differentiation of myeloid blasts into dendritic cells by calcium ionophore A23187. Int J Hematol 2005;81:131-7.

[11] Czerniecki BJ, Carter C, Rivoltini L, Koski GK, Kim HI, Weng DE, et al. Calcium ionophore-treated peripheral blood monocytes and dendritic cells rapidly display characteristics of activated dendritic cells. J Immunol 1997;159:3823-37.

[12] Koski GK, Schwartz GN, Weng DE, Czerniecki BJ, Carter C, Gress RE, et al. Calcium mobilization in human myeloid cells results in acquisition of individual dendritic cell-like characteristics through discrete signaling pathways. J Immunol 1999;163:82-92.

[13] Lindner I, Kharfan-Dabaja MA, Ayala E, Kolonias D, Carlson LM, Beazer-Barclay Y, et al. Induced dendritic cell differentiation of chronic myeloid leukemia blasts is associated with down-regulation of BCR-ABL. J Immunol 2003;171:1780-91.

[14] Kharfan-Dabaja MA, Ayala E, Lindner I, Cejas PJ, Bahlis NJ, Kolonias D, et al. Differentiation of acute and chronic myeloid leukemic blasts into the dendritic cell lineage: analysis of various differentiation-inducing signals. Cancer Immunol Immunother 2005;54:25-36.

[15] Houtenbos I, Westers TM, Ossenkoppele GJ, van de Loosdrecht AA. Feasibility of clinical dendritic cell vaccination in acute myeloid leukemia. Immunobiology 2006;211:677-85.

[16] Houtenbos I, Westers TM, Ossenkoppele GJ, van de Loosdrecht AA. Leukemia-derived dendritic cells: towards clinical vaccination protocols in acute myeloid leukemia. Haematol-Hematol J 2006;91:348-55.

[17] Ali OA, Huebsch N, Cao L, Dranoff G, Mooney DJ. Infection-mimicking materials to program dendritic cells in situ. Nat Mater 2009;8:151-8.

[18] Ali OA, Emerich D, Dranoff G, Mooney DJ. In situ regulation of DC subsets and T cells mediates tumor regression in mice. Sci Transl Med 2009;1:1-10.

[19] Mollenhauer HH, James Morré D, Rowe LD. Alteration of intracellular traffic by monensin; mechanism, specificity and relationship to toxicity. Biochim Biophys Acta-Rev Biomembranes 1990;1031:225-46.

[20] Guermonprez P, Valladeau J, Zitvogel L, Thery C, Amigorena S. Antigen presentation and T cell stimulation by dendritic cells. Annu Rev Immunol 2002;20:621-67.

[21] Shumilina E, Huber SM, Lang F. Ca2+ signaling in the regulation of dendritic cell functions. Am J Physiol Cell Physiol 2011;300:C1205-14.

[22] Connolly SF, Kusner DJ. The regulation of dendritic cell function by calcium-signaling and its inhibition by microbial pathogens. Immunol Res 2007;39:115-27.

[23] Randolph GJ, Angeli V, Swartz MA. Dendritic-cell trafficking to lymph nodes through lymphatic vessels. Nat Rev Immunol 2005;5:617-28.

Chapter 4
Enhancing Calcium Signaling *In Vivo* to Boost Local Inflammation

4.1 Introduction

Prior to the development of biomaterials for controlled drug delivery, the idea of harnessing calcium signaling *in vivo* to induce a potent and long-lasting immune response seemed impossible due to the universal role that calcium plays in the body and the detrimental side effects it could have on other cells and tissues. However, with the existence of biomaterials to target drugs to specific cells and locations in the body and their ability to sustain drug release, the idea of delivering calcium or calcium ionophores to white blood cells *in vivo* to enhance the immune response is now conceivable.

The effects of calcium release and A23187 *in vivo* have not been well-studied, and given the body's ability to buffer calcium and metabolize drugs, it is difficult to predict whether calcium or A23187 could have a potent effect on white blood cells in the body. Because the use of A23187 *in vivo* is rare, the pharmacokinetics and pharmacodynamics of the molecule are largely unknown. However, A23187 has been injected subcutaneously *in vivo* as a means to locally recruit lymphocytes [1, 2], which indicates that it can have a measurable inflammatory effect on surrounding tissue.

Contrary to A23187, calcium alginate gels encapsulating growth factors, cells, and/or cytokines have been used *in vivo* for a wide variety of applications such as type I diabetes treatment [3], angiogenesis [4] and cancer immunotherapy [5, 6]. Nevertheless, none of these studies specifically examined the potential contribution of calcium to the final outcome. Interestingly, in a study where calcium-crosslinked alginate gels were used to deliver pro-angiogenic factors to enhance blood vessel formation [4], and in another study where they were used to deliver activated DCs peritumorally to reduce tumor growth [6], alginate gels alone appeared to have a slight therapeutic effect, but further work would have to be done to determine the cause. Although minimal, the evidence suggests that the calcium crosslinker released from alginate gels can have a local stimulatory effect.

Consequently, because calcium and A23187 released from alginate gels had such potent effects on DCs *in vitro* and because of evidence that calcium alginate and A23187 could have observable effects *in vivo*, we were interested in determining whether barium and calcium alginate gels, with or without A23187, injected subcutaneously into C576BL/6J mice could stimulate white blood cells. We hypothesized that the calcium used to crosslink alginate gels and/or delivery of A23187 could increase local inflammation *in vivo*. To test this, we examined the effects of the injection site, days of implantation, calcium crosslinker concentration, gel volume, and LPS delivery on inflammatory cytokine secretion from surrounding tissue.

4.2 Materials and Methods

Subcutaneous Alginate Injections

Female C57BL/6J mice, ages 4-12 weeks, were anesthetized with isoflurane, and their backs were shaved and wiped with ethanol. A 2.5% MVG alginate solution in PBS was mixed with a sterile 20 mM $BaCl_2$ or 244 mM $CaSO_4$ solution in water using two 1 ml syringes connected by a coupler. The volumes were mixed in a 4:1 ratio so that the final gel contained 2% alginate and 4 mM $BaCl_2$ or 48.8 mM $CaSO_4$. For studies examining the effect of A23187, alginate gels encapsulating ionophore were fabricated according to methods described in Chapter 3 to yield 50 μl gels containing 0.4, 0.5, 0.6 or 0.8 μg of ionophore; for studies examining the effect of calcium crosslinker concentration, 375 and 500 mM $CaSO_4$ slurries were used to fabricate gels containing 75 and 100 mM calcium, respectively; and for alginate gels delivering LPS, MVG alginate was dissolved with PBS containing LPS so that final crosslinked gels contained 1 μg of LPS/50 μl gel. All gels were prepared aseptically. After mixing the dissolved alginate with the crosslinker, 50 or 100 μl of gel was injected subcutaneously with a 23 gauge needle in the left or right sides (lateral injection) or in the center of the back (medial injection) as indicated. Mice were allowed to recover and consume food and water *ad libitum*. At the timepoints specified, mice were

sacrificed and gels were removed with scissors and tweezers. Samples were frozen at -20°C until analysis.

Cytokine Analysis

Gels were digested with 100 μl of 10 unit/ml alginate lyase (Sigma) in a 37°C dry bath with occasional vortexing until fully dissolved. Digested alginate was analyzed with the Bio-Plex Pro™ Mouse Cytokine 23-plex Assay System or IL-1β and TNF-α Quantikine® Colorimetric Sandwich ELISA kits.

Calcium Release Assay

Gels were digested as described above, diluted 1:4 in PBS, and assayed using the QuantiChrom™ Calcium Assay Kit.

Graphs and Statistical Analysis

Graphs were made using Kaleidagraph® software. Statistical analysis was performed using Microsoft® Excel or Kaleidagraph® software. A two-tailed Student's t-test assuming equal variances was used when comparing two groups, and an ANOVA followed by a post-hoc Tukey test was used when comparing multiple groups. For all experiments n=3-4 unless otherwise noted. Data is reported as the mean ± standard deviation.

4.3 Results

To determine if the calcium in calcium alginate gels had an inflammatory effect *in vivo*, 50 μl barium (4 mM) and calcium (48.8 mM) alginate gels were injected subcutaneously into the lateral sides of mice. After 2 and 4 days, gels were removed and analyzed for IL-1β. For both timepoints, IL-1β was

undetectable for barium gels but detectable for calcium alginate gels, and there were no noticeable differences between days 2 and 4 (Figure 4.1).

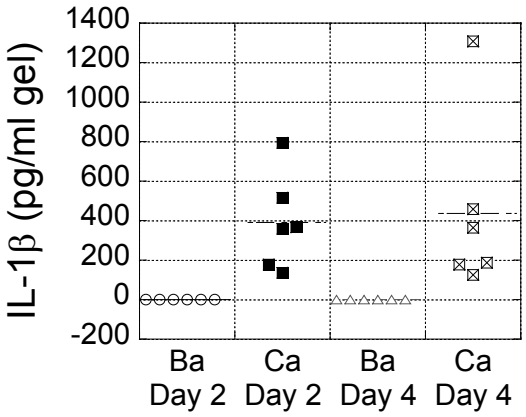

Figure 4.1: Calcium alginate gels enhanced IL-1β secretion *in vivo*. 50 μl barium or calcium alginate gels were injected subcutaneously into the lateral sides of mice. At days 2 and 4, gels were removed and analyzed for IL-1β.

In Chapter 3 it was demonstrated that A23187 encapsulated in alginate gels could be released to mature DCs *in vitro*. Furthermore, it was demonstrated that A23187 could enhance IL-1β secretion induced by calcium alginate. To determine whether this could be repeated *in vivo*, 50 μl calcium alginate gels encapsulating 0.4, 0.5, 0.6, or 0.8 μg of A23187 (which fall within the range of what has been previously used to recruit lymphocytes) were injected into the lateral sides of mice and after 2 days were removed and analyzed for IL-1β and TNF-α. Unlike its effects *in vitro*, A23187 delivered from calcium alginate matrices *in vivo* did not induce more inflammatory cytokine secretion compared to gels without A23187 (Figure 4.2). Because A23187 began to precipitate when it exceeded 0.8 μg/50 μl gel, we chose not to test concentrations greater than this.

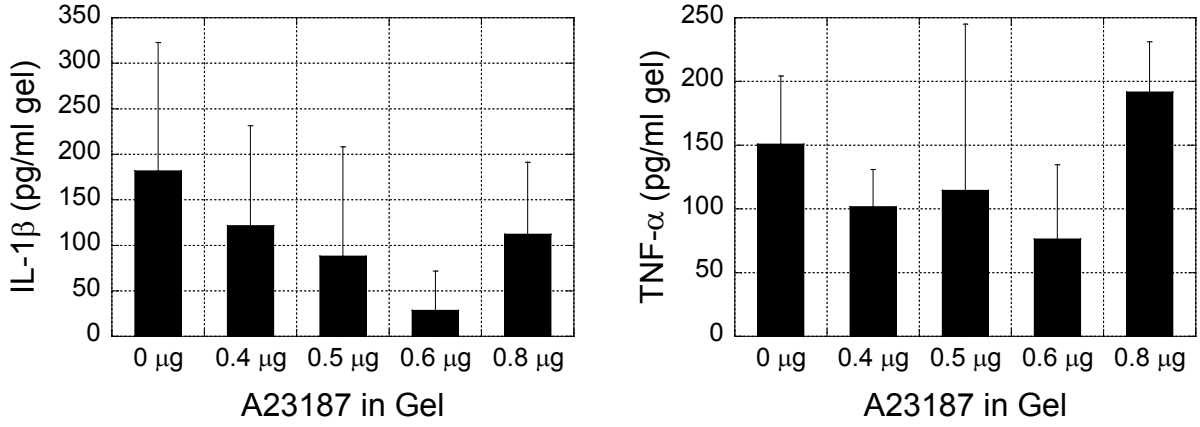

Figure 4.2: A23187 delivered from calcium alginate gels injected laterally did not enhance inflammatory cytokine secretion. 50 μl calcium alginate gels with or without A23187 were injected laterally into mice. At day 2, gels were removed and analyzed for IL-1β and TNF-α.

To determine if the injection site influenced the inflammatory response to alginate gels, 50 μl barium (4 mM) and calcium (48.8 mM) alginate gels were injected both laterally and medially into mice. At day 2, gels were removed and analyzed for IL-1β. It was observed that calcium alginate gels injected in the center of the back along the spine induced approximately 5 times more IL-1β secretion compared to calcium alginate gels injected laterally (Figure 4.3). There was also a slight increase in IL-1β secretion when barium alginate gels were injected medially versus laterally, but the results were not significant.

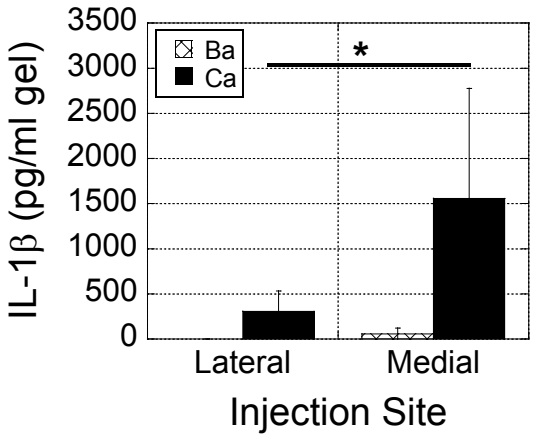

Figure 4.3: Alginate gels injected medially into mice induced more IL-1β secretion than gels injected laterally. 50 μl barium and calcium alginate gels were injected laterally or medially in mice. At day 2, alginate gels were removed and analyzed for IL-1β. n=4-12. *P≤0.05.

Because alginate gels were injected into the body, which is an open system where calcium can diffuse freely in and out, we were highly interested in analyzing calcium concentrations within the gels over time. When analyzing gels injected medially, more than 50% of the calcium originally incorporated within calcium alginate gels was released within the first 12 hours (Figure 4.4); the Ca^{2+} concentration within the gels was maintained at a steady-state thereafter. Interestingly, the calcium concentration in barium alginate gels increased over time and also reached steady state by approximately 12 hours. It appeared that while calcium alginate gels acted as a calcium source, barium alginate gels acted as a calcium sink.

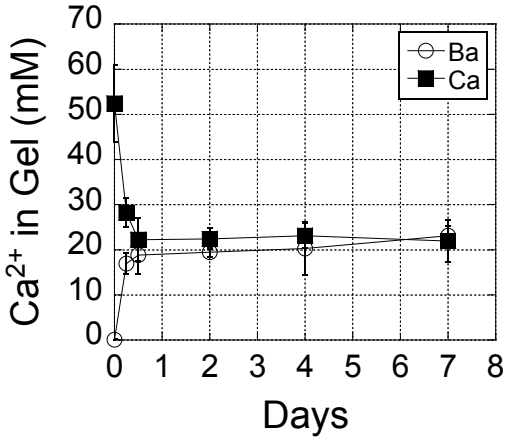

Figure 4.4: Ca^{2+} concentration in gels reached steady state by 12 hours after medial injection. 50 μl barium (4 mM) and calcium (48.8 mM) alginate gels were injected medially into mice. At various timepoints, alginate gels were removed and analyzed for Ca^{2+}.

In Chapter 2 it was demonstrated that increasing calcium crosslinker led to greater calcium release and enhanced inflammatory cytokine secretion by DCs *in vitro*. To determine if increasing calcium crosslinker could enhance cytokine secretion *in vivo*, 50 μl gels crosslinked with 4 mM barium or 48.8, 75, or 100 mM calcium were injected medially into mice. On days 1 and 2, gels were harvested and analyzed for IL-1β. Contrary to *in vitro* results, increasing calcium crosslinker did not enhance IL-1β secretion *in vivo* (Figure 4.5). It was also observed that cytokine secretion decreased after day 1.

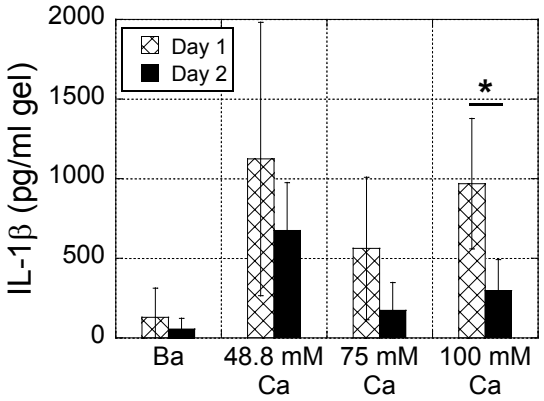

Figure 4.5: Increasing calcium crosslinker concentration did not enhance IL-1β secretion *in vivo*. 50 μl barium alginate gels or calcium alginate gels crosslinked with increasing concentrations of calcium were injected medially into mice. At days 1 and 2, gels were removed and analyzed for IL-1β. *P≤0.05.

Since alginate gels injected medially were able to induce significantly greater IL-1β secretion, we next tested whether calcium alginate gels containing A23187 could enhance inflammatory cytokine secretion if injected in the center of the back rather than the side flank. Fifty or 100 μl alginate gels crosslinked with 48.8 mM $CaSO_4$, and with or without 12 μg/ml A23187 (23 μM), were injected medially in the backs of mice and removed at day 2 for analysis. Rather than enhancing inflammatory cytokine secretion, delivering ionophore and increasing the gel volume decreased IL-1β and TNF-α expression (Figure 4.6).

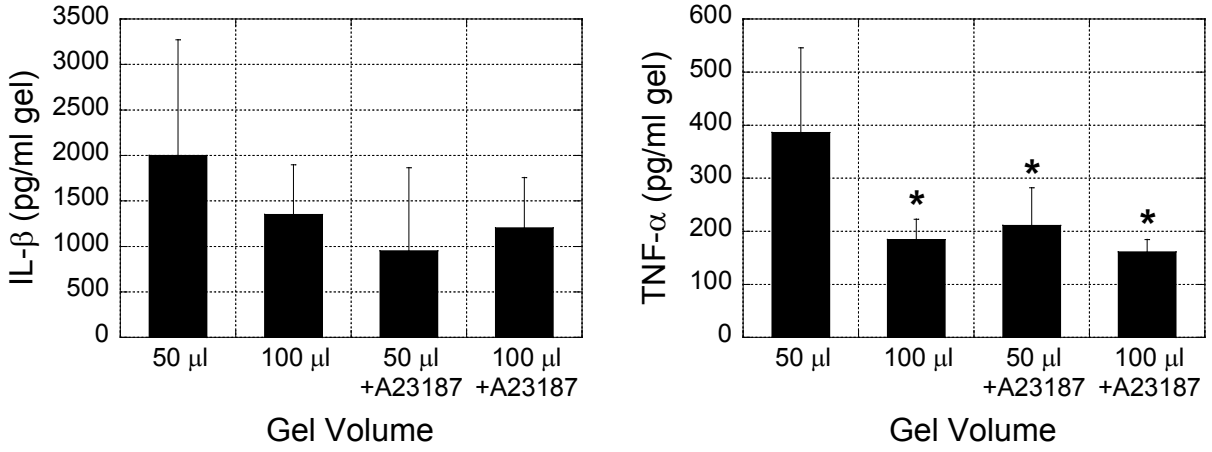

Figure 4.6

Figure 4.6 (Continued): Increasing gel volume and delivering A23187 from calcium alginate gels injected medially did not enhance inflammatory cytokine secretion *in vivo*. Fifty and 100 μl calcium alginate gels, with or without 12 μg/ml A23187, were injected medially into mice. At day 2, gels were removed and analyzed for IL-1β and TNF-α. Asterisks indicate that the condition is significantly different from the 50 μl calcium alginate control. *P≤0.05.

To determine if calcium alginate gels could enhance the effect of LPS as demonstrated *in vitro*, 50 μl alginate gels crosslinked with 4 mM barium or 48.8 mM calcium, with or without 1 μg LPS, were injected medially into mice. After 24 hours, gels were harvested and analyzed for IL-1β. Consistent with *in vitro* data, calcium alginate gels (Ca) induced more IL-1β secretion compared to barium alginate gels (Ba), and LPS delivered from calcium alginate gels (Ca+LPS) more than quadrupled IL-1β secretion relative to LPS delivered from barium alginate gels (Ba+LPS) (Figure 4.7).

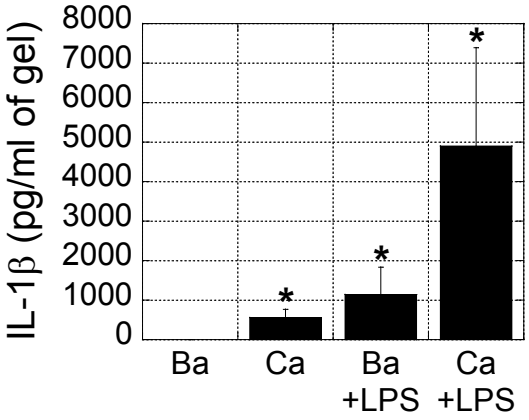

Figure 4.7: Calcium alginate gels induce greater IL-1β secretion compared to barium alginate gels and enhanced LPS-induced IL-1β secretion *in vivo*. 50 μl barium and calcium alginate gels, with or without LPS, were injected medially into mice. After 24 hours, gels were harvested and analyzed for IL-1β secretion. *P<0.05.

To get a more comprehensive analysis of other inflammatory mediators that calcium alginate gels induced from surrounding tissue, gels were multiplexed for 23 various cytokines and chemokines. Similar to DCs in Chapter 3, chemokines (MCP-1, MIP-1β, eotaxin, RANTES, MIP-1α and KC) were secreted in higher concentrations (Figure 4.8A). Interestingly, calcium gels alone upregulated IL-9 the most by ~9-fold (Figure 4.8B), and more than doubled the secretion of IL-1α, MIP-1β, IL-2, IL-1β, MCP-1α, KC, and MIP-1α. The upregulation of IL-9 was particularly striking because it is commonly expressed

by $CD4^+$ T-helper cells to stimulate proliferation and prevent apoptosis. Although several cytokines fell slightly below 1-fold upregulation (meaning that cytokine secretion was reduced with calcium-crosslinked gels), t-tests comparing the two types of crosslinker showed that the P-values did not fall below 0.05 and thus, were not significant. LPS delivered from both barium and calcium alginate gels upregulated overall inflammatory cytokine secretion (with the greatest fold increases occurring for G-CSF, IL-6, and MCP-1 for both types of gels) (Figure 4.8C). However, LPS delivered from calcium gels upregulated RANTES, IL-1β, MIP-1α, MIP-1β and IL-1α by approximately 3-5-fold more than LPS delivered from barium gels (Figure 4.8C). Overall, this data indicated that the calcium in calcium alginate gels promoted the secretion of a number of inflammatory mediators and enhanced inflammation induced by a TLR agonist *in vivo*, which is consistent with alginate *in vitro* data shown in Chapter 2.

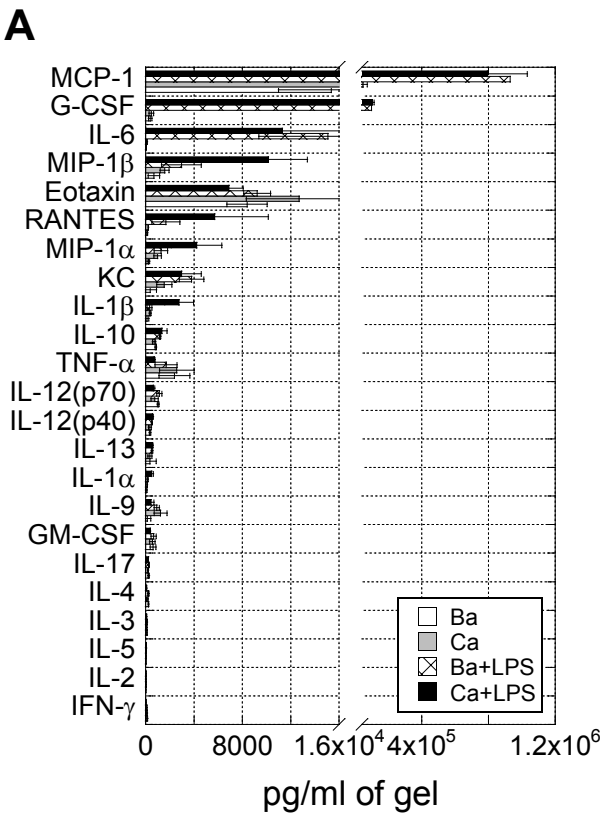

Figure 4.8

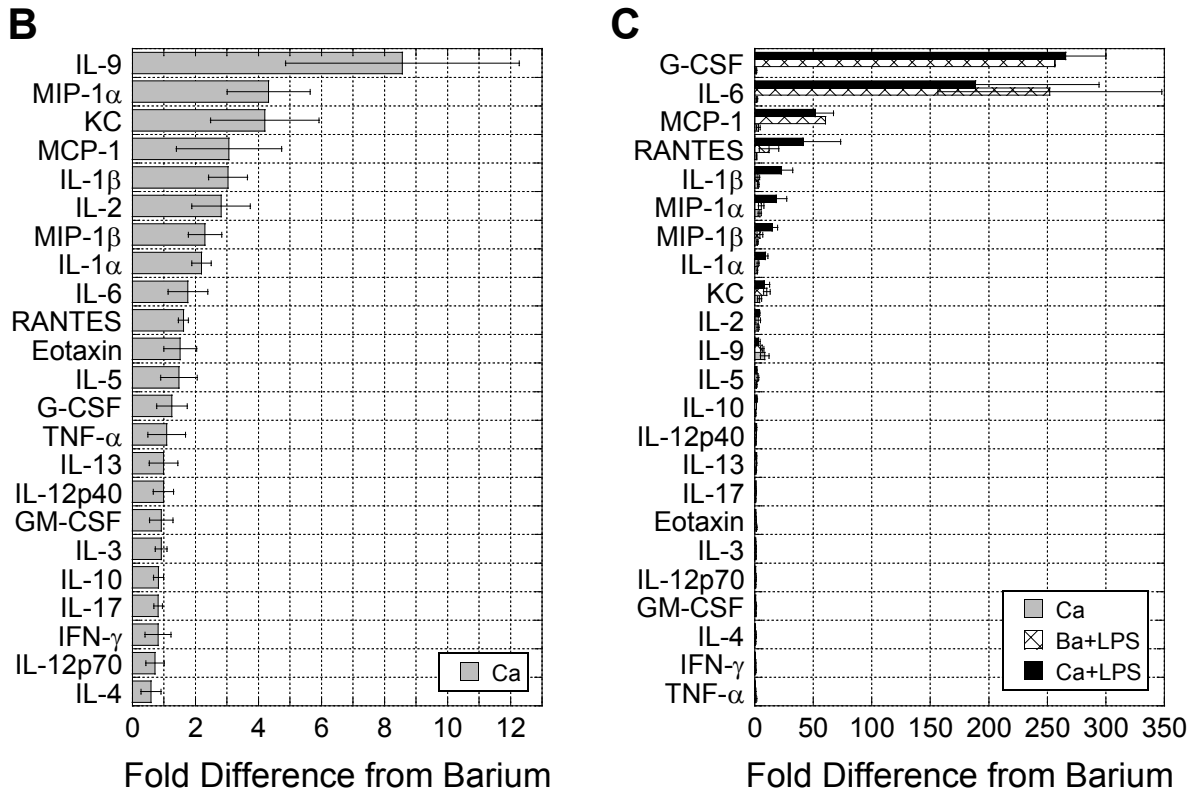

Figure 4.8 (Continued): Calcium alginate gels induce greater inflammatory cytokine secretion compared to barium alginate gels and enhanced LPS-induced inflammation *in vivo*. (A) The concentrations of cytokines and chemokines induced by barium and calcium gels with or without LPS were calculated. (B) The fold increase in cytokine secretion that calcium gels alone induced over barium gels alone was calculated. (C) The fold increases in cytokine secretion induced by barium gels with LPS and calcium gels with LPS over barium gels alone were calculated.

4.4 Discussion

The results of these studies revealed that despite enhancing IL-1β secretion *in vitro*, A23187 delivered from alginate gels did not enhance inflammatory cytokine secretion *in vivo*. However, they demonstrated that the calcium released from calcium alginate gels significantly promoted inflammatory cytokine secretion and enhanced the effects of LPS *in vivo*.

In Chapter 3, it was shown that A23187 delivered from calcium alginate gels had a more potent effect on IL-1β secretion compared to both calcium alginate gels and A23187 alone. Thus, we postulated that A23187 delivered from alginate gels *in vivo* would induce greater inflammation than alginate gels

alone. However, contrary to *in vitro* data, A23187 delivered from alginate gels could not enhance inflammatory cytokine secretion *in vivo*. A past report showed that a 50 μl injection of 1 μM A23187 in DMSO in the footpad of mice was able to recruit lymphocytes and enhance vascular permeability at the site within the first 4 hours [1]. These effects dropped steeply by 8 hours and returned near baseline by 24 hours. In another study, a 100 μl injection of 5 mM A23187 in DMSO into rats was able to locally recruit lymphocytes, which peaked at 2-3 hours after ionophore injection [2]. This suggests that although A23187 injected subcutaneously can have a measurable inflammatory effect on surrounding tissue, it loses its effectiveness within a few hours. This is likely due to the ionophore diffusing away quickly through the tissue or degradation of the molecule, and possibly explains why the quick delivery of A23187 from alginate gels was unsuccessful. In our studies, ~15-30 μM of A23187 was delivered in 50 or 100 μl alginate gels, which falls in the range of what has been previously used to recruit lymphocytes. It is possible that the ionophore was able to induce inflammation soon after injection, but had already returned to baseline by day 2 when the gels were analyzed, or that the levels of cytokines induced by A23187 fell below limits of detection. These results suggest that alternate materials should be considered as a delivery vehicle for ionophores to sustain their delivery for a more prolonged inflammatory effect.

While A23187 did not enhance cytokine secretion *in vivo*, it was demonstrated that the calcium-crosslinker itself was immunostimulatory. Similar to calcium release profiles *in vitro*, the majority of the calcium was released within the first few hours. An interesting finding was that the location of the injection altered the magnitude of cytokine secretion. Alginate gels injected down the center of the mouse's back induced up to 5 times more inflammatory cytokine secretion compared to gels injected in the side flanks. Perfusion varies between tissues, which may explain why the ability of calcium alginate gels to act as an immunostimulatory source was highly dependent on the location of alginate implantation [7]. Although a burst release of calcium occurred within the first 6 hours, after which the

calcium concentration in gels remained constant, cytokines could be detected within the gels for at least 4 days. It is possible that the alginate gels sequester cytokines induced by the burst release of calcium, but slowly release these cytokines as inflammation subsides, accounting for the drop in IL-1β seen after day 1. Consistent with results seen *in vitro*, calcium and LPS released from alginate gels had a synergistic effect and activated the most inflammatory cytokine secretion observed *in vivo*. Aside from IL-1β, strong upregulations in other inflammatory cytokines and chemokines were observed, which could be pursued further in future studies.

The results of this study confirmed that the calcium used to crosslink alginate gels was released *in vivo* and stimulated the local secretion of inflammatory cytokines and chemokines. Furthermore, calcium released from the gels enhanced signaling induced by LPS. This data strongly suggests that future work with calcium-crosslinked alginate gels should take into account the stimulatory effect of calcium when using this material for tissue engineering and drug delivery, and provides convincing evidence that calcium signaling can be harnessed *in vivo* to promote inflammation.

4.5 References

[1] Hayes JM, Simmons RL. The relative role of neutrophils and platelets in the local accumulation of circulating lymphocytes at sites of ionophore-A23187 inoculation. Transplantation 1991;51:674-81.

[2] Yeh T-C, Zhang W, Ildstad ST, Ho C. In vivo dynamic MRI tracking of rat T-cells labeled with superparamagnetic iron-oxide particles. Magn Reson Med 1995;33:200-8.

[3] Soonshiong P, Heintz RE, Merideth N, Yao QX, Yao ZW, Zheng TL, et al. Insulin independence in a type-1 diabetic patient after encapsulated islet transplantation. Lancet 1994;343:950-1.

[4] Silva EA, Mooney DJ. Spatiotemporal control of vascular endothelial growth factor delivery from injectable hydrogels enhances angiogenesis. J Thromb Haemost 2007;5:590-8.

[5] Hori Y, Winans AM, Huang CC, Horrigan EM, Irvine DJ. Injectable dendritic cell-carrying alginate gels for immunization and immunotherapy. Biomaterials 2008;29:3671-82.

[6] Hori Y, Stern PJ, Hynes RO, Irvine DJ. Engulfing tumors with synthetic extracellular matrices for cancer immunotherapy. Biomaterials 2009;30:6757-67.

[7] Hofer AM, Brown EM. Extracellular calcium sensing and signalling. Nat Rev Mol Cell Biol 2003;4:530-8.

Chapter 5
Conclusions, Implications and Future Work

5.1 Conclusions

Given the importance of calcium signaling in dendritic cell activation and the ability of biomaterials to specifically target dendritic cells *in vivo* for immunotherapy, we hypothesized that a biomaterial-based approach could be used to target calcium signaling in DCs *in vivo* to enhance their activation. The first sub-hypothesis was that the calcium used to crosslink alginate gels could activate DCs *in vitro*; the second sub-hypothesis was that calcium ionophore A23187 could be delivered from biomaterials to activate DCs *in vitro*; and the third sub-hypothesis was that calcium used to crosslink alginate gels and/or controlled delivery of A23187 could increase local inflammation *in vivo*. We found that both the calcium released from calcium alginate gels and A23187 matured DCs and enhanced TLR-induced inflammatory cytokine secretion *in vitro*. Although we were unable to effectively deliver A23187 *in vivo*, calcium alginate gels injected subcutaneously were able to upregulate a number of inflammatory cytokines and chemokines relative to barium alginate gels. Likewise, the inflammatory effects of LPS on surrounding tissue were enhanced when LPS was delivered from calcium alginate gels versus barium alginate gels. Thus, we confirmed that the calcium crosslinker in alginate gels could activate DCs, and provided a proof-of-principle that calcium signaling could be harnessed *in vivo* to enhance the immune response. Not only does this work impact the future of biomaterial design, but it may also enhance our understanding of DC biology.

5.2 Implications and Future Work

Based on the results presented in this thesis and previously published work, several implications can be drawn. These include expanding the ideas in this thesis to harness calcium signaling in other white blood cell types, taking into greater consideration the effects of calcium when using calcium

alginate gels for biomedical applications, improving the delivery of A23187 to DCs and other cell types *in vivo*, and finally, extending this work to other ionophores, such as monensin.

Alginate gels are commonly used for biomedical applications because they can encapsulate cells and drugs under physiological conditions and can be tailored to have different mechanical properties and degradation rates depending on the application. Here, we show that calcium, the most common ionic crosslinker used to crosslink alginate, can mature DCs, which should be taken into consideration when using this material for biological applications. Aside from DCs, many other leukocytes are heavily dependent on calcium signaling to carry out their effector functions and could potentially be sensitive to the calcium released from alginate gels [1]. For instance, it has been demonstrated that mast cells and neutrophils, important cells of the innate immune system, require calcium for degranulation, and that T cells require calcium signaling for the production of IL-2 and IL-4 [2-4]. Calcium's importance in the proper functioning of the immune system can be underscored by the fact that a single missense mutation in the gene encoding CRAC causes severe combined immunodeficiency in humans [2]. Because of calcium's importance in immune cell function, it has been proposed that calcium channels and calcium signaling pathways are promising therapeutic targets to control immune cell behavior [2, 4-7]. In Chapter 2, we also suggested that calcium alginate gels could potentially activate the inflammasome, which could have important implications in the field of vaccination. Thus, if using alginate gels for vaccination purposes, having calcium in the gels may be advantageous, but if trying to minimize inflammation, barium alginate gels may be recommended instead.

Although the majority of studies utilizing calcium alginate gels for biomedical purposes have not examined the effects of calcium crosslinker, evidence in some studies indicates that it contributed to the outcome. As alluded to earlier, in a study where activated dendritic cells were delivered in calcium-crosslinked alginate gels to reduce tumor size in mice, calcium alginate gels alone seemed to have a slight therapeutic effect. Consequently, it would be interesting to see if replacing the calcium with

barium would reduce vaccine efficacy [8]. Also mentioned earlier was that calcium-crosslinked alginate gels had a positive effect on angiogenesis in a mouse hindlimb ischemia model [9]. Although not statistically significant, alginate alone appeared to increase blood vessel density over untreated animals and animals injected with a bolus dose of vascular endothelial growth factor (VEGF). It is possible that the calcium in the gels promoted the secretion of endogenous pro-angiogenic factors from immune and/or non-immune cells leading to enhanced blood vessel formation. This could be easily tested by repeating barium and calcium alginate experiments described in this thesis but assaying for pro-angiogenic factors instead. Lastly, alginate has been used for decades in the management of acute and chronic wounds, although its exact molecular and cellular effects are not well-understood. A recent paper found that alginate promoted keratinocyte differentiation, which is critical for wound healing, and that this was due to the calcium released by the alginate [1]. This could potentially explain the benefits of using alginate in wound dressings. These examples illustrate that it is important to characterize the effects that the calcium crosslinker has on other leukocytes and non-immune cells both *in vitro* and *in vivo*.

Despite the use of A23187 to enhance the activation of DCs *in vitro* and the injection of A23187 to transiently recruit lymphocytes *in vivo* [10, 11], there has yet to be a study aimed at delivering the ionophore *in vivo* to sustain a potent and lasting immune response for immunotherapy. In our studies, A23187 delivered from calcium alginate gels did not enhance inflammatory cytokine secretion over calcium alginate gels alone *in vivo* (even though this was observed *in vitro*), and this was likely due to the quick release of ionophore from the material and its short-lived bioactivity. Additionally, although calcium alginate gels alone had an immunostimulatory effect, it was unclear what cell types were being affected by the calcium. For a more sustained and direct immunostimulatory effect, materials that can release ionophore over longer time periods or that can deliver payloads directly to dendritic cells will likely be more promising. In Chapter 3, porous PLG scaffolds encapsulating A23187 were described with

the idea that they could also contain GM-CSF and antigens to recruit and program DCs. More work could be done to characterize A23187 release from these scaffolds and to tune the PLG degradation rate (i.e. change the molecular weight and/or lactic to glycolic acid monomer ratio) for optimum release kinetics [12]. Another benefit of using PLG, aside from it being able to sustain the release of A23187, is that the material itself can be immunostimulatory [13-15]. Alternatively, different polymers could be selected to deliver A23187. One important consideration to keep in mind is that other local cells (both immune and non-immune) could be affected by the A23187 released from scaffolds, which may be desirable or undesirable.

Another approach would be to develop nanoparticles that can target A23187 to dendritic cells either in the periphery or in the lymph nodes. Nanoparticles could be a better approach as they can be targeted to specific cells (see Chapter 1) and release ionophore within the cell after internalization resulting in a more potent and specific effect. Particles less than ~100 nm are able to enter the lymphatics and be taken up by lymph node DCs, whereas larger nanoparticles tend to stay at the site of injection and be taken up by local DCs patrolling the area [16]. When the particle reaches the desired location and/or is taken up by DCs, it is important that the payload, in this case the ionophore, is released. This can be achieved by fabricating nanoparticles made of quickly degrading PLG/PLA polymers [17, 18] or a number of other materials that have been engineered to exploit the acidic, enzymatic and reductive environment of the endolysosome [19-23]. Interestingly, calcium phosphate nanoparticles (e.g. hydroxyapatite) have been commonly studied as vaccine delivery vehicles, since they have been shown to have potent adjuvant effects [24-26], and other studies have found that calcium phosphate crystals can activate the NLR3P inflammasome [27, 28]. Whether these effects are due to the calcium specifically or another property of the material is unclear, but these previous findings could make calcium phosphate an interesting and attractive choice for A23187 delivery.

To screen for optimal materials and dosage to deliver A23187, preliminary studies could be performed *in vitro* using 2D cultured DCs. It was previously shown that a 50 μl injection of a 1 μM A23187 solution (526 ng/ml), which is close to what was used to activate DCs *in vitro* (400 ng/ml), was able to induce lymphocyte infiltration *in vivo* [10]. These values can provide a starting point to help optimize the dose and release of A23187 from both scaffolds and nanoparticles.

Although our attention has been focused on targeting A23187 to DCs, other ionophores specific for Ca^{2+} or other ions (e.g. ionomycin or monensin) could be targeted to DCs and other cell types as a useful tool to control cellular functions *in vivo*. For example, ionomycin, another calcium ionophore, is already a commonly used experimental tool to stimulate T cells *in vitro*. In this thesis, we showed that monensin, a sodium ionophore, downregulated DC maturation markers compared to control cells, which suggests that it could potentially be used for immunosuppression. Monensin is commonly used to for intracellular cytokine staining because it disrupts the function of the Golgi apparatus trapping proteins within the cell. In instances where there is an undesirable immune response, as in the cases for allergy and autoimmunity, it could be useful to deliver monensin to specific T and B cells to suppress the progression of the disease. For transplantation, monensin delivery to DCs could be useful to minimize cross-presentation of tissue antigens and rejection of grafted tissue. Research studying mechanisms of immune tolerance and ways to induce regulatory responses has grown considerably over the past few years [29-32], and the controlled delivery of monensin could provide immunologists and bioengineers with a new tool to suppress the immune response.

The power of ion signaling to control cell fate is evident, and with the existence of a number of ionophores and an array of biomaterials that could be used to deliver them, one can begin to imagine the possibilities. If successful, the regulation of ion signaling *in vivo* may prove to have significant utility in the field of medicine.

5.3 References

[1] Stenvik J, Sletta H, Grimstad Ø, Pukstad B, Ryan L, Aune R, et al. Alginates induce differentiation and expression of CXCR7 and CXCL12/SDF-1 in human keratinocytes—the role of calcium. J Biomed Mater Res A 2012;100A:2803-12.

[2] Parekh AB. Store-operated CRAC channels: function in health and disease. Nat Rev Drug Discov 2010;9:399-410.

[3] Brown AP, Ganey PE. Neutrophil degranulation and superoxide production induced by polychlorinated biphenyls are calcium dependent. Toxicol Appl Pharmacol 1995;131:198-205.

[4] Li SW, Westwick J, Poll CT. Receptor-operated Ca2+ influx channels in leukocytes: a therapeutic target? Trends Pharmacol Sci 2002;23:63-70.

[5] Shumilina E, Huber SM, Lang F. Ca2+ signaling in the regulation of dendritic cell functions. Am J Physiol Cell Physiol 2011;300:C1205-14.

[6] Connolly SF, Kusner DJ. The regulation of dendritic cell function by calcium-signaling and its inhibition by microbial pathogens. Immunol Res 2007;39:115-27.

[7] Koski GK, Schwartz GN, Weng DE, Czerniecki BJ, Carter C, Gress RE, et al. Calcium mobilization in human myeloid cells results in acquisition of individual dendritic cell-like characteristics through discrete signaling pathways. J Immunol 1999;163:82-92.

[8] Hori Y, Stern PJ, Hynes RO, Irvine DJ. Engulfing tumors with synthetic extracellular matrices for cancer immunotherapy. Biomaterials 2009;30:6757-67.

[9] Silva EA, Mooney DJ. Spatiotemporal control of vascular endothelial growth factor delivery from injectable hydrogels enhances angiogenesis. J Thromb Haemost 2007;5:590-8.

[10] Hayes JM, Simmons RL. The relative role of neutrophils and platelets in the local accumulation of circulating lymphocytes at sites of ionophore-A23187 inoculation. Transplantation 1991;51:674-81.

[11] Yeh T-C, Zhang W, Ildstad ST, Ho C. In vivo dynamic MRI tracking of rat T-cells labeled with superparamagnetic iron-oxide particles. Magn Reson Med 1995;33:200-8.

[12] Anderson JM, Shive MS. Biodegradation and biocompatibility of PLA and PLGA microspheres. Adv Drug Del Rev 1997;28:5-24.

[13] Nilsson B, Ekdahl KN, Mollnes TE, Lambris JD. The role of complement in biomaterial-induced inflammation. Mol Immunol 2007;44:82-94.

[14] Anderson JM, Rodriguez A, Chang DT. Foreign body reaction to biomaterials. Semin Immunol 2008;20:86-100.

[15] Yoshida M, Babensee JE. Differential effects of agarose and poly(lactic-co-glycolic acid) on dendritic cell maturation. J Biomed Mater Res A 2006;79A:393-408.

[16] Reddy ST, Swartz MA, Hubbell JA. Targeting dendritic cells with biomaterials: developing the next generation of vaccines. Trends Immunol 2006;27:573-9.

[17] Panyam J, Labhasetwar V. Biodegradable nanoparticles for drug and gene delivery to cells and tissue. Adv Drug Del Rev 2012;64, Supplement:61-71.

[18] Vasir JK, Labhasetwar V. Biodegradable nanoparticles for cytosolic delivery of therapeutics. Adv Drug Del Rev 2007;59:718-28.

[19] Meng F, Cheng R, Deng C, Zhong Z. Intracellular drug release nanosystems. Mater Today 2012;15:436-42.

[20] Dierendonck M, De Koker S, Vervaet C, Remon JP, De Geest BG. Interaction between polymeric multilayer capsules and immune cells. J Control Release 2012;161:592-9.

[21] Ganta S, Devalapally H, Shahiwala A, Amiji M. A review of stimuli-responsive nanocarriers for drug and gene delivery. J Control Release 2008;126:187-204.

[22] Meng FH, Hennink WE, Zhong Z. Reduction-sensitive polymers and bioconjugates for biomedical applications. Biomaterials 2009;30:2180-98.

[23] Bae Y, Kataoka K. Intelligent polymeric micelles from functional poly(ethylene glycol)-poly(amino acid) block copolymers. Adv Drug Del Rev 2009;61:768-84.

[24] He Q, Mitchell AR, Johnson SL, Wagner-Bartak C, Morcol T, Bell SJD. Calcium phosphate nanoparticle adjuvant. Clin Diagn Lab Immunol 2000;7:899-903.

[25] Gupta RK, Siber GR. Adjuvants for human vaccines - current status, problems and future prospects. Vaccine 1995;13:1263-76.

[26] Singh M, Chakrapani A, O'Hagon D. Nanoparticles and microparticles as vaccine-delivery systems. Expert Rev Vaccines 2007;6:797-808.

[27] Pazar B, Ea HK, Narayan S, Kolly L, Bagnoud N, Chobaz V, et al. Basic calcium phosphate crystals induce monocyte/macrophage IL-1 beta secretion through the NLRP3 inflammasome in vitro. J Immunol 2011;186:2495-502.

[28] Jin CC, Frayssinet P, Pelker R, Cwirka D, Hu B, Vignery A, et al. NLRP3 inflammasome plays a critical role in the pathogenesis of hydroxyapatite-associated arthropathy. Proc Natl Acad Sci U S A 2011;108:14867-72.

[29] Sakaguchi S, Yamaguchi T, Nomura T, Ono M. Regulatory T cells and immune tolerance. Cell 2008;133:775-87.

[30] Poojary KV, Kong Y-cM, Farrar MA. Control of Th2-mediated inflammation by regulatory T cells. Am J Pathol 2010;177:525-31.

[31] Morelli AE, Thomson AW. Tolerogenic dendritic cells and the quest for transplant tolerance. Nat Rev Immunol 2007;7:610-21.

[32] Steinman RM, Banchereau J. Taking dendritic cells into medicine. Nature 2007;449:419-26.

- Appendices -

Preliminary Work for Related Studies and Detailed Protocols

Appendix 1

Effectiveness of an Implantable Cancer Vaccine in the C1498 Mouse Leukemia Model

A1.1 Introduction

The PLG *in situ* cell programming system described earlier in this thesis has been successful in reducing tumor growth and enhancing survival in mouse models of melanoma and glioma [1-3]. We hypothesized that we could apply this system in a mouse model of leukemia to reduce tumor burden and increase mouse survival. If successful, this could be a potential approach to treat leukemia patients in remission and prevent relapse caused by minimal residual disease. To test this, we chose to use the C1498 cell line, a myeloid leukemia line derived from C57BL/6J mice, because it can be easily injected into C57 mice to induce leukemia [4-6]. We vaccinated C57 mice with anti-C1498 scaffolds (with or without A23187), challenged them with C1498 cells two weeks later, and determined vaccine efficacy by monitoring mouse survival.

A1.2 Materials and Methods

Cell culture

C1498 cells (ATCC, Manassas, VA) were cultured in Dulbecco's Modified Eagle's Medium (DMEM) (Life Technologies) containing 10% heat-inactivated FBS, 100 U/ml penicillin, and 100 μg/ml streptomycin.

Survival Studies

PLG scaffolds (8.5 mm diameter) were fabricated according to standard methods in the lab [1, 2]. They contained 18 mg of PLG microspheres, ~2 μg of GM-CSF, 10^7 C1498 tumor cell lysates, and 300 μg of condensed CpG. To test the effects of A23187, A23187 was incorporated into the scaffolds by

adding it to the PLG oil phase during microsphere fabrication so the final concentration (assuming 89% encapsulation efficiency) equaled 10 μg/scaffold. Blank and drug-loaded scaffolds were implanted subcutaneously in the backs of C57BL/6J mice, and two weeks later they were injected with $2x10^6$ C1498 cells/100 μl PBS via the tail vein. Survival was monitored over several weeks.

DC Recruitment Studies

For comparison of DC recruitment between blank and drug-loaded scaffolds, scaffolds containing GM-CSF only were fabricated as above. After 7 days of implantation, scaffolds were removed, cut into small pieces, placed in tubes containing 10 ml of type IV collagenase (250 U/ml PBS) (Lot#40E11931) (Worthington Biochemical, Lakewood, NJ), and incubated in a 37°C water bath for 30 minutes with vortexing every 10 minutes. Dissociated cells were strained through a 40 μm cell strainer, washed in stain buffer, and stained with APC-conjugated anti-mouse CD11c for analysis by flow cytometry.

A1.3 Results

Drug-loaded scaffolds containing C1498 lysates were able to enhance survival of mice challenged with C1498 leukemia by roughly one week when compared to blank scaffolds (Figure A1.1A). In a second trial, the vaccine was able to extend survival longer than one week for one mouse and completely cured another mouse (Figure A1.1B). Although A23187 has been shown to enhance DC activation, scaffolds containing A23187 actually reduced survival compared to scaffolds without it (Figure A1.1B).

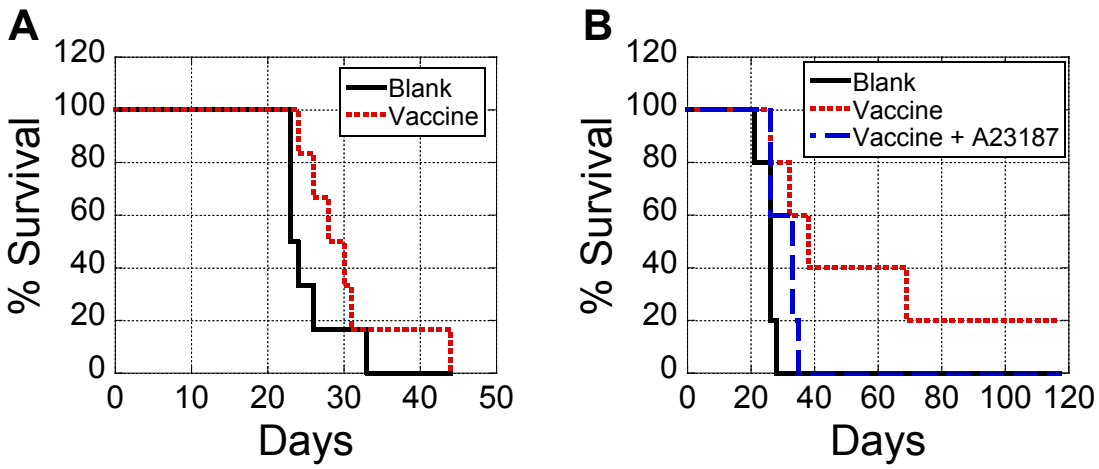

Figure A1.1: Implantable cancer vaccine enhanced survival in C1498 leukemia model while A23187 reduced its efficacy. (A) Blank and drug-loaded PLG scaffolds were implanted subcutaneously in mice. 2 weeks later, mice were challenged with C1498 leukemia cells and survival was monitored over several weeks. n=6. (B) Drug-loaded scaffolds containing 10 μg of A23187 were tested for their ability to enhance survival. n=5.

When analyzing the effect of GM-CSF on DC recruitment, we found that scaffolds containing GM-CSF enhanced overall cell numbers (Figure A1.2A) but decreased the percentage of CD11c positive cells (Figure A1.2B). When the number of DCs recruited to the scaffolds was calculated, it was determined that although scaffolds containing GM-CSF recruited more cells, the number of DCs was approximately the same as blank scaffolds accounting for the decreased percentage of CD11c positive cells (Figure A1.2C).

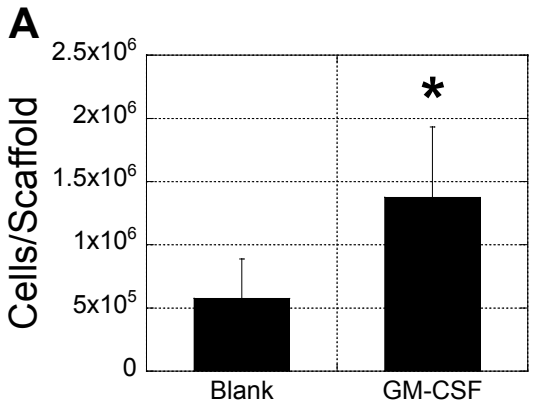

Figure A1.2

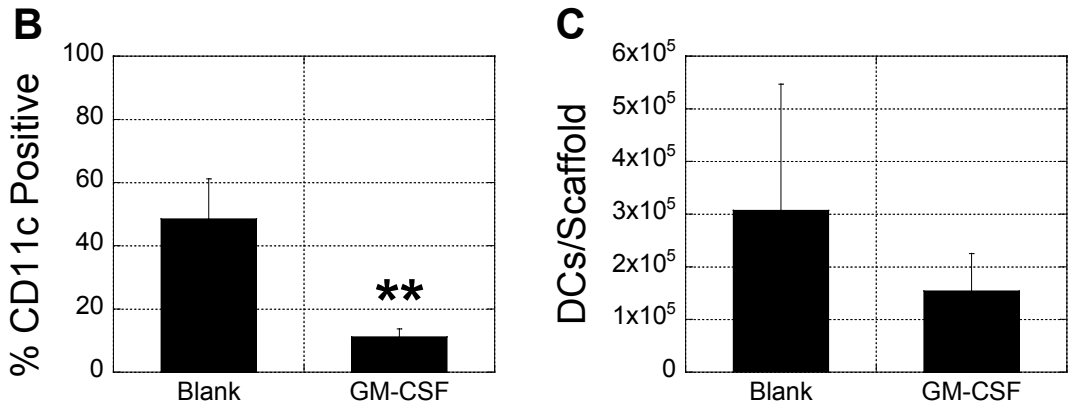

Figure A1.2 (Continued): Scaffolds containing GM-CSF recruited more cells overall, but the number of recruited DCs remained the same. (A) After 7 days of implantation, blank scaffolds or scaffolds containing GM-CSF were removed and analyzed for total cell number. (B) Cells isolated from scaffolds were stained with CD11c and analyzed by flow cytometry. (C) The number of DCs recruited to each scaffold was calculated based on the data in (A) and (B). Data is presented as mean ± standard deviation. *P<0.05; **P<0.001.

A1.4 Conclusion

The PLG *in situ* programming system was successful at enhancing survival in the C1498 mouse model of myeloid leukemia. Although A23187 has been shown to enhance DC activation *in vitro*, it reduced vaccine efficacy in this *in vivo* model. It is possible that interactions between A23187 and other components of the scaffold reduced its overall efficacy, or that the amount of ionophore encapsulated in the scaffolds was so great that they destabilized cellular membranes leading to toxicity. Further experiments would be needed to determine the cause. Lastly, although GM-CSF enhanced overall cell recruitment to the scaffold, it did not significantly enhance $CD11c^+$ DC recruitment.

A1.5 References

[1] Ali OA, Huebsch N, Cao L, Dranoff G, Mooney DJ. Infection-mimicking materials to program dendritic cells in situ. Nat Mater 2009;8:151-8.

[2] Ali OA, Emerich D, Dranoff G, Mooney DJ. In situ regulation of DC subsets and T cells mediates tumor regression in mice. Sci Transl Med 2009;1:1-10.

[3] Ali O, Doherty E, Bell W, Fradet T, Hudak J, Laliberte M-T, et al. Biomaterial-based vaccine induces regression of established intracranial glioma in rats. Pharm Res 2011;28:1074-80.

[4] Blazar BR, Taylor PA, Boyer MW, PanoskaltsisMortari A, Allison JP, Vallera DA. CD28/B7 interactions are required for sustaining the graft-versus-leukemia effect of delayed post-bone marrow transplantation splenocyte infusion in murine recipients of myeloid or lymphoid leukemia cells. J Immunol 1997;159:3460-73.

[5] Boyer MW, Vallera DA, Taylor PA, Gray GS, Katsanis E, Gorden K, et al. The role of B7 costimulation by murine acute myeloid leukemia in the generation and function of a CD8(+) T-cell line with potent in vivo graft-versus-leukemia properties. Blood 1997;89:3477-85.

[6] Weigel BJ, Panoskaltsis-Mortari A, Diers M, Garcia M, Lees C, Krieg AM, et al. Dendritic cells pulsed or fused with AML cellular antigen provide comparable in vivo antitumor protective responses. Exp Hematol 2006;34:1403-12.

Appendix 2

Differentiating Myeloid Leukemia Cells into Antigen Presenting Cells *In Situ* for Anti-Leukemia Therapy

A2.1 Introduction

This thesis demonstrated that A23187 could mature DCs and enhance TLR-induced DC activation. In addition to maturing DCs, A23187 has been used along with phorbol 12-myristate 13-acetate (PMA) to differentiate patients' myeloid leukemia cells into APCs *ex vivo*. The hope has been that these leukemia-derived APCs can be re-introduced into the patient while they are in remission, home to the lymph nodes, and present leukemia antigens to T cells to generate anti-leukemia responses that would prevent relapse caused by minimal residual disease (MRD) [1-4]. However, critical issues with this procedure (and *ex vivo* manipulation, in general) are that primary tumor cells are difficult to isolate and culture, and the majority of cells re-injected into the patient do not home to the lymph nodes [5, 6]. This may explain why this approach to combat myeloid leukemia has not been successful in the clinic [7]. To address issues associated with the *ex vivo* manipulation of leukemia cells, we hypothesized that we could apply the PLG *in situ* programming system described in this thesis to recruit and differentiate myeloid leukemia cells into APCs using A23187 and/or PMA for anti-leukemia therapy [8, 9]. To demonstrate proof-of-principle, we needed to choose a model myeloid leukemia line that could be differentiated into an APC phenotype using A23187 and/or PMA and could be recruited with chemoattractants. We chose to test the human myeloid leukemia cell line HL-60, which has been previously shown to engraft well in nude mice and to differentiate into an APC phenotype with exposure to A23187 and PMA [2, 10]. We also tested the C1498 cell line because it easily engrafts in C57BL/6J mice. In the following studies, we wanted to verify that HL-60 and C1498 cells could be differentiated by A23187 and/or PMA *in vitro* and that we could establish an *in vivo* HL-60 nude mouse model. We also tested the bacterial peptide N-Formyl-L-methionyl-L-leucyl-L-phenylalanine (fMLP) as a recruiting factor

in vitro, since it has been shown to be a strong chemoattractant for HL-60, and then assessed its encapsulation and release from PLG scaffolds *in vitro* [11, 12].

A2.2 Materials and Methods

Cell Culture

HL-60 cells (ATCC) were cultured in Iscove's Modified Dulbecco's Medium (IMDM) (Life Technologies) containing 20% heat-inactivated FBS, 100 U/ml penicillin, and 100 μg/ml streptomycin.

C1498 cells were cultured in DMEM containing 10% heat-inactivated FBS, 100 U/ml penicillin, and 100 μg/ml streptomycin.

Differentiation Assays

HL-60 cells were resuspended at a concentration of 333,333 cells/ml of control IMDM or IMDM containing 400 ng/ml A23187 and/or 10 ng/ml PMA (Sigma-Aldrich). 10^6 cells (3 ml) of each condition were plated in 6-well plates. After 20-24 hours, differentiated cells were collected and stained with PE-conjugated anti-human CD80 (BioLegend, San Diego, CA), APC-conjugated anti-human CD86 (BioLegend), and Pacific Blue™-conjugated anti-human MHC class I (human leukocyte antigen (HLA) – A, B, C) (BioLegend). Fluorescence was quantified using an LSR II or LSR Fortessa™ flow cytometer. Photomicrographs of cells were taken with an Olympus IX81® inverted microscope.

For C1498 differentiation, 10^6 cells/1.5 ml were plated in 6-well plates. After 1 hour of incubation, 1.5 ml of control DMEM or DMEM containing A23187 and/or PMA was added to each well so that the final concentrations equaled 400 ng/ml A23187 and/or 10 ng/ml PMA. After 20-24 hours, cells were scraped from each well and stained with PE-conjugated anti-mouse CD86, APC-conjugated anti-mouse CD80, and FITC-conjugated anti-mouse MHC class I (eBioscience). Fluorescence was quantified as above using flow cytometry.

Migration Assays

To confirm that fMLP was a strong chemoattractant of HL-60, 0.6 ml medium containing 10^{-8} M GM-CSF, CCL21, or fMLP were plated in 24 well plates. Transwells (Corning, Lowell, MA) containing 5 μm size pores were inserted into each well, and 500,000 cells in 0.3 ml medium were pipetted into each transwell. At 2, 4 and 6 hours, the transwells were removed, and cells that had migrated through the transwell were counted with a Z2 particle counter. To test optimum fMLP concentration, a similar experiment was repeated, but this time medium contained of 10^{-9}, 10^{-8} or 10^{-7} M fMLP and cells were collected after 1 hour.

To determine if fMLP could induce differentiation of HL-60 cells into APCs, cells were cultured in control medium or medium containing 10^{-8} M fMLP or 400 ng/ml A23187 (a positive control) for 20-24 hours. Cells were then stained with APC-conjugated anti-human CD86, Pacific Blue™-conjugated anti-human MHC class I, and FITC-conjugated anti-human CCR7 (eBioscience) and analyzed using flow cytometry.

Scaffold Fabrication, Encapsulation Efficiency, and Release Assays

PLG scaffolds (8.5 mm diameter) containing fMLP were fabricated using methods described previously [8, 9]. The amount of fMLP added to the PLG/oil phase during microsphere fabrication was such that the final amount in each 18 mg scaffold equaled 1.8 mg fMLP (assuming 100% encapsulation efficiency). To analyzed fMLP encapsulation efficiency and release, the same protocol described in Chapter 3 to determine A21387 release was used.

HL-60 Induction in Nude Mice

To develop an HL-60 *in vivo* mouse model to test the *in situ* programming system, 6 week-old NU/J mice (Jackson Laboratory) were injected with $30x10^6$ HL-60 cells in a 150 μl volume via the tail

vein. At 1, 2, 4, and 6 weeks, blood was collected and mice were sacrificed so that their inguinal lymph nodes and spleens could be harvested and analyzed for HL-60. For blood collection, mice were anesthetized with isoflurane, and 300 μl of blood was collected through the orbital sinus with capillary tubes. To prevent clotting, blood was emptied into polypropylene tubes containing 50 μl of 600 USP/ml heparin solution. After blood collection, mice were sacrificed so their lymph nodes and spleens could be harvested. For HL-60 detection in blood, 100 μl of each blood sample was pipetted into 15 ml tubes, and 1 μg of Pacific Blue™-conjugated anti-human MHC class I in 10 μl of stain buffer was added. After 30 minutes of incubation on ice, red blood cells (RBCs) were lysed with ammonium-chloride-potassium (ACK) lysing buffer. Remaining cells were washed and resuspended in staining buffer for analysis. Spleens were mashed with a back of a syringe and lymph nodes were dissociated using needles in a small Petri dish containing HBSS+. Cells were passed through a 70 μm cell strainer, and RBCs in spleen samples were lysed using ACK lysing buffer. Organ samples were then washed and stained with Pacific Blue™-conjugated anti-human MHC class I antibody for flow cytometry analysis.

To improve HL-60 engraftment, mice were injected intraperitoneally (I.P.) with 3 mg cyclophosphamide/100 μl PBS 3 days prior to HL-60 injection via the tail vein. At 3, 6, and 7 weeks after leukemia induction, blood, inguinal lymph nodes, and spleens were harvested for HL-60 analysis as described above.

A2.3 Results

A23187 was found to upregulate HL-60 expression of CD80, CD86, and MHC class I (Figure A2.1A). Although results were less striking, PMA (which in addition to A23187 has also been shown to induce HL-60 cells into an APC phenotype [2]) was also able to increase CD80 and CD86. The combination of PMA and A23187 did not seem to significantly enhance differentiation compared to A23187 alone. A23187 also increased CD86 expression by C1498 cells, but overall, induced less C1498

differentiation compared to HL-60 cells (Figure A2.1B). Thus, A23187 and HL-60 cells were used for the remainder of the study. Interestingly, it was observed that A23187 caused HL-60 cells to form dendrites characteristic of activated DCs, while PMA caused them to acquire a more fibroblastic-like appearance (Figure A2.1C). The combination of PMA and A23187 caused cells to cluster into colonies.

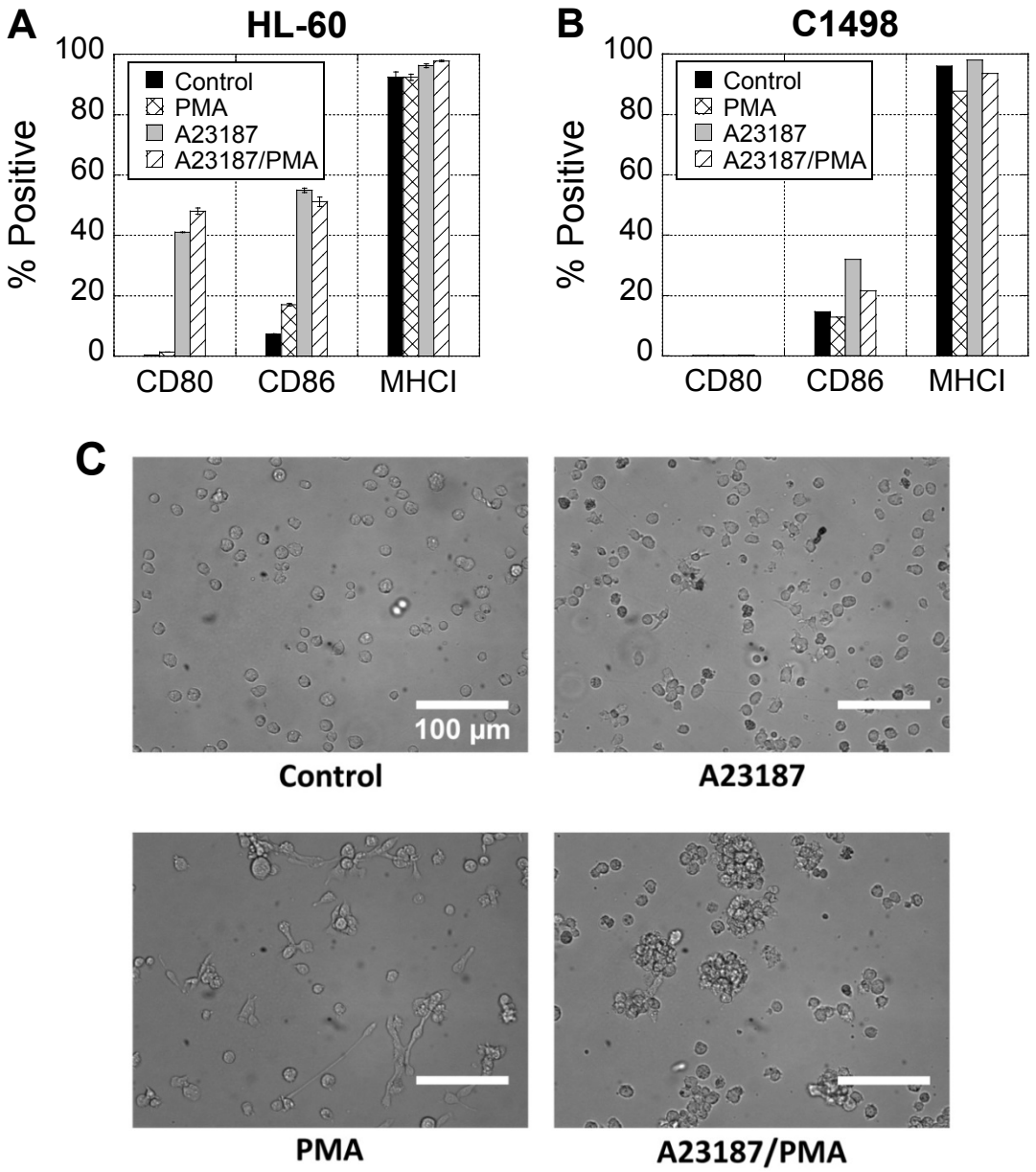

Figure A2.1: A23187 strongly induced HL-60 cells to acquire an APC phenotype. (A) HL-60 cells were cultured overnight in control medium or medium containing A23187 and/or PMA. Cells were stained for CD80, CD86 and MHC class I to gauge differentiation. n=3. Data is presented as mean ± standard deviation. (B) C1498 cells were cultured overnight with A23187 and/or PMA and analyzed as above. n=1. (C) Photomicrographs of HL-60 cells were taken 24 hours after culture with control or differentiation medium.

fMLP has been shown to be a potent chemoattractant of HL-60. We found that compared to GM-CSF and CCL21, strong chemoattractants of myeloid cells, fMLP was able to induce more cell migration (Figure A2.2A) with an optimum concentration of 10^{-8} M (Figure A2.2B). Unlike A23187, fMLP was not able to induce HL-60 differentiation (Figure A2.2C).

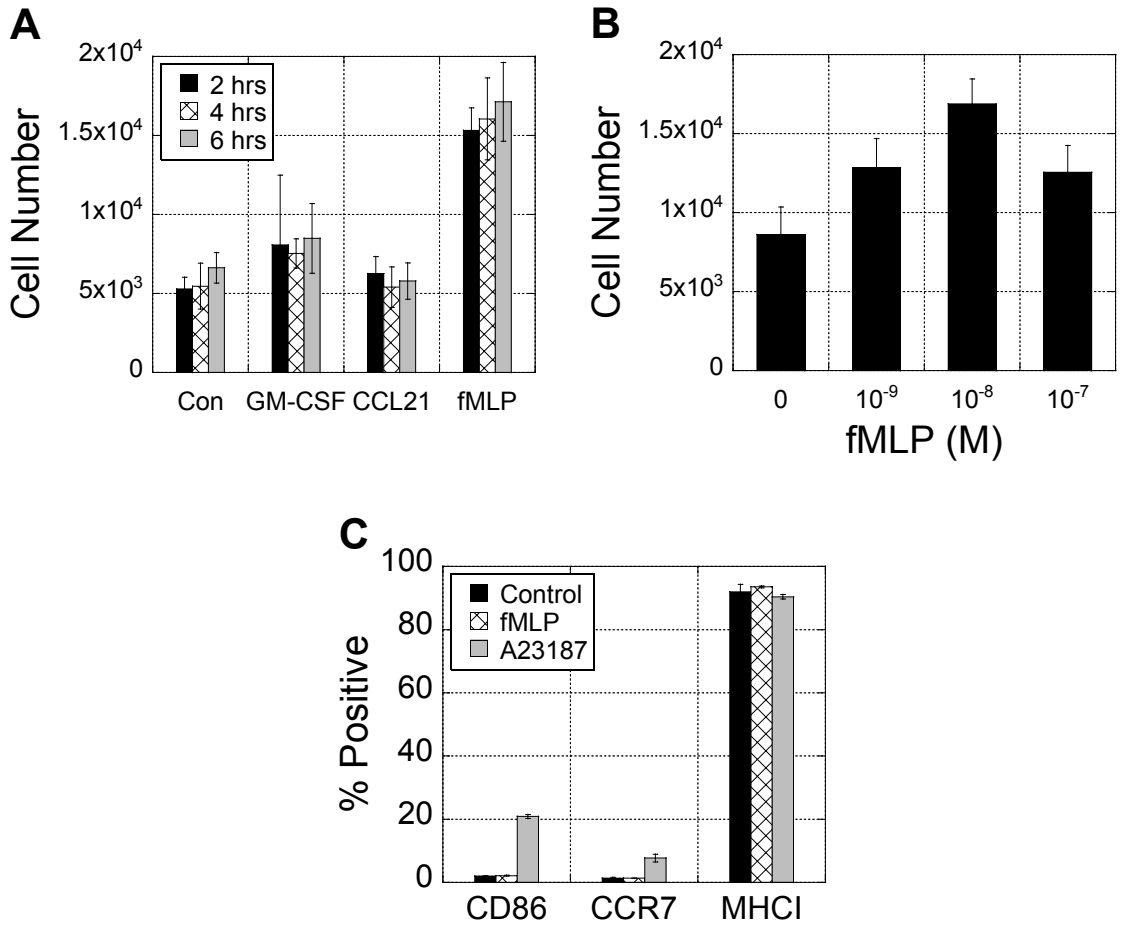

Figure A2.2: fMLP was a potent HL-60 chemoattractant. (A) 10^{-8} M of GM-CSF, CCL21, and fMLP were tested for their ability to attract HL-60 cells using a transwell migration assay. n=3. (B) Transwell migration assays were also used to determine the optimum fMLP dose. n=3. (C) HL-60 cells were cultured with fMLP overnight and stained for CD86, CCR7, and MHC class I to determine if it could induce HL-60 differentiation into an APC phenotype. n=3. Data is presented as mean ± standard deviation.

LC-MS was used to test the release of fMLP from PLG scaffolds. Using the LC-MS protocol described in Chapter 3, fMLP was found to elute at approximately 2.95 minutes (Figure A2.3A) and have a mass of 438.2 g/mol (Figure A2.3B). The lower limit of detection was ~0.001 mg/ml.

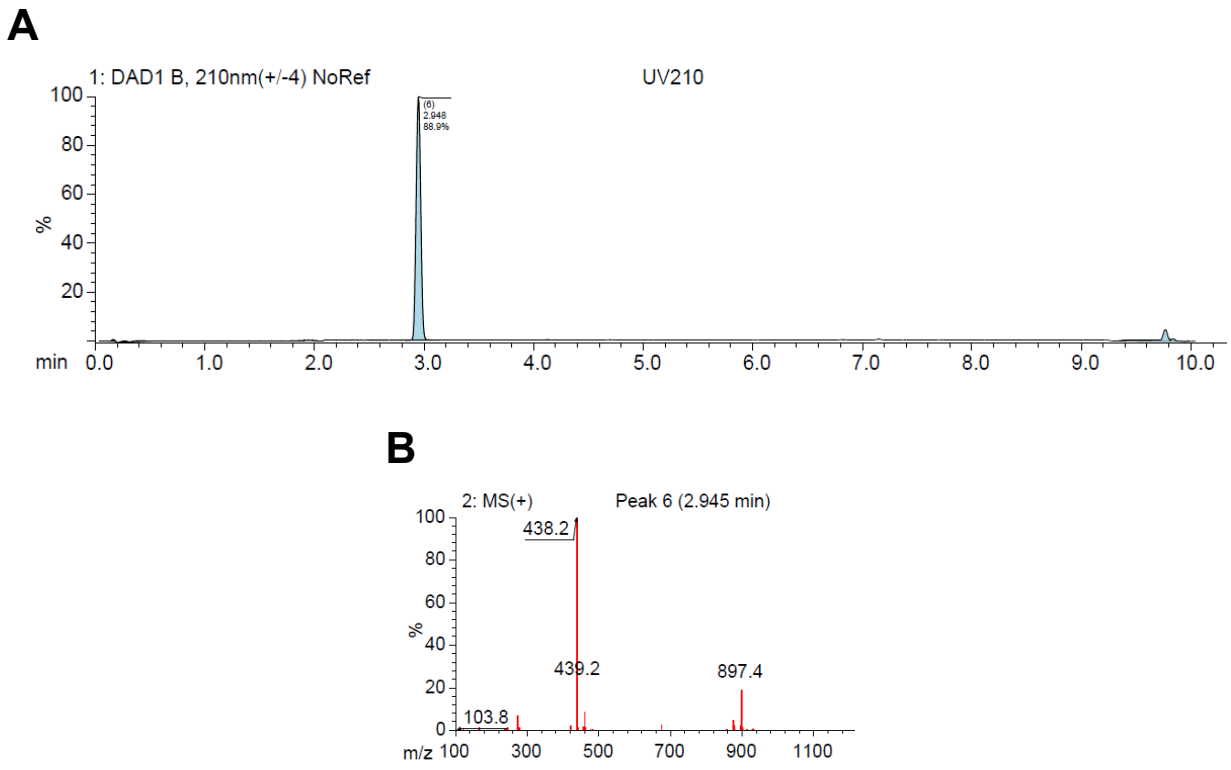

Figure A2.3: fMLP was detected with LC-MS. (A) Chromatogram of 1 mg/ml fMLP. fMLP eluted at ~2.95 minutes. (B) Mass spectrum of fMLP.

Unlike A23187 (see Chapter 3), fMLP had a much lower encapsulation efficiency of 2-8%, meaning that of the original 1.8 mg of fMLP used for scaffold fabrication, only 40-150 μg was actually encapsulated. A signficant amount (~66 μg) was released during the porogen leach, and the remainder was released within the first day of the release study (Figure A2.4).

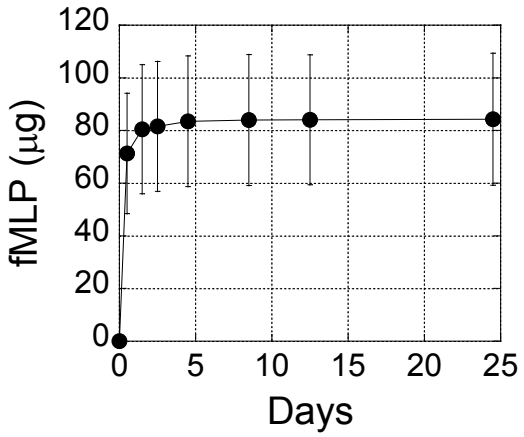

Figure A2.4: fMLP released quickly from PLG scaffolds. Cumulative release of fMLP from PLG scaffolds. fMLP was detected using LC-MS. n=3. Data is presented as mean ± standard deviation.

To establish an *in vivo* leukemia model in which the *in situ* programming scaffold could be tested, nude mice were injected via the tail vein with $30x10^6$ HL-60 cells. To determine whether HL-60 cells were able to persist and cause disease, peripheral blood, inguinal lymph nodes, and the spleens of mice were analyzed at 1, 2, 4, and 6 weeks for HL-60 infiltration. At each of the timepoints, organs were negative for HL-60. However, between 5-7 weeks, palpable tumors began to grow in some mice, particularly on the back of the neck (Figure A2.5). Cells isolated from these tumors stained ~96% positive for HLA indicating that they consisted mainly of HL-60 cells. Aside from tumor growth, mice appeared otherwise healthy.

Figure A2.5: Nude mice injected with HL-60 cells via the tail vein developed tumors at 5-7 weeks. Photograph of a mouse with an HL-60 tumor on the back of the neck.

In a previous study, it was reported that cyclophosphamide administration aided in HL-60 engraftment in nude mice [10]. To promote HL-60 engraftment, mice were given 3 mg cyclophosphamide injections 3 days prior to HL-60 induction. HL-60 infiltration of organs was then monitored at 3, 6, and 7 weeks. Unlike the reported results, we could not detect HL-60 in the peripheral blood or in any of the harvested organs, and no solid tumor formation was observed.

A2.4 Conclusion

HL-60 myeloid leukemia cells were strongly induced by A23187 to acquire an APC phenotype and were strongly attracted by the bacterial derived chemoattractant fMLP. However, A23187 and fMLP release need to be optimized (for both concentration and release kinetics) in order for the leukemia cells to be significantly affected *in vivo*. This could be accomplished by tuning the PLG (such as its degradation rate) or by choosing alternative materials to deliver the factors.

In this study, HL-60 cells were not able to properly engraft in nude mice, and it is likely that mice with a more severe form of immunodeficiency will be necessary to establish an HL-60-mediated leukemia model. Ultimately, an immunocompetent mouse will be needed to test the ability of myeloid leukemia-derived APCs to induce adaptive anti-leukemia immune responses and reduce leukemia progression.

A2.5 References

[1] Lindner I, Kharfan-Dabaja MA, Ayala E, Kolonias D, Carlson LM, Beazer-Barclay Y, et al. Induced dendritic cell differentiation of chronic myeloid leukemia blasts is associated with down-regulation of BCR-ABL. J Immunol 2003;171:1780-91.

[2] Kharfan-Dabaja MA, Ayala E, Lindner I, Cejas PJ, Bahlis NJ, Kolonias D, et al. Differentiation of acute and chronic myeloid leukemic blasts into the dendritic cell lineage: analysis of various differentiation-inducing signals. Cancer Immunol Immunother 2005;54:25-36.

[3] Houtenbos I, Westers TM, Ossenkoppele GJ, van de Loosdrecht AA. Feasibility of clinical dendritic cell vaccination in acute myeloid leukemia. Immunobiology 2006;211:677-85.

[4] Houtenbos I, Westers TM, Ossenkoppele GJ, van de Loosdrecht AA. Leukemia-derived dendritic cells: towards clinical vaccination protocols in acute myeloid leukemia. Haematol-Hematol J 2006;91:348-55.

[5] Cheuk ATC, Guinn BA. Immunotherapy of acute myeloid leukaemia: development of a whole cell vaccine. Front Biosci-Landmrk 2008;13:2022-9.

[6] Steinman RM, Banchereau J. Taking dendritic cells into medicine. Nature 2007;449:419-26.

[7] Westers TM, Ossenkoppele GJ, van de Loosdrecht AA. Dendritic cell-based immunotherapy in acute and chronic myeloid leukaemia. Biomed Pharmacother 2007;61:306-14.

[8] Ali OA, Huebsch N, Cao L, Dranoff G, Mooney DJ. Infection-mimicking materials to program dendritic cells in situ. Nat Mater 2009;8:151-8.

[9] Ali OA, Emerich D, Dranoff G, Mooney DJ. In situ regulation of DC subsets and T cells mediates tumor regression in mice. Sci Transl Med 2009;1:1-10.

[10] Xu Y, Scheinberg DA. Elimination of human leukemia by monoclonal antibodies in an athymic nude mouse leukemia model. Clin Cancer Res 1995;1:1179-87.

[11] Gallagher R, Collins S, Trujillo J, Mccredie K, Ahearn M, Tsai S, et al. Characterization of the continuous, differentiating myeloid cell-line (HL-60) from a patient with acute promyelocytic leukemia. Blood 1979;54:713-33.

[12] Kress H, Park JG, Mejean CO, Forster JD, Park J, Walse SS, et al. Cell stimulation with optically manipulated microsources. Nat Methods 2009;6:905-9.

Appendix 3
Effect of Extracellular Matrix on Dendritic Cell Maturation

A3.1 Introduction

It is widely appreciated that cell-matrix interactions can play a critical role in cell phenotype and behavior [1, 2]. For example, integrin signaling has been shown to converge with immunoreceptor signaling and plays an important role in leukocyte effector functions [3]. Specifically, extracellular matrix (ECM) proteins have been shown to influence DC development and phagocytosis, which in turn influence the quality of T cell stimulation [4-6]. To verify that ECM proteins could influence DC maturation, we cultured bone marrow-derived DCs overnight on increasing densities of fibronectin or laminin, as well as encapsulated in calcium-crosslinked alginate matrices modified with increasing densities of RGD peptide, in the presence or absence of TLR-ligands. Supernatants were analyzed for the inflammatory cytokine IL-12p70 to gauge maturation.

A3.2 Materials and Methods

Fibronectin and Laminin Studies

50 μl of sterile human fibronectin (hFN) (Sigma-Aldrich), mouse fibronectin (mFN) (Innovative Research, Novi, MI), or mouse laminin (mLN) (BD Biosciences) in carbonate buffer (15 mM Na_2CO_3 (Sigma-Aldrich), 35 mM $NaHCO_3$ (Sigma-Aldrich), pH 9.4) was plated onto non-tissue culture treated 96-well plates overnight at 4°C so that the plating density of each protein equaled 0, 10, 100, 1,000, or 10,000 ng/cm^2. The next day, the solutions were aspirated, and 200 μl of a sterile solution of 1 mg/ml Pluronic® F-127 (P127) (Sigma-Aldrich) in PBS was plated per well for 1 hour at room temperature to block non-specific binding. To control for P127, unmodified wells lacking both ECM protein and P127 were included in the experiment. Wells were washed twice with PBS and 100,000 DCs/180 μl of R10

medium were plated per well (see Chapter 2 for protocol on generating primary bone-marrow derived DCs). One hour or 18 hours after attachment, cells were pulsed with 20 μl of LPS or CpG such that the final concentration equaled 100 ng/ml or 5 μM, respectively. After 20-24 hours, supernatants were collected and frozen at -20°C for IL-12p70 analysis by Quantikine® ELISA.

DC Encapsulation in RGD-Modified Alginate Matrices

MVG alginate was modified with increasing amounts of RGD peptide (Peptides International, Louisville, KY), using standard methods developed in the lab [7], so that the degree of substitution per alginate chain was 2, 10, or 20. DCs were encapsulated in RGD-modified MVG alginate discs as described in Chapter 2 and placed in medium. After one hour of incubation at 37°C and 5% CO_2, cells were activated with CpG such that the final concentration equaled 5 μM. To compare encapsulation time on DC activation, cells were encapsulated in MVG alginate beads as described in Chapter 2, and after 1 or 18 hours after encapsulation, were pulsed with 5 μM CpG. After 24 hours, supernatants were collected and analyzed for the DC maturation cytokine IL-12p70.

A3.3 Results

To determine if fibronectin density could influence DC activation, DCs were cultured on increasing densities of human and mouse fibronectin blocked with Pluronic F127, and one hour later, were stimulated with control medium, LPS or CpG. DCs plated on hFN without TLR stimulation did not secrete detectable cytokine (data not shown), but DCs activated with LPS or CpG secreted increasing concentrations of IL-12p70 with increasing hFN density (Figure A3.1A). Interestingly, DCs plated on mFN without TLR stimulation and DCs plated on mFN with CpG activation secreted increasing concentrations of IL-12p70 with increasing mFN density, but there was no obvious trend with LPS (Figure A3.1B). Overall, the data strongly suggested that increasing fibronectin density promoted DC activation *in vitro*.

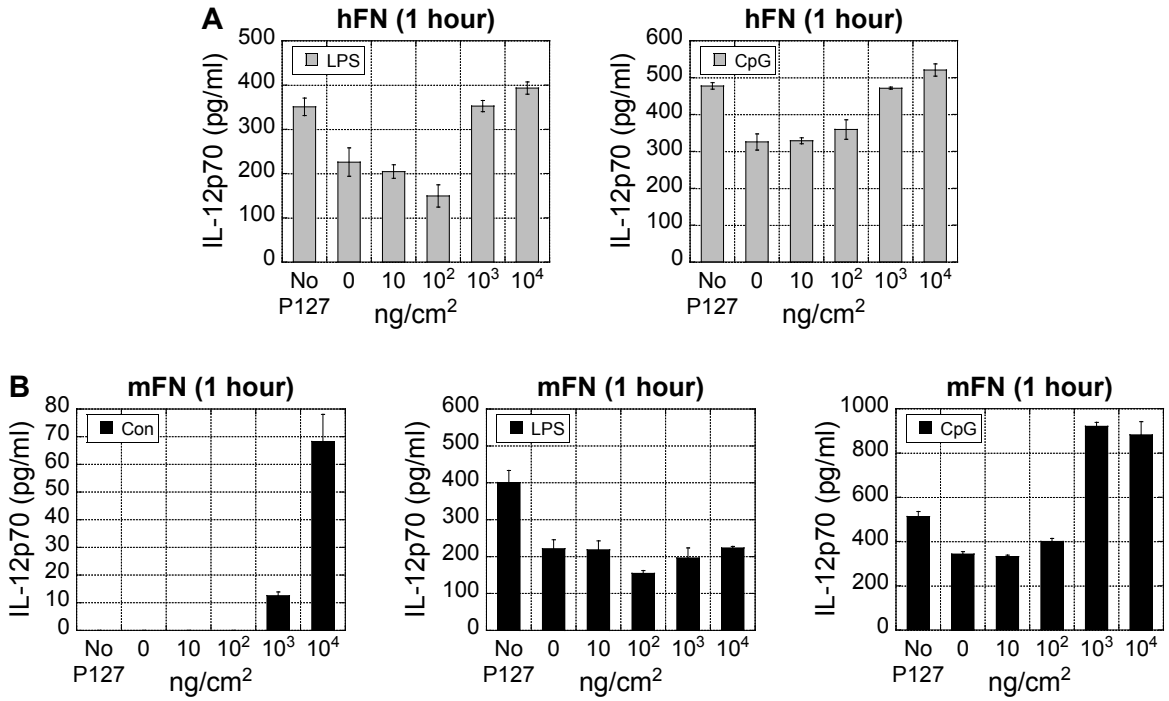

Figure A3.1: Effect of ECM protein density on DC activation (DCs plated 1 hour before activation). (A) DCs were plated onto wells with increasing densities of hFN blocked with Pluronic F127 (P127). As a control, DCs were plated onto unmodified wells (No P127). One hour after plating, DCs were stimulated with control medium (not shown), LPS, or CpG. After 20-24 hours of stimulation, supernatants were collected and analyzed for IL-12p70 by ELISA. n=3. (B) DCs were plated onto wells with increasing densities of mFN and stimulated with control medium (Con), LPS, or CpG as above. After 20-24 hours of stimulation, supernatants were collected and analyzed for IL-12p70 by ELISA. n=3. Data is presented as mean ± standard deviation.

It has been shown that when DCs mature they become less responsive to subsequent stimulation. Given that mFN alone was able to induce IL-12p70 secretion, we wanted to establish whether DC plating on ECM proteins caused DCs to mature and lose their ability to be stimulated over time. The above experiments were repeated except DCs were stimulated 18 hours after plating instead of 1 hour. DCs plated on hFN and stimulated with LPS secreted increasing concentrations of IL-12p70 with increasing hFN density, but when DCs were stimulated with CpG, IL-12p70 secretion seemed to peak at 10^2 ng/cm^2 (without LPS stimulation, IL-12p70 was undetectable (data not shown)) (Figure A3.2A). DCs plated on mFN without TLR stimulation secreted increasing concentrations of IL-12p70 with increasing mFN density, but when DCs were stimulated with LPS or CpG, IL-12p70 secretion peaked at 10^2 ng/cm^2 (Figure A3.2B). Lastly, DCs plated on mLN secreted increasing concentrations of IL-12p70

with increasing mLN density when stimulated with LPS (without LPS stimulation, IL-12p70 was undetectable (data not shown)) (Figure A3.2C). Taken together, these results indicate that delaying activation of bone-marrow derived DCs *in vitro* may reduce their ability to be activated depending on the ECM protein, the concentration that the protein is plated, and the TLR agonist.

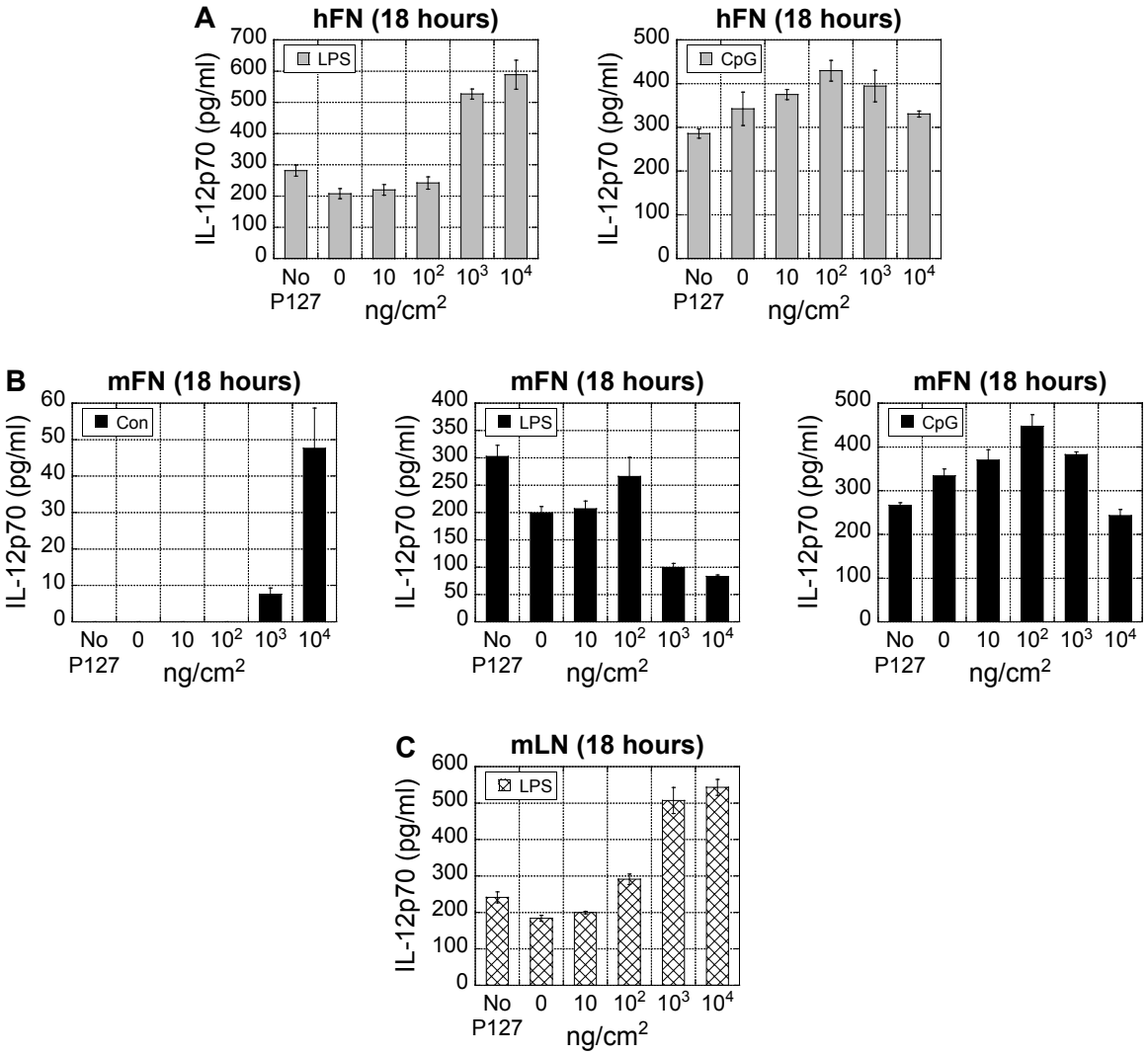

Figure A3.2: Effect of ECM protein density on DC activation (DCs plated 18 hours before activation). (A) DCs were plated onto wells with increasing densities of hFN blocked with Pluronic F127 (P127). As a control, DCs were plated onto unmodified wells (No P127). Eighteen hours after plating, DCs were stimulated with control medium (not shown), LPS, or CpG. After 20-24 hours of stimulation, supernatants were collected and analyzed for IL-12p70 by ELISA. n=3. (B) DCs were plated onto wells with increasing densities of mFN and stimulated with control medium, LPS, or CpG as above. After 20-24 hours of stimulation, supernatants were collected and analyzed for IL-12p70 by ELISA. n=3. (C) DCs were plated onto wells with increasing densities of mLN and treated with control medium (data not shown) or LPS. After 20-24 hours of stimulation, supernatants were collected and analyzed for IL-12p70 by ELISA. n=4. Data is presented as mean ± standard deviation.

Similar to the above 2D studies, we were interested in determining if 3D culture of DCs in calcium alginate gels caused them to lose their ability to be stimulated over time. DCs were encapsulated in alginate beads, and 1 hour or 18 hours after encapsulation were stimulated with control medium or CpG. Control DCs did not secrete detectable IL-12p70 (data not shown). However, we found that culturing DCs in alginate gels for 18 hours reduced their ability to secrete IL-12p70 in response to CpG (Figure A3.3A).

To determine whether matrix protein density could influence DC activation in 3D, DCs were encapsulated in alginate discs with increasing densities of RGD peptide and treated with control medium or CpG 1 hour after encapsulation. DCs cultured in control medium did not secrete detectable IL-12p70 (data not shown), and unlike studies done on 2D TCPS, IL-12p70 secretion in 3D alginate matrices was not influenced by integrin-matrix interactions (Figure A3.3B).

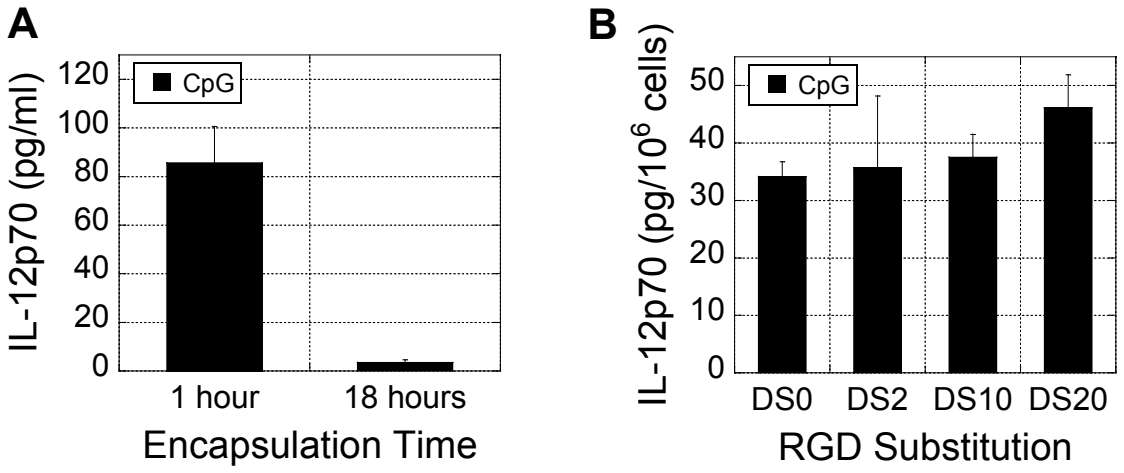

Figure A3.3: Effect of encapsulation time and RGD density on activation of DCs in alginate matrices. (A) After 1 hour or 18 hours of encapsulation in calcium alginate beads, DCs were stimulated with control medium (not shown) or CpG. After 20-24 hours of stimulation, supernatants were collected and analyzed for IL-12p70 by ELISA. n=3. (B) After 1 hour of encapsulation in calcium alginate discs with increasing RGD densities, DCs were stimulated with control medium (not shown) or CpG. After 20-24 hours of stimulation, supernatants were collected and analyzed for IL-12p70 by ELISA. n=4. Data is presented as mean ± standard deviation.

A3.4 Conclusion

Increasing ECM protein density generally promoted IL-12p70 secretion when DCs were cultured on 2D surfaces. However, after 18 hours, DCs cultured on both 2D surfaces (depending on the ECM protein and its plating density) and within calcium alginate matrices tended to lose their ability to be stimulated. Because DCs easily mature after being manipulated and have a diminished capability of being activated after maturation, it is recommended that DCs be assayed soon after plating or encapsulation. The results of this study also suggest that DC behavior can be modulated by controlling DC-matrix interactions, which could be useful for biomedical applications.

A3.5 References

[1] Discher DE, Janmey P, Wang YL. Tissue cells feel and respond to the stiffness of their substrate. Science 2005;310:1139-43.

[2] Ingber DE. Mechanical control of tissue growth: function follows form. Proc Natl Acad Sci U S A 2005;102:11571-2.

[3] Abram CL, Lowell CA. Convergence of immunoreceptor and integrin signaling. Immunol Rev 2007;218:29-44.

[4] Brand U, Bellinghausen I, Enk AH, Jonuleit H, Becker D, Knop J, et al. Influence of extracellular matrix proteins on the development of cultured human dendritic cells. Eur J Immunol 1998;28:1673-80.

[5] Acharya AP, Dolgova NV, Clare-Salzler MJ, Keselowsky BG. Adhesive substrate-modulation of adaptive immune responses. Biomaterials 2008;29:4736-50.

[6] Andersen CAS, Handley M, Pollara G, Ridley AJ, Katz DR, Chain BM. Beta 1-integrins determine the dendritic morphology which enhances DC-SIGN-mediated particle capture by dendritic cells. Int Immunol 2006;18:1295-303.

[7] Rowley JA, Madlambayan G, Mooney DJ. Alginate hydrogels as synthetic extracellular matrix materials. Biomaterials 1999;20:45-53.

Appendix 4
Effect of Collagenase Type on Dendritic Cell CD11c Staining

A4.1 Introduction

Various cell-surface antigens are susceptible to cleavage by trypsin, which is commonly found in collagenase used to digest tissues. When analyzing tissue-extracted cells for surface markers, it is important to choose collagenase type with caution, as any contaminating trypsin could cleave markers of interest. CD11c, a DC marker, is an example of a cell-surface protein that is cleavable by trypsin, and we hypothesized that exposing DCs to collagenase with higher trypsin content would lead to greater CD11c cleavage [1, 2]. To test this, we incubated bone-marrow derived DCs in collagenase type II and IV (the latter containing less trypsin) at 37°C for 15, 30 and 60 minutes, and analyzed the DCs for CD11c and CD86 using flow cytometry.

A4.2 Materials and Methods

Bone marrow-derived DCs were cultured as described in Chapter 2. On Day 10 of culture, LPS was added to the Petri dishes so that the final concentration equaled 100 ng/ml. After 24 hours, cells were collected and washed. $2x10^6$ cells were pipetted into 15 ml tubes, spun, and resuspended in 250 U/ml of collagenase type II (Lot#S9E11242) or type IV (Lot#40E11931) (Worthington) in PBS. Tubes were placed in a 37°C water bath and vortexed every 10 minutes. At 15, 30, and 60 minutes, cells were spun down, washed in stain buffer and stained with APC-conjugated anti-mouse CD11c or PE-conjugated anti-mouse CD86 for analysis by flow cytometry.

A4.3 Results

As hypothesized, we found that type II collagenase, which contained 1.23 u/mg of tryptic activity, reduced DC expression of CD11c significantly more than type IV collagenase, which contained

0.03 u/mg of tryptic activity. When digestion was allowed to occur for 30 minutes, CD11c staining decreased by approximately 5% and for 60 minutes decreased by 10%. CD86 was less affected by type II collagenase digestion (Figure A4.1).

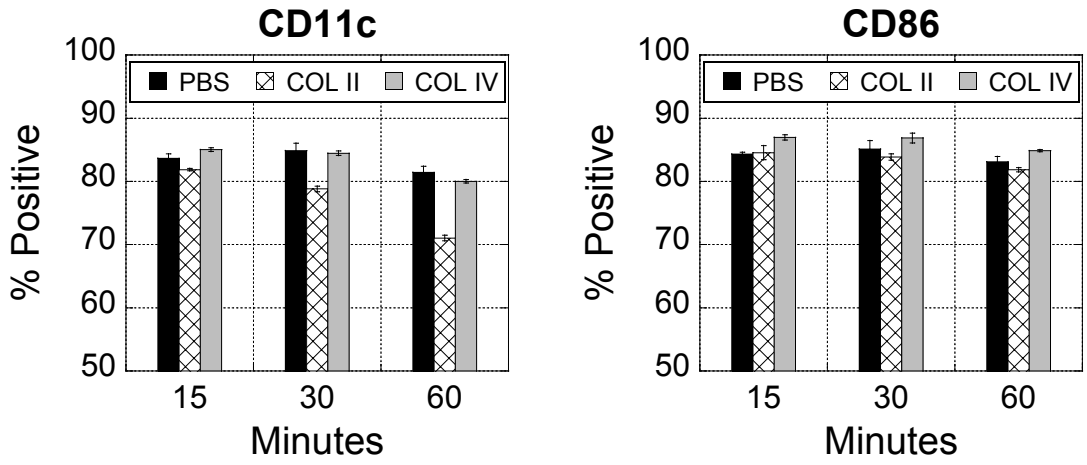

Figure A4.1: Type II collagenase significantly cleaved CD11c on bone marrow derived DCs. DCs were treated with type II and type IV collagenase for 15, 30, and 60 minutes at 37°C and stained for CD11c and CD86.

A4.4 Conclusion

When digesting scaffolds and tissues for CD11c analysis, it is recommended that for optimum staining, type IV collagenase should be used instead of type II.

A4.5 References

[1] Stutte S, Jux B, Esser C, Forster I. CD24a expression levels discriminate Langerhans cells from dermal dendritic cells in murine skin and lymph nodes. J Invest Dermatol 2008;128:1470-5.

[2] Byrne SN, Halliday GM. Phagocytosis by dendritic cells rather than MHC IIhigh macrophages is associated with skin tumour regression. Int J Cancer 2003;106:736-44.

Appendix 5
Optimal Temperature for Dendritic Cell CCR7 Staining

A5.1 Introduction

It has been demonstrated that the anti-CCR7 4B12 antibody clone stains more brightly at 37°C than 4°C [1]. To confirm this, we stained bone-marrow derived DCs with the PE-Cy7-conjugated 4B12 anti-CCR7 antibody at 4°C and 37°C and compared staining using flow cytometry.

A5.2 Materials and Methods

Bone marrow-derived DCs were cultured as described in Chapter 1. On Day 10 of culture, LPS was added to the Petri dishes so that the final concentration equaled 100 ng/ml. After 24 hours, cells were collected, washed, and stained with APC-conjugated anti-mouse CD11c , PE-conjugated anti-mouse CD86, and PE Cy7-conjugated anti-mouse CCR7 (Clone 4B12; eBioscience) at either 4°C or 37°C for analysis by flow cytometry.

A5.3 Results

CCR7 staining was brighter when it was performed at 37°C rather than 4°C, while CD86 staining and CD11c staining were unaffected by staining temperature (Figure A5.1).

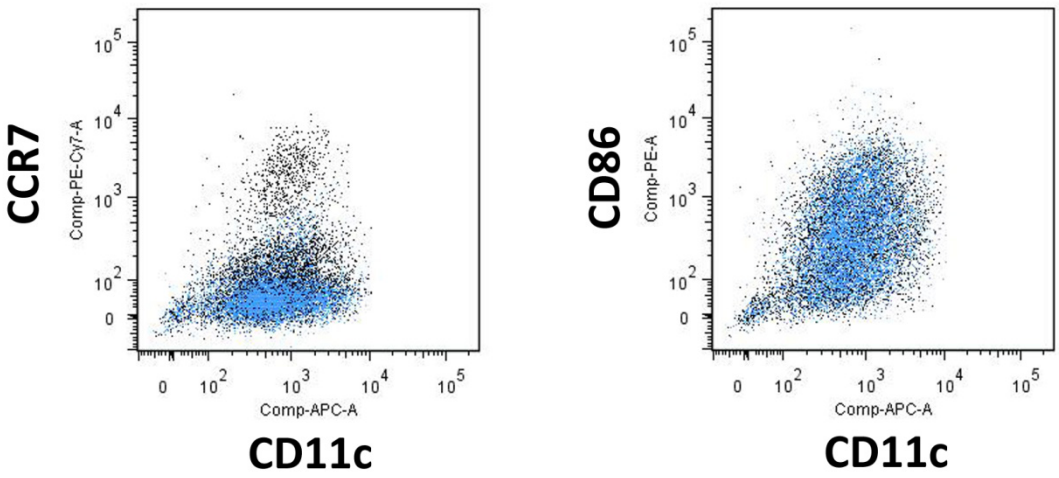

Figure A5.1: CCR7 (Clone 4B12) staining was brighter when performed at 37°C. CCR7, CD86 and CD11c staining were performed at 4°C (blue) and 37°C (black).

A5.4 Conclusion

When performing CCR7 staining with antibody clone 4B12, it is recommended that staining be done at 37°C according to the manufacturer's instructions.

A5.5 References

[1] eBioscience. Anti-Mouse CD197 (CCR7) PE-Cy7. Online. 2013 February. Available from URL: http://www.ebioscience.com/media/pdf/tds/25/25-1971.pdf.

Appendix 6
General Staining Protocol for Flow Cytometry

A6.1 Materials

Stain buffer with BSA
FC blocking antibody, staining antibodies, and isotype controls
96-well non-TC U-bottom plate
Multichannel pipette
Polystyrene tubes (BD Falcon, 352058)

A6.2 Procedure

1. Wash cells in ice cold stain buffer and resuspend each sample at a concentration of 10^6 cells/50 μl stain buffer.

2. Pipet 50 μl of cell suspension into a well of a 96-well non-TC U-bottom plate. Keep plate on ice during entire staining protocol.

3. For each sample being stained with antibodies, add 0.5-1 μg FC block in 10 μl stain buffer (pipet up and down to mix). Add 10 μl to each well being stained and incubate on ice for 15 minutes. In the meantime, prepare the staining antibodies (see step 4).

4. Since the cells are already in a 60 μl volume, prepare multi-stains, single stains, and isotype controls in stain buffer so that when 40 μl is added to each well, the final concentration equals the highest recommended concentration by the manufacturer for 10^6 cells in a 100 μl volume.

5. After the FC blocking step, add 40 μl of staining or isotype antibody to each well (pipet up and down to mix) and incubate on ice for 30 minutes. Protect from light.

6. Wash wells by pipetting an additional 100 μl stain buffer using a multichannel pipette. Spin plate at 1200 RPM (~300 RCF) for 5 minutes and flick plate into sink to remove supernatant. Wash cells 2 more times as above with 200 μl stain buffer.

7. After the last wash, resuspend cells in 200 μl stain buffer and add to a polystyrene tube containing 300 μl stain buffer.

8. Keep cells on ice or at 4°C until analysis and protect from light. If staining is being done on a different day, you can resuspend cells in 0.1% PFA in PBS instead.